

Synthesis of Metal-Organic Frameworks (MOFs): Routes to Various MOF Topologies, Morphologies, and Composites[†]

Norbert Stock* and Shyam Biswas

Institut für Anorganische Chemie, Christian-Albrechts-Universität zu Kiel, Max-Eyth-Str. 2, 24118 Kiel, Germany

CONTENTS

1. Introduction	933	List of Acronyms and Abbreviations	964
1.1. Historical Developments	935	References	965
2. Conventional Synthesis	935		
2.1. Reaction Scaleup	936		
3. Systematic Investigations of MOF Synthesis	937		
3.1. High-Throughput Methods	937		
3.2. Ex Situ and In Situ Studies of MOF Crystallization	939		
4. Alternative Synthesis Routes	941		
4.1. Microwave-Assisted Synthesis	942		
4.2. Electrochemical Synthesis	944		
4.3. Mechanochemical Synthesis	945		
4.4. Sonochemical Synthesis	946		
5. Various Aspects of MOF Synthesis	948		
5.1. Solvents and Structure-Directing Agents	949		
5.1.1. Solvents	949		
5.1.2. Structure-Directing Agents	949		
5.2. Mineralizers	950		
5.3. Precursor Approach	950		
5.4. In Situ Linker Synthesis	951		
5.5. Control of Catenation	952		
6. MOF Crystals, Films/Membranes, and Composites	953		
6.1. Crystal Size and Morphology	953		
6.1.1. Compositional and Process Parameters	954		
6.1.2. Temperature Program	955		
6.1.3. Additives	956		
6.1.4. Reverse Microemulsions	957		
6.2. Thin Films and Membranes	957		
6.2.1. Direct Growth	958		
6.2.2. Layer-By-Layer Growth	960		
6.2.3. Secondary Growth	960		
6.2.4. Chemical Solution Deposition	961		
6.3. Composites	961		
6.3.1. MOF-Organic Matrix Composites	961		
6.3.2. MOF-Inorganic Matrix Composites	962		
7. Conclusions and Future Prospects	963		
Author Information	963		
Biographies	963		
Acknowledgment	964		

1. INTRODUCTION

The synthesis of metal-organic frameworks (MOFs) has attracted immense attention during the last 2 decades due to the possibility to obtain a large variety of aesthetically interesting structures that could also be of great interest for applications in a number of fields related to porous materials. This includes the more traditional areas of storage, separation, and catalysis, which are based on the pore size and shape as well as the host–guest interactions involved. In addition, biomedical applications or the use as sensor materials are currently intensively investigated. Extensive reviews have been published that also partially cover the synthesis of MOFs.^{1–4}

Regarding the synthesis of MOFs, often the term “design” has been used. There have been controversial discussions about this term and an interesting personal view has been given recently.⁵ The more stringent definition of “design”, which implies “to create, fashion, execute, or construct according to plan” (Webster’s Dictionary),⁶ generally is not applicable in MOF synthesis. Nevertheless, the definition and its implications have helped to promote the field. The knowledge of possible topologies, the functionality of multitopic organic linker molecules, as well as the understanding of typical metal coordination environments or the formation conditions of typical inorganic building blocks (sometimes termed as bricks) help one to understand and direct the synthesis efforts. The main goal in MOF synthesis is to establish the synthesis conditions that lead to defined inorganic building blocks without decomposition of the organic linker. At the same time, the kinetics of crystallization must be appropriate to allow nucleation and growth of the desired phase to take place. These complex relationships explain why only for selected examples isorecticular series of MOFs could be obtained and why for the discovery of the majority of MOFs still exploratory syntheses are mandatory. To speed up the discovery of MOFs, high-throughput methods, which were at first developed in pharmaceutical research, have been developed (section 3.1). The concepts of miniaturization and parallelization in combination with the automation within the workflow allow not only speeding up the discovery of MOF but also facilitate synthesis optimization as well as the extraction of reaction and structural

Special Issue: 2012 Metal-Organic Frameworks

Received: August 4, 2011

Published: November 18, 2011

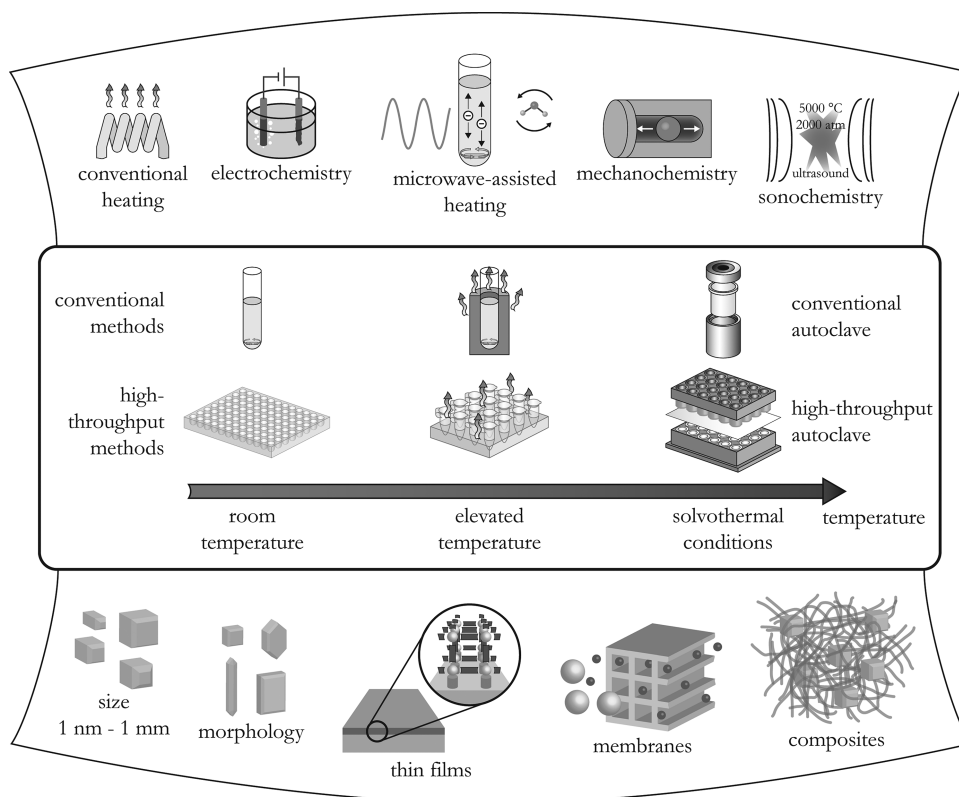


Figure 1. Overview of synthesis methods, possible reaction temperatures, and final reaction products in MOF synthesis.

trends. While these methods are very helpful in relating reaction conditions to the formation of MOFs, they do not result in a deeper understanding of the crystallization processes. Therefore, detailed ex and in situ studies have been performed to shed more insight on the formation of MOFs (section 3.2).

The historical development of the still relatively young field of MOFs is an excellent example of interdisciplinary research that has evolved during the last 2 decades (section 1.1). Developments in the more molecule-based field of crystal engineering led coordination chemists at the beginning of the 1990s to focus on the assembly of organic and inorganic building blocks in order to form porous structures.⁷ Since weak interactions between the building blocks were anticipated, rather mild reaction conditions were applied (section 2). At the same time, chemists with a background in the synthesis of zeolites and zeolite-related materials started to look at the use of organic molecules not only as structure-directing agents but also as reactants to be incorporated in as a part of the framework structure.⁸ For these studies, elevated reaction temperatures are generally employed (section 2). These different scientific backgrounds explain the diverse synthetic methods employed in MOFs synthesis nowadays by various groups around the world, especially regarding reaction temperatures and reactors. They also explain the variety of synthetic methodologies and strategies adopted in the field of MOF synthesis. Coordination chemistry has accounted for introducing electrochemical and mechanochemical synthesis as well as concepts like the precursor approach or in situ linker synthesis. On the other hand, from zeolite chemistry the concepts of solvothermal reaction conditions, structure-directing agents, mineralizers, as well as microwave-assisted synthesis or steam-assisted conversion have been also introduced.⁹

Why are different syntheses methods necessary for MOFs? Starting from the same reaction mixtures, they can lead to different MOFs. They may have a strong impact on reaction time, yields, or particle size and morphology, or may be differently well suited for the implementation in large-scale processes.

Figure 1 summarizes the scope of this review. An account is given on the different synthesis methods that have been applied in the last 20 years. Thus, in addition to room temperature synthesis, conventional electric (CE) heating, microwave (MW) heating, electrochemistry (EC), mechanochemistry (MC), and ultrasonic (US) methods have been employed. Conventional step-by-step methods as well as high-throughput methods have been employed in some of the studies, and these will also be covered in this review. There have been various objectives regarding the morphology of the MOF products. In addition to the crystal size or shape, thin films, membranes, and various other shapes made of MOFs have been reported, which require the application of different synthesis methods.

Although we take already a very restricted definition for the class of compounds labeled MOFs, i.e., 3D framework structures that exhibit porosity and/or guest exchange properties, it is still not possible to review the syntheses of all the MOFs presented in the literature. Thus, most conventional syntheses are not covered, but concepts and nonstandard investigations are summarized.

We will not cover the activation of MOFs, although this is an extremely important step to unlock the full potential of MOFs. Well-activated MOFs are also crucial for postsynthetic modification reactions, in order to diminish the number of side reactions that can take place. This rapidly expanding field, which relates

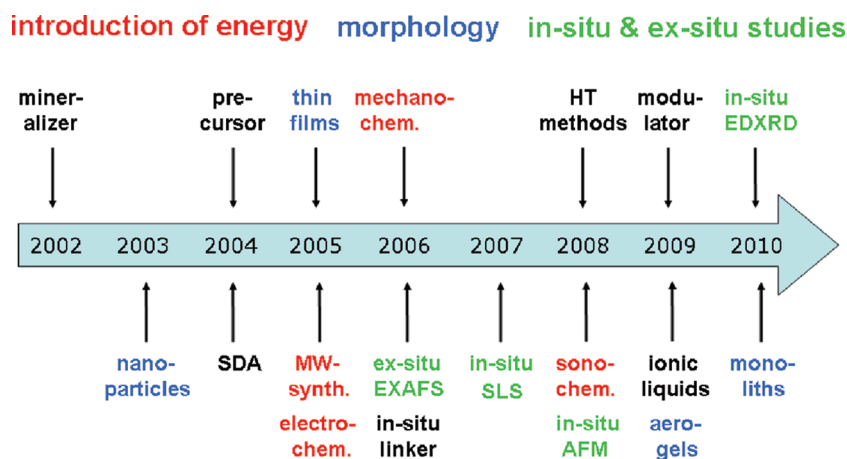


Figure 2. Historical developments in the synthesis of porous MOFs. Details of the different synthetic issues can be found in the respective sections (cf. contents). The dates given refer to the synthesis of porous MOFs, whose porosity was demonstrated by sorption experiments or solvent exchange experiments.

more to organic solid-phase synthesis, will also not be covered, but a number of reviews have recently been published.¹⁰ Over the last years, many reviews and perspectives have been published in the field of MOFs. Information has been taken from these sources as well as from the primary literature.

1.1. Historical Developments

The still relatively young field of MOF synthesis has been recognized to have evolved from the fields of coordination and solid-state/zeolite chemistry. Coordination chemistry has a long history of investigating compounds that were labeled as coordination polymers¹¹ since they were formed by connection of metal ions as connectors and organic ligands as linkers.^{1–4} This area was first reviewed in 1964.¹² The interest in porous coordination polymers surfaced much later, although some complexes such as Prussian blue compounds and Hofmann clathrates had been known to show reversible sorption properties. Thus, the interest in porous coordination polymers and MOFs started only around 1990. In 1989¹³ and 1990,⁷ the seminal work by Hoskins and Robson set the basis for the future of MOFs. In their paper, they already envisioned what has been subsequently shown by many scientists around the world:¹⁴ the formation of a large range of crystalline, microporous, stable solids, possibly using structure-directing agents, with ion-exchange, gas sorption, or catalytic properties that further allow introducing functional groups by postsynthetic modification.

The term MOF was popularized by Yaghi et al. around 1995^{15,16} for a layered Co–trimesate that showed reversible sorption properties. In 1997, a 3D MOF was reported by Kitagawa et al. that exhibited gas sorption properties at room temperature.¹⁷ In 1999, the syntheses of MOF-5¹⁸ and HKUST-1¹⁹ were reported that in the following years and up to now are among the most studied MOFs. Starting in 2002, Férey et al. reported on nonflexible as well as flexible porous MOFs, i.e., MIL-47²⁰ and MIL-53²¹/MIL-88,²² respectively. The concept of isorecticular chemistry²³ was made popular in 2002 for a series of Zn dicarboxylates but has also been extended to other materials. Especially, the mixed-linker compounds $[M_2(\text{dicarboxylate})_2(\text{diamine})]$ ($M = \text{Zn}, \text{Cu}$) have shown to be a versatile class, and numerous studies have been carried out by varying the two organic components.²⁴ The first structural model

for the mixed-linker compounds was published in 2001.²⁵ In 2002, the family of MOFs was extended to imidazolate-based compounds that are nowadays known as zeolitic imidazole frameworks (ZIFs).^{26,27} Although there is a large number of exciting compounds that need to be mentioned, this section will be concluded by providing a list of MOFs that are currently investigated due to their high stability: e.g., Ni–CPO-27,²⁸ UiO-66,²⁹ Cr–MIL-100,³⁰ Cr–MIL-101,³¹ MIL-125,³² CAU-1,³³ and ZIF-8.³⁴ Historical developments taking into account the different synthetic issues covered in this paper are summarized on a time line in Figure 2.

2. CONVENTIONAL SYNTHESIS

The term conventional synthesis is usually applied to reactions carried out by conventional electric heating without any parallelization of reactions. The reaction temperature is one of the main parameters in the synthesis of MOFs, and two temperature ranges, solvothermal and nonsolvothermal, are normally distinguished, which dictate the kind of reaction setups that have to be used. Although a common definition of solvothermal reactions has not been established,³⁵ we use the one by Rabenau,³⁶ i.e., reactions taking place in closed vessels under autogenous pressure above the boiling point of the solvent. Accordingly, nonsolvothermal reactions take place below or at the boiling point under ambient pressure, which simplifies synthetic requirements. The latter reactions can further be classified as the ones at room-temperature or the ones taking place at elevated temperatures.

As exemplified by the work of Hoskins and Robson,⁷ early work has mainly relied on low-temperature routes. Thus, a precipitation reaction followed by recrystallization or the slow evaporation of the solvent was reported. These methods are well-known to grow simple molecular or ionic crystals, since it is possible to tune the reaction conditions, i.e., the rate of nucleation and crystal growth. To grow crystals from clear solutions, the concentration of the reactants has to be adjusted in a way that the critical nucleation concentration is exceeded. This is commonly achieved by changing the temperature or by evaporating the solvent. Once particles exceeding the critical radius are formed, crystal growth takes place. Methods such as solvent evaporation of a solution of reactants, layering of solutions, or slow diffusion

Table 1. Summary of MOFs That Have Been Synthesized in Larger Amounts

MOF	comment	STY ^a (kg m ⁻³ d ⁻¹)	ref
MOF-2	organic solvent, open vessel, 87% yield (Zn)		52
MOF-5	organic solvent, open vessel, 91% yield (Zn)		52
IRMOF-8	organic solvent, open vessel, 15% yield (Zn)		52
Al-MIL-53	commercially available as Basolite A100	160	49, 55
HKUST-1	solvothermal batch synthesis		51
	commercially available as Basolite C 300	225	49, 55
	organic solvent, electrochemical synthesis		52, 56
	continuous synthesis; microwave-assisted heating	2000	46, 47, 50
Fe-BTC	commercially available as Basolite F300	20	49, 55
ZIF-8	commercially available as Basolite Z1200	100	49, 55
[Mg(O ₂ CH) ₂]	commercially available as Basosiv M050	>300	49, 55
Fe-MIL-100	hydrothermal reaction, 10 L reactor	>120	48, 50
	hydrothermal reaction, 100 L reactor	300	57

^a Space–time yields given in this table are not based on the reactor volume, but on the volume of the reaction mixture.

of reactants into each other lead to concentration gradients that allow the formation of MOFs. Concentration gradients can also be accomplished using temperature as a variable, i.e. by applying a temperature gradient or slow cooling of the reaction mixture. Often large crystals suitable for structure determination are obtained by these methods.

Some prominent MOFs have even been obtained at room temperature by just mixing the starting materials; these are, for example, MOF-5, MOF-74, MOF-177, HKUST-1 or ZIF-8.^{37–39} This method is sometimes termed as direct precipitation reaction and shows that the crystallization of some MOFs must take place on a short time-scale. Surprisingly, some of these MOFs, e.g. ZIF-8, show good thermal and chemical stabilities. Variation of the reaction temperature has a strong influence on the product formation and often more condensed/dense structures are observed at higher temperatures.^{40,41} An increase of reaction temperature is also necessary in some systems to attain suitable crystallinity and reaction rates, especially if kinetically more inert ions are used. Nevertheless, the temperature can also have a strong influence on the morphology of the crystals,⁴² and prolonged reaction times can even lead to the degradation of the MOF.⁴³

2.1. Reaction Scaleup

Although a large number of different MOFs as well as many potential applications have been reported in the literature, the synthesis up-scaling to the gram-scale or larger and the large-scale production of these materials have surprisingly been neglected. Most of the reports on scaled-up reactions can be found in patents,^{44–48} but some have also been published, with varying amounts of details, in the scientific literature.^{49,50} The first successful scaleup was demonstrated for HKUST-1 on the 80 g scale,⁵¹ and subsequently MOF-5 was synthesized on a 50 g scale.⁵² Recently, a press release was issued on “the first industrial-scale MOF synthesis” and the testing of the material for natural gas storage in heavy-duty vehicles.⁵³ The identity of the MOF was not disclosed.

The challenges for the use of MOFs in industrial applications lie in their inherent properties as well as their production. Requirements of the MOFs that must be fulfilled include high porosity, thermal and chemical stability, as well as sustainability. Laboratory syntheses, which were established in the search of new MOFs, must also be adapted. Hence, the following issues

need to be taken into account: (1) availability and cost of the starting materials, (2) synthesis conditions (low temperature, ambient pressure), (3) workup procedure, (4) activation process, (5) necessity of obtaining high yields, (5) avoiding large amount of impurities, and (6) using only small amounts of solvents. The latter plays an important role and the use of organic solvents in synthesis, workup, and activation are preferentially avoided. High space–time yields (STY) σ_p (in kg m⁻³ s⁻¹), i.e., “the mass of a product formed per volume of the reactor and time”,⁵⁴ need to be accomplished, which should be as high as possible. The exclusion of anions such as nitrate, perchlorate, or chloride during the synthesis mixtures that often pose challenges on the process control and the reactor layout has led to the development of electrochemical synthesis procedures (section 4.2).

The efforts in recent years have resulted in the scaleup of well-known MOFs in good space–time yields, such as MOF-5, Al-MIL-53, HKUST-1, ZIF-8, and Fe-MIL-100 and some products are also commercially available (Table 1).

The reported scale-up procedures do not comply with most of the criteria for industrial-scale syntheses. Thus, MOF-2 was obtained in 87% yield, based on Zn, starting from 52.2 g of Zn(NO₃)₂·4H₂O and 24.9 g of H₂BDC in a mixture of organic solvents, i.e., NMP, chlorobenzene, and DMF, by adding 30 g of triethylamine at 70 °C.⁵² MOF-5 was synthesized in 91% yield, based on Zn, at 130 °C by reaction of 193 g of Zn(NO₃)₂·4H₂O and 41 g of DEF.⁵² Large crystals of the isorecticular compound IRMOF-8 could be isolated in 15% yield based on Zn or 91% yield based on H₂NDC by reacting 67.4 g of Zn(NO₃)₂·4H₂O and 7.5 g of H₂NDC in 883 g of DEF.⁵² The continuous electrochemical synthesis of HKUST-1 in methanol was scaled up to the 100-g scale per batch (see also section 4.3).⁵⁶

A detailed report on the batch scale-up synthesis of Fe-MIL-100 will be published soon.^{48,50} Thus, it was possible to accomplish the HF-free synthesis of well-crystalline Fe-MIL-100 in Teflon-lined autoclaves ($V = 10$ L, 160 °C) by changing the metal source from elemental Fe to Fe(NO₃)₃·9H₂O and by using high concentrations of starting materials. Activation was accomplished by treatment with NH₄F, and a STY > 120 kg m⁻³ d⁻¹ was obtained. For synthesis up-scaling to a 100 L reactor, a STY of 300 was even accomplished.⁵⁷

The synthesis of HKUST-1 was first scaled up to the 80-g scale by using a batch reactor.⁵¹ The systematic investigation of different

Table 2. Summary of High-Throughput Investigations of Porous MOFs

MOF	comment	ref
Imidazolate-Based MOFs		
ZIFs	9600 microreactions lead to 25 different Co- and Zn-containing ZIFs, 10 mixed-linker ZIFs, 16 new compositions and structures, and five new topologies; fully automated HT methodology	34
Carboxylate-Based MOFs		
Fe–MIL-53–NH ₂ ; Fe–MIL-88B–NH ₂ ; Fe–MIL-101–NH ₂	investigation of solvent; influence of pH, reaction temperature, overall concentration for scaleup	63
MOF-5; HKUST-1	influence of metal salt, reaction time, and temperature on phase purity, crystal size, and morphology	42
Al–MIL-53–NH ₂	investigation of the influence of solvents for Al-based MOFs	64
CAU-1	investigation of the influence of solvents for Al-based MOFs; new inorganic brick; methanol as solvent and reactant	33
Al–MIL-101–NH ₂	investigation of the influence of solvents for Al-based MOFs; DMF as solvent	33
MIL-121	influence of starting pH on the selective formation of MIL-118, -120, and -121;	65
	Al–MIL-53–(COOH) ₂	
CAU-4	investigation of the influence of solvents for Al-based MOFs; use of DMF and synthesis optimization; [Al(BTB)]	66
Cr–MIL-101–NDC	isoreticular to Cr–MIL-101 with mesoporous cages; acetic acid as additive improves crystallinity	67
Ni–HKUST-1	[Ni ₃ (BTC) ₂ (Me ₂ NH) ₃]; investigation of Ni paddle wheel containing MOFs	68
Ni–MOF-14	[Ni ₃ (BTB) ₂ (HMIIm) _{1.5} (H ₂ O) _{1.5}]; investigation of Ni paddle wheel containing MOFs	68
[Ni ₂ (BDC) ₂ (DABCO)]	investigation of Ni paddle wheel containing MOFs; discovery and optimization of polymorphs	68
Phosphonate-Based MOF		
[NaLa(H ₄ L)]	[NaLa((HO ₃ P) ₂ CH–C ₆ H ₄ –CH(PO ₃ H) ₂)]]; anionic open framework; alkaline metal ions as structure-directing agent	69
Tetrazolate-Based MOF		
Fe–BTT	fully automated HT methodology; open Fe ²⁺ sites, sodalite-type MOF	61

solvent mixtures, the reaction temperature, and the influence of stirring resulted in a procedure that yielded after 18 h at 383 K a product that showed after activation a specific surface area of 964 m² g⁻¹, which is far below the values reported for other HKUST-1 products. On the basis of results obtained by MW-assisted heating,⁵⁰ a continuous MW-assisted synthesis of HKUST-1 was developed,^{46,47} and using a total solvent volume of 9 L a STY of 2000 kg m⁻³ d⁻¹ was achieved.⁵⁷ It has to be kept in mind that there are limitations regarding reactor design utilizing MW-assisted heating. Currently a 50-L MWreactor is being realized.⁵⁷

3. SYSTEMATIC INVESTIGATIONS OF MOF SYNTHESIS

To investigate the formation of MOFs, many parameters, such as compositional (molar ratios of starting materials, pH, solvent, etc.) and process parameters (reaction time, temperature, and pressure), are varied. This can be done in a serial way, but it is a time-consuming process that is still used for most of the synthetic investigations. High-throughput methods have been shown to be the ideal tool to accomplish this cumbersome task. Thus, they present a new and more systematic way to establish the fields of formation (section 3.1). Nevertheless, their application does not shed any light on the reaction mechanism or the formation of intermediate phases. Thus, recently *in situ* and *ex situ* investigations under solvothermal conditions have been carried out that demonstrate the fast crystallization of selected MOFs (section 3.2).

3.1. High-Throughput Methods

High-throughput (HT) methods for solvothermal syntheses are a powerful tool to accelerate the discovery of new compounds and to optimize syntheses procedures.^{34,58} Large amounts of data are generated that allows one to establish crystallization fields and to extract relevant reaction trends. This in turn can contribute to a better understanding of the role of individual reaction parameters on the product formation. HT methods are closely connected with the concepts of automation, parallelization, and miniaturization. Thus, parallel reactors, often based on the 96 well-plate format, have been employed, which can hold reaction mixtures ranging from a few microliters to a few milliliters. In order to facilitate the synthesis—handling of small amounts of starting materials in different ratios—as well as the rapid characterization of products, at least a minimum degree of automation is necessary. But also fully automated HT setups have been described.⁵⁹ In addition to automated liquid handling, the fully automated dosing in the milligram-range has also been demonstrated.^{60,61} The proof of concept for the successful application of HT methods in solvothermal syntheses was first demonstrated for zeolites in the late 1990s.⁶² Since then a large number of inorganic–organic hybrid compounds as well as MOFs (Table 2) have been discovered and optimized. Most of the latter are metal–carboxylates, but also imidazolate-, phosphonate- and tetrazolate-based compounds were investigated.

Most of the reported studies focus on the discovery and synthesis optimization, i.e., the crystallinity or crystal size. Characterization of

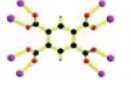

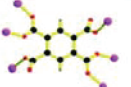
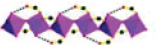
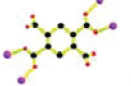

MOF-type Aluminum Pyromellitate	Organic ligand configuration	Inorganic sub-network configuration	Starting pH value
MIL-120			12.2
MIL-118			2
MIL-121			1.4

Figure 3. Influence of pH related to the formation of MOF-type Al pyromellitate frameworks. Reproduced with permission from ref 65. Copyright 2010 American Chemical Society.

the reaction products is routinely carried out by automated XRPD measurements, and the patterns are compared to databases containing simulated powder patterns of the known compounds in the system under investigation. In addition, automated optical microscopy has also been employed to identify products containing suitable single crystals.³⁴

The first two studies, reported in 2008, dealt with ZIFs and amino-functionalized derivatives of Fe–MIL-53, -88, and -101.^{34,63} In the study on ZIFs,³⁴ 9600 reactions were performed in 96-well plates in the range of 65–150 °C. Nine imidazolate-type linkers and mixtures thereof were reacted with zinc or cobalt nitrate in mixtures of DMF and DEF at various concentrations and molar ratios of metal to linker. Although 16 new compounds and five new topologies were identified, only seven out of 16 discovered ZIFs could be scaled up in order to permit bulk characterization. The results of the 9600 reactions allowed establishing the optimal synthesis conditions for ZIFs, i.e., a concentration level of 0.20 M, a reaction time of 72 h, and an isothermal temperature of 85 or 100 °C.

The influence of reaction temperature, molar ratios of starting materials, overall concentration, and pH of the reaction mixture as well as the role of the solvent was studied for the system Fe³⁺/H₂BDC–NH₂/base/solvent.⁶³ Reactions were carried out in protic as well as aprotic reaction media, i.e. DMF, water, acetonitrile, and methanol. The fields of formation of the three amino-functionalized Fe-based compounds MIL-53–NH₂, MIL-88–NH₂, and MIL-101–NH₂ could be determined, and up-scaling of the reaction products was demonstrated. The following parameters could be established to have the most profound impact on the product formation: (a) reaction medium, (b) reaction temperature, and (c) overall concentration.

The thorough investigation of the corresponding system containing Al³⁺ as the metal ion was also carried out.^{33,64–66} Al–MIL-53–NH₂ was obtained when water was employed as the solvent.⁶⁴ The optimal molar ratio (Al³⁺:H₂BDC–NH₂) as well as the optimal reaction temperature was determined, and on the basis of these results the scaleup was successfully performed. The –NH₂ groups were shown to be accessible to postsynthetic modification reaction. Al–MIL-101–NH₂ could be isolated using DMF and working under diluted conditions.³³ When methanol was employed as the solvent, a new, highly porous MOF denoted as CAU-1 was discovered.³³ This compound contains the new Al-based octameric brick [Al₈(OH)₄(OCH₃)₈]¹²⁺ that is connected

by organic linkers to form a 12-connected net. The structure is related to a cubic centered packing motive in which the octameric units replace individual atoms. Thus, distorted octahedral and tetrahedral cages with effective accessible diameters of 1 and 0.45 nm, respectively, are formed. On the basis of the results of the HT investigation, the syntheses could be scaled-up to the 250 mL scale. Other Al-containing MOFs that have been discovered by employing HT methods are MIL-121⁶⁵ and CAU-4.⁶⁶ MIL-121 is an Al–MIL-53 analogue containing two extra noncoordinating carboxylic acid functions per ligand. It was discovered as the third member in the chemical system Al(NO₃)₃·9H₂O/H₄BTEC/H₂O/NaOH during the detailed investigation of the influence of the starting pH and the overall concentration on the phase formation. The HT methods enabled the authors to establish reaction conditions for the selective formation of the three compounds (MIL-118, -120, and -121), and on the basis of the data, synthesis–structure correlations could be established. Thus, low pH favors the formation of corner-sharing [AlO₆] polyhedra as observed in MIL-118 and -121, while higher pH values lead to edge-sharing, as observed in MIL-120. The increase of the starting pH leads to a higher degree of deprotonation of H₄BTEC, and thus for MIL-121, -118, and -120, four, six, and eight carboxyl O atoms are connected to Al³⁺ ions, respectively (Figure 3).

One outstanding example of a stable and highly porous MOF is Cr–MIL-101,³¹ a Cr terephthalate that has been the focus of many investigations. It contains two kinds of accessible cages with diameters of ~29 and ~34 Å. Replacing BDC²⁻ by NDC²⁻ ions has led to an isoreticular compound with pore diameters of ~39 and ~46 Å, denoted as Cr–MIL-101-NDC.⁶⁷ Employing a 24-well high-throughput reactor system, the influence of chemical (solvents, starting materials, molar ratio, etc.) and process parameters (temperature and reaction time) was investigated. More than 600 individual reactions were performed to determine the appropriate synthesis conditions for Cr–MIL-101-NDC. The temperature control (heating and cooling rate), the Cr³⁺ source, the solvent as well as the presence of aliphatic acids play an important role. Although the compound was unambiguously characterized, it is only obtained in combination with an X-ray amorphous byproduct.

One of the most abundant inorganic bricks in MOFs is the so-called paddle wheel unit. According to the CSD database, most of the compounds containing paddle wheel units are based on Cu and Zn, but examples with other ions such as Mo, Fe, and Cr were also reported. Prominent examples are the compounds HKUST-1,¹⁹ MOF-14,⁷⁰ PCN-6,⁷¹ or mixed-linker materials with the composition [M₂(dicarboxylate)₂(diamine)].^{72,73} Recently, a systematic HT investigation of Ni-based paddle wheel containing MOFs was conducted using H₃BTC, H₃BTB, and the mixed-linker system H₂BDC/DABCO. Six new compounds were discovered: four porous Ni-based MOFs with paddle wheel building units and two compounds with dense layered structures. As a first step in the study, a comprehensive screening of compositional and process parameters allowed establishing the reaction conditions for the Ni analogue of HKUST-1. Applying these reaction conditions and replacing H₃BTC with the extended tritopic linker H₃BTB, the Ni analogue of MOF-14 was discovered. In the mixed-linker system H₂BDC/DABCO, two pillared–layered structures with the composition [Ni₂(BDC)₂(DABCO)] were achieved. HT methods involving MW-assisted heating as well as stirring of the reaction mixture allowed establishing the synthesis condition for each polymorph.

Table 3. Summary of Ex Situ Studies of MOF Crystallization

MOF	method	investigation	ref
MIL-89	EXAFS	indication of the retention of inorganic brick over the complete crystallization process	75
[Mg ₂ (Hcam) ₃ (H ₂ O) ₃][NO ₃]	ESI-MS	detection of the inorganic brick in the supersaturated crystallization solution	76
M–MIL-53; V–MIL-47	XRPD	influence of metal ions on crystallization kinetics of isostructural M(III)–BDCs (M = Cr, Al)	77
M–MOF-76	XRPD	influence of metal ions on crystallization kinetics of isostructural lanthanide–BTCs (M = Ce, Tb, Y)	78
Fe–MIL-53	XRPD	influence of heating methods (conventional electric, microwave, and ultrasound) on crystallization kinetics	79
ZIF-8	XRPD	evaluation of crystallization kinetics by the Avrami model	80

Compared to the large number of carboxylate-based MOFs, there are only a few porous metal phosphonates known in literature.^{69,74} Recently, the anionic flexible open-framework metal phosphonate [NaLa((PO₃H)₂CH–C₆H₄–CH(PO₃H)₂)], [NaLa(H₄L)] was reported.⁶⁹ In a systematic study on the role of the alkaline metal ions on the product formation, Na⁺ was identified as the best structure-directing agent for this framework. The molar ratios of the starting materials, the reaction temperature, and the degree of dilution as well as influence of the order of addition of the metal ions to the reaction mixture were scrutinized in a very systematic way. This allowed the presence of a Na₄(H₄L)_{solv} precursor complex in solution to be proposed and the order of suitability for the alkaline ions to be determined.

A fully automated HT methodology employing a solid- and liquid-dispensing robotic module, optical monitoring of the reaction progress, as well as automated workup and HT powder diffraction were used for the synthesis optimization of the tetrazolate-based compound Fe₃[(Fe₄Cl)₃(BTT)₈(CH₃OH)₄]₂ (Fe–BTT).⁶¹ Although this compound is isostructural with Mn– and Cu–BTT, many optimization cycles were necessary to obtain a phase-pure compound. The final optimized conditions were observed to be vastly different from those for Mn–BTT and Cu–BTT, high-lighting the benefit of HT methods. Unfortunately, only the final synthesis procedure but no details about the synthetic strategy or the observed trends were reported.

The synthetic parameters are not only responsible for the phase formation but they also present a way to influence the crystal morphology. In a study on MOF-5 and HKUST-1, the influence of the metal source, the compositional parameters, reagent concentrations, and pH as well as reaction temperature and time were recently investigated.⁴² The characterization of the samples was performed by X-ray powder diffraction and high-resolution scanning electron microscopy. Attention was focused on the phase purity and the crystal morphology of the resulting compounds. The metal acetates were identified as preferable starting materials to obtain well-developed small crystals. For HKUST-1, the optimal reaction conditions for phase-pure compound and X-ray quality crystals were determined by controlling the reactant concentration as well as reaction time and temperature.

3.2. Ex Situ and In Situ Studies of MOF Crystallization

Time-resolved investigations of MOF crystallization allow the detection of crystalline intermediates, the assessment of individual reaction parameters, i.e., reaction rate constants and activation energies, and formulating an idea about the crystallization mechanism. Thus, the optimization of the synthesis conditions of new compounds can be achieved. In addition, they can be used to monitor and adjust the crystal size of the final product.

To follow the crystallization, ex situ or in situ studies can be performed. In ex situ investigations, the reaction is quenched after certain time intervals. This and the following workup can lead to changes in the nature of the sample and thus to nonreliable results. Nevertheless, ex situ studies can be more easily carried out under laboratory conditions and are fairly straightforward to conduct. In contrast, in situ studies require often the use of special equipment and synchrotron radiation, but the reactions are monitored continuously, which leads normally also to a better time resolution. Various methods have been employed for these investigations. EXAFS spectroscopy, ESI-MS, and XRPD measurements were used for the ex situ studies (Table 3), while EDXRD, SAXS/WAXS, SLS, SPR, and AFM measurements were employed for in situ studies (Table 4).

An ex situ EXAFS study was carried out for the synthesis of Fe–MIL-89.⁷⁵ The trimeric brick [Fe₃(μ₃-O)(O₂C–R)₆]⁺ was detected over the complete solvothermal crystallization process.

ESI-MS measurements of a supersaturated crystallization solution for the synthesis of [Mg₂(Hcam)₃(H₂O)₃][NO₃] allowed the direct identification of the inorganic brick [Mg₂(Hcam)₃]⁺.⁷⁶

XRPD measurements were mostly used for ex situ studies of MOF synthesis. The extent of reaction is obtained from the relative intensities of the most intense Bragg reflections. Using this method, the influence of metal ions in the synthesis of isostructural metal(III)–BDCs⁷⁷ and lanthanide–BTCs⁷⁸ was investigated. In both cases, the synthesis rate was found to be directly proportional to the lability of the metal ions ($r_{\text{Cr-MIL-53}} < r_{\text{Al-MIL-53}} < r_{\text{V-MIL-47}}; r_{\text{Ce-BTC}} > r_{\text{Tb-BTC}} > r_{\text{Y-BTC}}$). The deprotonation of the linkers is much faster than the complexation of the metal ions. The same group also investigated the influence of the heating method on the reaction kinetics of Fe–MIL-53.⁷⁹ Compared to CE heating, the use of US or MW irradiation substantially accelerated the synthesis rate of Fe–MIL-53 ($r_{\text{US}} > r_{\text{MW}} \gg r_{\text{CE}}$). The acoustic cavitation, which leads to hot spots, is possibly responsible for the acceleration of US synthesis. The higher rates of MW synthesis may be attributed to the fast and uniform heating of the reaction solutions. In another ex-situ study, the Avrami model was applied to describe the crystallization kinetics of ZIF-8 at room temperature.⁸⁰ The Avrami exponent suggested homogeneous nucleation and growth of spherical particles.

In a time-resolved in situ EDXRD study, the influence of the heating method (MW and CE heating) on the crystallization process of CAU-1–(OH)₂ was investigated (Figure 4).⁸¹ Complete crystallization was observed in the range of 10–280 min depending on the reaction temperature, and MW heating led to shorter induction periods as well as shorter reaction times compared to CE heating. A kinetic analysis of the data according to the Sharp–Hancock method suggested that the reaction mechanism varied with the heating method. The Avrami exponents indicated a phase-boundary controlled reaction under

Table 4. Summary of in Situ Studies of MOF Crystallization

MOF	method	investigation	ref
CAU-1-(OH) ₂	EDXRD	evaluation of crystallization kinetics using the Avrami–Erofe'ev model; influence of heating methods (conventional electric and microwave) on crystallization kinetics	81
HKUST-1	EDXRD	evaluation of crystallization kinetics using the Avrami–Erofe'ev as well as Gualtieri model	43, 82
Fe–MIL-53	EDXRD	evaluation of crystallization kinetics using the Avrami–Erofe'ev model; detection and isolation of MOF-235 as an intermediate	82
MOF-14	EDXRD	evaluation of crystallization kinetics using the Gualtieri model; determination of solvothermal stability of the MOF	43
Al–MIL-101–NH ₂	SAXS/WAXS	evaluation of the competitive formation of Al–MIL-53–NH ₂ , Al–MOF-235–NH ₂ , and Al–MIL-101–NH ₂ employing the Gualtieri model	83
	SAXS/WAXS	evaluation of the competitive formation of Al–MOF-235–NH ₂ and Al–MIL-101–NH ₂ in the presence of Keggin polyanions employing the Gualtieri model	84
HKUST-1	SLS	elucidation of crystal growth mechanism from a supersaturated crystallization solution	85
MOF-5	SLS	elucidation of crystal growth mechanism from a supersaturated crystallization solution; control of particle size by using a modulator	86
ZIF-8	SLS	adjustment of particle size by adding modulators; determination of the role of modulators in the crystallization process	87
HKUST-1	SPR	indication of the formation of inorganic brick during layer-by-layer growth by varying the Cu ²⁺ ion source	88
HKUST-1	AFM	elucidation of mechanism of crystal growth as well as nature of building units	89, 90

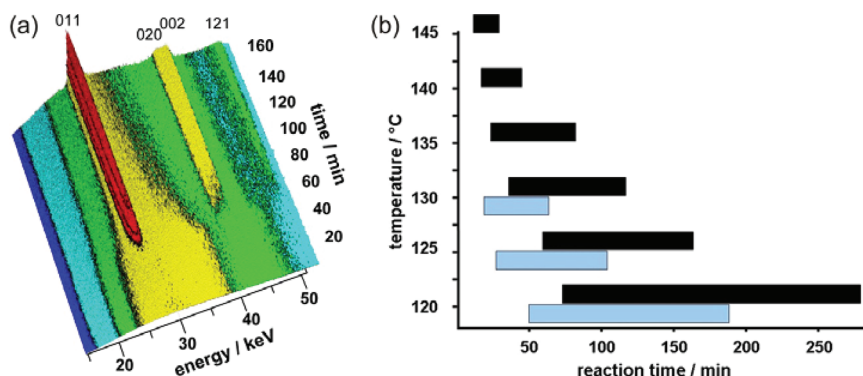


Figure 4. (a) Time-resolved in situ EDXRD data measured during the crystallization of CAU-1-(OH)₂ at 125 °C using conventional heating. (b) Comparison of induction and reaction times between microwave (blue) and conventional (black) heating for the crystal growth of CAU-1-(OH)₂ in the range 120–145 °C. Reproduced with permission from ref 81. Copyright 2011 Wiley-VCH Verlag GmbH & Co. KGaA.

CE heating and a diffusion-controlled reaction under MW heating. In the EDXRD investigations of the solvothermal crystallization of HKUST-1 and Fe–MIL-53, two different crystallization scenarios were noticed.⁸² The crystal growth kinetics of HKUST-1 was evaluated using the Avrami–Erofe'ev model by applying the Sharp–Hancock method. A classical nucleation-controlled reaction was observed, in which nucleation continued after crystallization had begun. The formation of Fe–MIL-53 occurred via the metastable precursor MOF-235, which could also be isolated by quenching. In an EDXRD study of the solvothermal crystallization of MOF-14 and HKUST-1,⁴³ the former compound was found to decompose at longer reaction times. Thus, the material possesses a lower solvothermal stability compared to HKUST-1. The kinetics of crystallizations of both MOFs was examined by the Gualtieri model, which allowed separation of the nucleation and growth regimes. The occurrence of secondary nucleation in MOF-14 prior to the decomposition was proposed by the kinetic analysis and proven by SEM images.

Employing in situ SAXS/WAXS measurements, the crystal growth kinetics of product formation in the system Al³⁺/H₂BDC–NH₂/solvent was evaluated using the Gualtieri model.^{83,84} In the first report, the influence of solvent, reactant concentration, and reaction temperature was systematically investigated.⁸³ When the synthesis is carried out in DMF at low reactant concentration, both Al–MIL-53–NH₂ and Al–MIL-101–NH₂ are observed. The increase of the reactant concentration or the replacement of DMF by water as solvent leads to the formation of Al–MIL-53–NH₂. In the intermediate temperature range in DMF, Al–MOF-235–NH₂ appears as a kinetically stable phase, which transforms into the thermodynamically stable Al–MIL-101–NH₂ as the reaction temperature rises. The DMF facilitates the dissolution of H₂BDC–NH₂, increasing the availability of the building blocks and thus favoring the formation of Al–MOF-235–NH₂. The intermediate Al–MOF-235–NH₂ phase could be isolated by quenching the reaction mixture at intermediate temperatures. In DMF/water

mixtures, the Al–MOF-235–NH₂ phase is hydrolyzed and the Al–MIL-53–NH₂ phase is formed at high temperatures. The fast formation of Al–MOF-235–NH₂ is supported by the higher rate of nucleation compared to crystal growth. In the second report, the encapsulation of Keggin polyoxometalate ions (POMs) in Al–MIL-101–NH₂ was confirmed by the dramatic change of relative intensity of the Bragg peaks after the addition of POM to the synthesis mixture.⁸⁴ The crystal growth kinetics of Al–MIL-101–NH₂ was almost unaffected by this addition. It has been inferred that the POM acts as nucleation sites and stabilizes the precursor MOF-235 phase that aggregates rapidly. When the crystallization of Al–MIL-101–NH₂ begins, such agglomerates separate and finally the POM nuclei are encapsulated in the cages of Al–MIL-101–NH₂.

Static light scattering (SLS) measurements were used to monitor the crystal growth of HKUST-1 from a supersaturated solution at room temperature.⁸⁵ After a reaction time of 10 min, the particle mass continued to increase linearly, but there was no further increase of the particle size. It has been concluded that the nucleation is slow and continues while the particles grow fast (i.e., nucleation-controlled reaction). In a similar in situ SLS study on the crystallization process of MOF-5,⁸⁶ the same group observed that both mass and size of the particles continued to increase until precipitation took place. For MOF-5, the reaction is not nucleation-controlled; the nucleation being faster compared to successive crystal growth. The particle size of MOF-5 was adjusted by using *p*-perfluoromethylbenzoic acid as a capping agent. Monodentate ligands, such as sodium formate, 1-methylimidazole, or *n*-butylamine, were successfully employed as modulators to tune the size of ZIF-8 crystals in the range from 10 nm to 1 μm.⁸⁷ The modulators acted as competitive ligands in the coordination equilibria and bases in the deprotonation equilibria during nucleation and crystal growth. Time-resolved in situ SLS investigations revealed that nanocrystal formation is characterized by continuous, comparatively slow nucleation and fast crystal growth. Focusing and defocusing of the particle size distribution was noticed at earlier and later stages of growth, respectively. The growth of microcrystals took place by a particle–monomer attachment mechanism, and a change of crystal shape from cubes to rhombic dodecahedra occurred in later stages of growth. Indications for the occurrence of a coalescence mechanism during early stages of the growth were also obtained.

Surface plasmon resonance (SPR) spectroscopy was applied to monitor the layer-by-layer growth of HKUST-1 thin films on OH- or COOH-terminated Au surface.⁸⁸ Virtually no deposition of MOF was detected when copper nitrate was used as a Cu²⁺ ion source. Using copper acetate, fast growth of the layer was observed. This fact was rationalized considering that the [Cu₂(CH₃CO₂)₄(H₂O)₂] unit already contains the paddle-wheel structure and is more efficiently attached compared to the mononuclear Cu²⁺ species present in copper nitrate solution.

Atomic force microscopy measurements were also used to study the formation of HKUST-1. The step height on the {111} facet of a HKUST-1 crystal should be multiples of 1.1 or 1.3 nm, if the crystal growth mechanism involves only attachment of the paddle wheel units. However, during the time-resolved in situ AFM imaging using a ~50 μm crystal, the measured heights were not multiples of 1.1 or 1.3 nm, and many growth hillocks exhibited steps of less than 1.1 nm.⁸⁹ This suggests that the actual growth species (possibly, solvated Cu²⁺ ions or BTC units) are smaller than the expected inorganic brick. The crystal

growth followed a 2D “birth and spread” mechanism with the occurrence of defects as well as isotropic growth steps. The same group later investigated the in situ growth of the {111} facet of a ~0.6 μm sized, defect-free HKUST-1 crystal on OH-terminated Au surface.⁹⁰ In this case, the authors proposed a 2D step-by-step growth mechanism. The height of the anisotropic growth steps corresponded to *d*₁₁₁ crystal spacing (1.5 nm). The difference in growth mechanisms between the two studies was attributed to the difference in crystal size and nature of solvent used for crystallization.

4. ALTERNATIVE SYNTHESIS ROUTES

Chemical reactions require some form of input of energy, and only at temperatures close to 0 K do reactions stop. As described in the previous sections, normally MOF syntheses take place in a solvent and at temperatures ranging from room temperature to approximately 250 °C. The energy is generally introduced using conventional electric heating, i.e., heat is transferred from a hot source, the oven, through convection. Alternatively, energy can also be introduced through other means, for example by an electric potential, electromagnetic radiation, mechanical waves (ultrasound), or mechanically.⁹¹ The energy source is closely related to the duration, pressure, and energy per molecule that is introduced into a system,⁹² and each of these parameters can have a strong influence on the product formed and its morphology.

Why is it important to use different synthesis methods? Obviously, different methods can lead to new compounds that cannot be obtained otherwise. Furthermore, alternative routes can lead to compounds with different particle sizes and size distributions as well as morphologies that can have an influence on the material's properties. For example, different particle sizes in porous materials can influence the diffusion of guest molecules, which has a direct impact on catalytic reactions or the adsorption and separation of molecules. Small crystals may also be employed for the formation of membranes using a seeded growth procedure (section 6.2.3). Nanocrystalline, nontoxic MOFs with high loading capacities are also envisioned for biomedical application.⁹³ For these objectives, sonochemical and microwave-assisted methods have been applied. On the other hand, larger single crystals (in the 100 μm range) are necessary to routinely determine the structure and to establish structure–property relationships.

Since many groups working in the field of MOFs envision their commercial use, it is also important to establish facile, inexpensive, rapid, and commercially viable routes. Fast reactions could lead to continuous syntheses, which are advantageous for large-scale production. Reducing reaction time and temperature would lead to more energy-efficient processes and less demanding synthesis equipment. Thus, a number of investigations have recently been carried out to evaluate the influence of the synthetic method on the formation of MOFs (section 3.2). Crystallization rate, particle size, and sorption properties are just a few variables that have been the focus of these studies. Comparison of these results show one problem in MOF science: a very detailed characterization of all materials using complementary characterization methods is mandatory, since already small changes in synthesis procedures can lead to compounds with immense diverging properties.^{94,95}

In the following sections, alternative synthesis routes are described where energy is introduced through microwave irradiation

Table 5. Summary of Studies Dealing with the Microwave-Assisted Synthesis of Porous MOFs

MOF	comment	ref
Metal(III)–Carboxylate-Based MOFs		
Cr–MIL-100	first MW synthesis of MOFs	100
Fe–MIL-100	nanoscale particles; imaging and drug delivery	101
Cr–MIL-101	nanoscale particles; benzene sorption	102
	nanoscale particles	103
Fe–MIL-101	nanoscale particles	104
Fe–MIL-101–NH ₂	nanoscale particles; imaging and drug delivery	104
	nanoscale particles; imaging and drug delivery	101
Fe–MIL-88A	CE, MW and US synthesis; nanoscale particles	105
Fe–MIL-53	CE, MW and US synthesis; ex-situ crystallization study	79
CAU-1	CE and MW synthesis; in situ crystallization study	81
V–dicarboxylates	isoreticular frameworks with MIL-47 topology	106
	growth on polyacrylonitrile	107
[Ce ₂ (PYDC) ₂ (HPYDC)(H ₂ O) ₂]Cl	lanthanide-based MOF	108
Metal(II)–Carboxylate-Based MOFs		
IRMOF- <i>n</i>	IRMOF-1	109–112
	IRMOF-1; 3 ² statistical design used for synthesis optimization; consecutive application of US and MW irradiation	113
	IRMOF-1 film	114
	IRMOF-1 membrane	115
	IRMOF-2, -3	110
	IRMOF-16-(OH) ₂ ; activation by supercritical CO ₂	116
MOF-177	CE, MW, and US synthesis	117
HKUST-1	systematic study of Cu–trimesates	118
	comparison with other synthesis methods	119
	kinetics of crystallization	120
	activation by supercritical CO ₂	121
Ni–glutarates	phase-selective and rapid crystallization	122
Ni–CPO-27	epoxidation catalysis	123
[M ₃ (NDC) ₃ (DMF) ₄]	M = Co, Mn	124
[Mg ₂ (BTEC)(H ₂ O) ₄]	single-crystal-to-single-crystal transformation; selective gas sorption	125
[Cu ₂ (OBA) ₂ (DMF) ₂]	dynamic framework	126
Azolate-Based MOFs		
ZIF-7 and -8	ZIF-8 powder	127
	ZIF-8 membrane	128
	ZIF-7 membrane	129
[Co ₄ O(BDPB) ₃]	catalytic oxidation	130
[Zn ₃ Cl ₄ (BBTA) ₃]	triazolate-based MOF; selective gas sorption	131
[Zn ₃ Cl ₄ (BTDD) ₃]	triazolate-based MOF; hydrogen sorption	132
Mixed-Linker MOFs		
[Zn ₂ (NDC) ₂ (DPNI)]	selective gas sorption	133
[Ni ₂ (BDC) ₂ (DABCO)]·(DMF) ₄ ·(H ₂ O) ₄	phase selectivity, polymorphs	68

(microwave-assisted synthesis, section 4.1), application of an electric potential (electrochemistry, section 4.2), mechanically (mechanochemistry, section 4.3) or through ultrasound (sonochemistry, section 4.4).

4.1. Microwave-Assisted Synthesis

Introduction of energy using microwave irradiation is a well-established method in synthetic chemistry⁹⁶ but has been mainly used in organic chemistry.^{97,98} Nevertheless, solid–solid reactions

as well as solution-based syntheses, for examples of zeolites⁹ and MOFs, have also been described. The latter has been recently summarized in a perspective covering nonporous coordination polymers as well as MOFs.⁹⁹ Here, we present a short summary of the work presented in ref 99 and focus on the most recent examples.

Microwave-assisted synthesis relies on the interaction of electromagnetic waves with mobile electric charges. These can be polar solvent molecules/ions in a solution or electrons/ions in

a solid. In the solid, an electric current is formed and heating is due to electric resistance of the solid. In solution, polar molecules try to align themselves in an electromagnetic field and in an oscillating field so that the molecules change their orientations permanently. Thus, applying the appropriate frequency, collision between the molecules will take place, which leads to an increase in kinetic energy, i.e., temperature, of the system. Due to the direct interaction of the radiation with the solution/reactants, MW-assisted heating presents a very energy efficient method of heating. Thus, high heating rates and homogeneous heating throughout the sample is possible. Attention must be paid to the choice of appropriate solvents and selective energy input, since starting materials may strongly interact with the MW radiation.

Microwave ovens suited for materials syntheses allow one to monitor temperature and pressure during the reaction and thus allow a more precise control of reaction conditions. Nevertheless, transfer of the syntheses to MW ovens from different vendors is often critical, since these differ in their specifications. MW-assisted MOF syntheses have mainly focused on (1) the acceleration of crystallization and (2) the formation of nanoscale products, but it has been also used (3) to improve product purity and (4) for selective synthesis of polymorphs. This is due to the direct heating of the solvents and the higher nucleation rate that have been observed. Table 5 summarizes the investigations that deal with MW-assisted synthesis of MOFs.

MW-assisted synthesis of MOFs has often been carried out at a temperature above 100 °C with reaction times rarely exceeding 1 h. Only a few reports describe the systematic variation of compositional and process parameters (solvent, irradiation time, reaction temperature, power level, molar ratio of the reactants, reactant concentration, etc.) in order to optimize the reaction conditions. In general, MW irradiation allows faster synthesis of smaller crystals compared to CE heating.

Several metal(III) carboxylate-based MOFs ($M = \text{Fe}, \text{Al}, \text{Cr}, \text{V}, \text{Ce}$) have been prepared by MW-assisted synthesis route. The first MW synthesis of MOFs dealt with Cr–MIL-100.¹⁰⁰ The compound was synthesized in 4 h at 220 °C under MW irradiation with 44% yield, which is comparable with that of CE synthesis. The analogous Fe compound was prepared in 30 min at 200 °C.¹⁰¹ The MW-assisted synthesis of nanoscale Cr–MIL-101 was demonstrated in two reports.^{102,103} In the earlier report, the dimensions of the nanoparticles increased from 40–80 to 70–90 nm and became more homogeneous in size with increasing reaction time.¹⁰² In the later report, the use of HF was avoided, and nanocrystals of Cr–MIL-101 with sizes of ~50 nm in 37% yield were obtained by lowering the reactant concentration or increasing the pH of the reaction mixture.¹⁰³ However, the particle size was not affected by the reaction time. Nanocrystals of Fe–MIL-101 having an average diameter of ~200 nm were synthesized by using DMF as the solvent at 150 °C in 10 min.¹⁰⁴ The formation of nanocrystals of amino-functionalized Fe–MIL-101 was investigated in two reports.^{101,104} In the first report,¹⁰⁴ only small amounts of BDC–NH₂ were incorporated in the mixed-linker nanocrystals synthesized in DMF at 150 °C in 10 min. In the later report,¹⁰¹ octahedral nanocrystals of 173 ± 60 nm containing exclusively BDC–NH₂ were prepared in water at 60 °C in 5 min. In a systematic study showing the effect of compositional and process parameters on nanoscale Fe–MIL-88A formation, only MW-assisted hydrothermal synthesis ensured the fast synthesis of small (<100 nm) and monodispersed nanoparticles with high yields.¹⁰⁵ An ex situ and a time-resolved in situ

crystallization study were carried out on Fe–MIL-53⁷⁹ and CAU-1–(OH)₂,⁸¹ respectively. In both cases, MW irradiation resulted in faster reaction rates compared to CE heating. Six isorecticular V–dicarboxylates having MIL-47 topology were synthesized under similar MW conditions (200 °C, 10 min, VCl₃ as metal salt).¹⁰⁶ Later, the same group studied the direct growth of MIL-47 on polyacrylonitrile as a function of MW irradiation time.¹⁰⁷ In contrast to the above-mentioned studies on nanocrystals, X-ray quality single-crystals of [Ce₂(PYDC)₂(HPYDC)(H₂O)₂]Cl were obtained in 20 min at 200 °C by applying MW irradiation.¹⁰⁸

A wide variety of metal(II)–carboxylate-based MOFs were synthesized by applying MW irradiation. IRMOF-1 and HKUST-1 are among the most studied materials. In the earliest study, cubic microcrystals of IRMOF-1 with the length of 2–4 μm were obtained in 9 min at 95 °C in 27% yield.¹⁰⁹ In another report, both size and regularity of the cubic microcrystals (4 ± 1 μm) of IRMOF-1 decreased up to 1 μm with reducing the concentration of H₂BDC in the starting solution.¹¹⁰ The size of the microcrystals did not change remarkably when the reaction time was varied from 25 s to 1 min. The MW synthesis of the microcrystals of IRMOF-2 and -3 was also described, but the adjustment of crystal size was demonstrated only for IRMOF-1. In a recent report on IRMOF-1, the MW-assisted method yielded higher quality crystals with better CO₂ adsorption properties, compared to the ambient pressure dynamic CE synthesis.¹¹² A ramped-temperature MW synthesis led to crystals with higher crystallinity compared to a constant temperature experiment. In a systematic study on microscale IRMOF-1 (20–25 μm), the increase in MW irradiation time, power level, and concentration of the substrates beyond an optimal condition led to a reduction in synthesis time at the expense of crystal quality.¹¹¹ In another work, uniform IRMOF-1 microcrystals (5–15 μm) were synthesized by applying a consecutive combination of US and MW irradiation.¹¹³ This combined two-step technique resulted in smaller and more regularly shaped crystals, compared to CE synthesis. Thin films and membranes of IRMOF-1 were also deposited on porous alumina by using MW irradiation.^{114,115} Oriented but poorly intergrown films of IRMOF-1 crystals were grown on graphite-coated alumina by the direct growth method.¹¹⁴ In another study, continuous and ordered membranes of IRMOF-1 were deposited on α-alumina by employing the crystals produced by direct growth as seeds for secondary growth.¹¹⁵ In the MW synthesis of microscale IRMOF-16–(OH)₂ (20 μm), the crystal quality as well as porosity of the material improved with an increase in irradiation time.¹¹⁶ The effect of the heating method was investigated for the synthesis of microscale MOF-177 (5–50 μm).¹¹⁷ Both crystallinity and porosity of the material prepared by MW irradiation were inferior to those obtained by US and CE synthesis. The MW synthesis of HKUST-1 was systematically investigated in four reports, and the results were compared with other synthesis methods.^{118–121} In the first report on HKUST-1, the results of MW and CE syntheses were compared.¹¹⁸ MW-assisted heating was found to be the method of choice to rapidly synthesize HKUST-1 crystals in the range of 10–20 μm in high yields (~90%) within 1 h. The crystal size increased with MW irradiation time and reactant concentration. In the second report on HKUST-1, the compound was obtained using six different synthetic routes (static and dynamic CE, MW, US, EC, and MC conditions).¹¹⁹ The results show that MW-assisted synthesis is the best method to produce crystalline HKUST-1 in a short time (30 min) associated with high purity, high micropore volume (0.79 cm³ g⁻¹), and quantitative yield. In the third report on HKUST-1, the crystallization kinetics was investigated by ex situ XRPD measurements.¹²⁰ A comparison between MW and CE

Table 6. Summary of Studies Dealing with the Electrochemical Synthesis of Porous MOFs

MOF	comment	ref
Zn- and Cu-carboxylates	patent; first electrochemical synthesis; systematic investigation of Zn, Cu, Mg, Co as anode materials and 1,3,5-H ₃ BTC, 1,2,3-H ₃ BTC, H ₂ BDC, and H ₂ BDC-(OH) ₂ as linkers	56
Zn-imidazolates	patent; synthesis of [Zn(MIm) ₂] and [Zn(BIm) ₂]	134
HKUST-1	synthesis; gas purification, storage and separation	52
	comparison with other synthesis methods	119
	synthesis; isobutene-isobutane separation	135
	patterned film growth	136
	patterned film growth by galvanic displacement	137

synthesis suggests that the acceleration in MW synthesis is due to a highly increased pre-exponential factor of the Arrhenius equation rather than decreased activation energy. In the fourth report on HKUST-1, MW irradiation led to an increase in the porosity of the material compared to CE heating.¹²¹ The influence of pH, reaction temperature, and heating method was investigated for the synthesis of two Ni-glutarates. The formation of the cubic phase [Ni₂₀(GLU)₂₀-(H₂O)₈] occurred at low pH, low temperature, and especially under CE heating. In contrast, the tetragonal phase [Ni₂₂(GLU)₂₀(OH)₄-(H₂O)₁₀] was formed at high pH, high temperature, and especially with MW irradiation.¹²² In the MW synthesis of Ni-CPO-27, the effect of irradiation time and reaction temperature on the porosity and morphology of the compound was investigated.¹²³ The crystallinity as well as the porosity of the material decreased with an increase in reaction temperature. However, the variation of reaction temperature (90–130 °C) or irradiation time (2–60 min) had negligible effect on the crystal size (22–28 nm). In a study on [M₃(NDC)₃(DMF)₄] (M = Co, Mn), MW irradiation led to 5–20 μm sized crystals with a narrow size distribution, whereas CE heating resulted in 50–200 μm sized single-crystals.¹²⁴ In contrast to the above-mentioned reports on micro- or nanosized crystals, single-crystals of [Mg₂(BTEC)-(H₂O)₄]¹²⁵ and [Cu₂(OBA)₂(DMF)₂]¹²⁶ were obtained under MW irradiation. Whereas a phase-pure synthesis of the former required a careful adjustment of pH or reaction temperature, the latter could only be obtained in multistep MW irradiation mode.

The MW-assisted synthesis of azolate-based MOFs has been described in only a few reports. Rhombic dodecahedral shaped crystals (~20 μm) of the imidazolate-based ZIF-8 were synthesized at 140 °C in 4 h.¹²⁷ The ZIF-8 crystals obtained by MW irradiation showed a larger specific surface area compared to the material synthesized under CE heating. Membranes on ZIF-7 and -8 were also prepared by using MW radiation. In a report of ZIF-8, a dense, crack-free membrane was deposited on bare titania using the direct growth method.¹²⁸ In another report, high-quality membrane of ZIF-7 was grown on α-alumina by a secondary growth technique.¹²⁹ In order to produce a seed layer prior to secondary growth, α-alumina was dip-coated with dispersions containing presynthesized nanocrystals and PEI. The pyrazolate-based compound [Co₄O(BDPB)₃] was synthesized at 155 °C in 2 min under MW radiation.¹³⁰ The small, uniform crystals synthesized by MW irradiation exhibited higher catalytic activity in cyclohexene oxidation, compared to the material obtained by CE heating. The MW synthesis of two triazolate-based MOFs, [Zn₃Cl₄(BBTA)₃]¹³¹ and [Zn₅Cl₄(BTDD)₃]¹³² was accomplished at 155 °C in 10 and 30 min, respectively.

Two mixed-linker MOFs were synthesized under MW irradiation. The microwave sample of [Zn₂(NDC)₂(DPNI)] shows slightly lower capacity for CO₂ and CH₄ compared to the sample prepared by CE heating, but it has much higher selectivity of CO₂ over CH₄.¹³³

In another work, one of the polymorphs of the pillared-layered [Ni₂(BDC)₂(DABCO)] framework was synthesized by employing a high-throughput MW-assisted method.⁶⁸ A combination of MW irradiation, low overall concentration, stirring of the reaction mixtures, and an excess of DABCO yielded the phase-pure polymorph [Ni₂(BDC)₂(DABCO)] · (DMF)₄ · (H₂O)₄.

4.2. Electrochemical Synthesis

The electrochemical synthesis of MOFs was first reported in 2005 by researchers at BASF.⁵⁶ Their main objective was the exclusion of anions, such as nitrate, perchlorate, or chloride, during the syntheses, which are of concern to large-scale production processes. Rather than using metal salts, the metal ions are continuously introduced through anodic dissolution to the reaction medium, which contains the dissolved linker molecules and a conducting salt. The metal deposition on the cathode is avoided by using protic solvents, but in the process H₂ is formed. Another option is the use of compounds such as acrylonitrile, acrylic, or maleic esters that are preferentially reduced. Other advantages of the electrochemical route for industrial process are the possibility to run a continuous process and the possibility to obtain a higher solids content compared to normal batch reactions. Studies dealing with the electrochemical synthesis of porous MOFs are listed in Table 6.

To date the electrochemical formation of microcrystalline powders and films was reported. Researchers from BASF have performed the pioneering work and have established synthesis procedures for some Cu- and Zn-based MOFs.⁵⁶ In their study various combinations of anode materials (Zn, Cu, Mg, Co) and linkers [1,3,5-H₃BTC, 1,2,3-H₃BTC, H₂BDC, and H₂BDC-(OH)₂] as well as different experimental setups were reported, which also allowed the up-scaling of the syntheses. From these combinations, four Cu- or Zn-containing compounds with high porosity were obtained. The HKUST-1 product was tested for its use in gas purification, i.e., removal of tetrahydrothiophene from natural gas, H₂ storage, and the separation of Kr–Xe mixtures.⁵² This work was further extended to the chemistry of ZIFs.¹³⁴ Synthesis procedures were reported that led to the formation of [Zn(MIm)₂] and [Zn(BIm)₂] showing specific surfaces of 1746 and 465 m² g⁻¹, respectively. Studies by other groups have exclusively focused on the electrochemical synthesis of HKUST-1.

In a comparative study on the influence of the synthesis procedure on the properties of HKUST-1, the compound was synthesized using solvothermal, ambient pressure, and electrochemical routes in pure ethanol and ethanol/water mixtures.¹¹⁹ Although XRPD investigations demonstrated that in all cases HKUST-1 was formed, TG experiments, elemental analyses, and sorption experiments showed the inferior quality of the electrochemically synthesized product. This was explained by

Table 7. Summary of Studies Dealing with the Mechanochemical Synthesis of Porous MOFs

MOF	comment	ref
Carboxylate-Based MOFs		
[Cu(INA) ₂]	first report; solvent-free synthesis; known phase	144
[Cu(INA) ₂]; HKUST-1	array approach: 12 metal salts and five organic linkers; solvent-free synthesis, known and unknown phases	145
HKUST-1	formation and properties	146
	evaluation of competitive formation of Cu-BTC phases	119
	yields and properties	147
	H ₂ storage	148
MOF-14	yields and properties	147
[Ln(BTC)(H ₂ O)]	homo- and hetero-Ln MOFs (Ln = Y, Sm, Gd, Tb, Dy, Er, Yb)	149
Imidazolate-Based MOFs		
[Zn(EIm) ₂]	dense and porous ZIFs; ILAG; ZnO as starting material; metal salts as structure-directing agents	150
[Co ₃ Cl ₆ (L') ₂]	tripodal imidazole frameworks; manual grinding	151
Mixed-Linker, Pillared-Layered MOFs		
[Zn ₂ (FMA) ₂ (BPY)]; [Zn ₂ (FMA) ₂ (BPE)]	ZnO as starting material; LAG	152
[Zn ₂ (FMA) ₂ (BPY)]	varying amount of AcOH and H ₂ O in the pores; solvent-free grinding	153
[Zn ₂ (BDC) ₂ (BPY)]; [Zn ₂ (BDC) ₂ (DABCO)]	ZnO as starting material; LAG of Zn terephthalates with BPY or DABCO	154
[Zn ₂ (BDC) ₂ (DABCO)]	ZnO as starting material; ILAG; polymorphs; salt inclusion; anion as structure-directing agent; additives enhance MOF formation	155

the incorporation of linker molecules and/or the conducting salt in the pores during crystallization.

The formation of films and patterned coatings of HKUST-1 has also been reported.¹³⁶ Careful adjustment of the reaction conditions allowed the growth of films in the range of 2–50 μm. By extending the reaction time, self-completing growth of uniform HKUST-1 films was demonstrated. The method was extended to Cu-patterned substrates and a Cu-coated QCMB sensor. The latter was shown to be suitable to monitor the adsorption of water vapor. Patterned growth by anodic oxidation is only possible if continuous electrical contact of the complete metallic pattern to the power source must be guaranteed. An alternative method based on a galvanic replacement reaction was reported for the patterned growth of HKUST-1 on glass slides.¹³⁷ A pattern of metallic Cu was deposited on a glass substrate. Spin-coating of a reaction solution containing H₃BTC, DMSO, and AgNO₃ led to the oxidation of Cu by the Ag⁺ ions. Evaporation of the solvent resulted in the formation of dense films of small intergrown octahedral crystallites with sizes between 100 and 200 nm. Sonication of the coated substrates did not lead to a significant loss of crystallites, which demonstrates the strong adherence of the crystals.

4.3. Mechanochemical Synthesis

Mechanical force can induce many physical phenomena (mechanophysics) as well as chemical reactions.¹³⁸ In mechanochemical synthesis, the mechanical breakage of intramolecular bonds followed by a chemical transformation takes place. Mechanochemistry has a long history in synthetic chemistry¹³⁹ and it has recently been employed in multicomponent (ternary and higher) reactions to form pharmaceutically active cocrystals and in inorganic solid-state chemistry, organic synthesis, and polymer science, just to name a few.^{140–142} Its use for the synthesis of porous MOFs was first reported in 2006¹⁴⁴ and results of selected mechanochemical studies were summarized recently.¹⁴³ Table 7

lists all the reports on MOFs obtained by mechanically activated synthesis.

The interest in mechanically activated MOF synthesis is due to multiple reasons. One important point is environmental issues. Reactions can be carried out at room temperature under solvent-free conditions, which is especially advantageous when organic solvents can be avoided.¹⁴¹ Short reaction times, normally in the range of 10–60 min, can lead to quantitative yields, and generally products containing small particles are obtained. Moreover, in some cases metal salts can be replaced by metal oxides as a starting material, which results in the formation of water as the only side product. For example, ZnO has recently been shown to be suitable for the synthesis of pillared–layered MOFs and ZIFs.^{152,154,155} In contrast, metal oxides are rarely used in solvent-based reactions due to their low solubility.

First studies were performed under solvent-free conditions.^{144,145} The use of organic reactants with a low melting point and hydrated metal salts, preferentially the ones containing basic anions, were shown to be advantageous. Thus, well-crystalline compounds were obtained using metal acetates or carbonates. As a result, acetic acid is often observed as the byproduct that is present in the pores, but it can easily be removed by thermal activation. The addition of minute amounts of solvents, the so-called liquid-assisted grinding (LAG), has been shown to have profound advantages.¹⁵² It leads to the acceleration of mechanochemical reactions, which is probably due to an increase of mobility of the reactants on the molecular level. At the same time, the liquid can exert structure-directing properties. Recently, the extension of the method to ion- and liquid-assisted grinding (ILAG) was demonstrated to be highly efficient for the selective construction of pillared–layered MOFs, and it was shown that the ions as well as solvents exert a structure-directing effect.^{150,155}

The following paragraphs summarize the results on mechanochemical synthesis reported so far. The first investigation dealt

with the solvent-free grinding of $\text{Cu}(\text{OAc})_2 \cdot \text{H}_2\text{O}$ and isonicotinic acid.¹⁴⁴ Treatment of the starting materials for 10 min in a 20 mL steel reactor containing a steel ball led to a highly crystalline and single-phase product of $[\text{Cu}(\text{INA})_2]$ with acetic acid and water molecules in the pores.¹⁴⁴ These can be removed by thermal activation to yield the guest-free porous compound. Interestingly, the grinding was only required to initiate the reaction. As proven by XRPD experiments, a sample that was ground for just 1 min yielded in the course of 6 h a single-phase product. The same group also reported a systematic study on solvent-free mechanochemical syntheses using 60 mixtures between 12 metal salts (Ni, Cu, or Zn with various counterions) and five carboxylate-based organic linker molecules.¹⁴⁵ On the basis of XRPD results, 38 mixtures resulted in crystalline products, and 29 reactions were quantitative. Two porous compounds ($[\text{Cu}(\text{INA})_2]$ and HKUST-1) as well as other known and previously unknown coordination polymers were obtained. Due to the large amount of data, the reaction trends mentioned in the previous paragraph could be established.

The mechanochemical synthesis of HKUST-1 has also been studied in detail. Five publications deal with the formation and properties of the resulting products.^{119,145–148} Starting from a stoichiometric ratio of Cu^{2+} to H_3BTC (3:2), solvent-free grinding as well as LAG resulted in the desired product. Cu salts, grinding conditions (time and frequency), presence/absence of a solvent, and nature of the solvent (DMF, methanol, H_2O /ethanol) were studied. Copper acetate was shown to be the starting material of choice and LAG led to better crystalline products with better sorption properties. The pores of the products contain residual reactants and/or acetic acid and water molecules, which was proven by TG and TG–MS measurements as well as spectroscopic methods. The guest molecules could be removed by washing followed by thermal treatment, but thermal treatment alone led only to small specific surface areas (S_{BET}). Thus, the S_{BET} values differ substantially for the optimized products of the different studies (739,¹⁴⁸ 1364,¹⁴⁶ 1421,¹¹⁹ and 1713¹⁴⁷ $\text{m}^2 \text{g}^{-1}$). Interestingly, the products obtained by short grinding times exhibit mesoporosity,^{146,147} which was proven by SAXS and sorption experiments. In one of the studies on HKUST-1, the BTC linker was replaced by the extended BTB linker and the Cu carboxylate denoted as MOF-14 was also obtained by ball milling.¹⁴⁷

LAG of mixtures of H_3BTC with seven rare-earth carbonates in the presence of DMF gave a series of isostructural products with the composition $[\text{Ln}(\text{BTC})(\text{H}_2\text{O})]$ ($\text{Ln} = \text{Y}, \text{Sm}, \text{Gd}, \text{Tb}, \text{Dy}, \text{Er}, \text{Yb}$), which have previously also been obtained from solvothermal reactions.¹⁴⁹ Activation using methanol followed by thermal treatment led to porous structures. Switching the solvent from DMF to water resulted in the formation of a nonporous coordination polymer, while changing the starting material from the rare-earth carboxylates to the oxides and acetates led to new, so far unidentified phases.

Imidazolate-based compounds have also been synthesized by mechanochemical synthesis.^{150,151} While the reaction of HIm with ZnO or ZnCl_2 led only to nonporous $\text{Zn}(\text{Im})_2$, LAG of ZnO in the presence of DMF was shown to yield quantitatively ZIF-4 and ZIF-8 in the presence of HIm and HMIm, respectively.¹⁵⁰ Since ILAG had been shown to accelerate the formation and direct the phase formation,¹⁵⁵ various combinations ZnO/RIm/solvent/ammonium salts were investigated (RIm = HIm, HMIm and HEIm). The synthesis of ZIFs was facilitated in the presence of the ammonium ions. All components were shown to have an

influence on the phase formation, and the results illustrate that ILAG assists the construction of porous as well as nonporous materials. By variation of the reaction time, the time-dependent ZIF transformation was demonstrated. Thus, short reaction times led to a more open structure, which was stepwise transformed to finally yield the Zn imidazolate with qtz topology. In addition to this detailed study, another paper reports the mechanochemical formation of a MOF containing a tripodal imidazole linker.¹⁵¹ The focus of the work is on the solvothermal synthesis, but by using a pestle and mortar one of the porous compounds was also obtained.

Zn-based, mixed-linker MOFs with the composition $[\text{M}_2(\text{dicarboxylate})_2(\text{diamine})]$ exhibit pillared–layered structures, i.e., 2D metal carboxylate sheets containing inorganic paddle wheel units are pillared by ditopic amines.^{24,73} LAG of ZnO, fumaric acid, BPY, or BPE in the presence of DMF, methanol, ethanol, or 2-propanol yielded the corresponding pillared–layered structures.¹⁵² Starting from a mixture of zinc acetate, fumaric acid, and BPY, the synthesis was repeated in the absence of a solvent, and the interpenetrated structure was refined using Rietveld methods.¹⁵³ The product contains varying amounts of disordered acetic acid and water molecules in the pores, which can be thermally removed.

The reactivity of MOFs under mechanochemical reaction conditions has also been investigated.¹⁵⁴ Thus, the mechanochemical synthesis and grinding-induced transformation of three different nonporous solvated Zn terephthalates were demonstrated, showing the lability of the compounds under grinding conditions. These compounds were also used as starting materials to synthesize pillared–layered MOFs through the reaction with BPY or DABCO. Direct mechanochemical synthesis starting from ZnO or $\text{Zn}_5(\text{CO}_3)_2(\text{OH})_6$ or direct immersion of the nonporous Zn terephthalates in a solvent containing DABCO or BPY were generally not successful. Surprisingly, the formation of two pseudopolymorphs of pillared–layered compounds in the system ZnO/ H_2BDC /DABCO/DMF was observed upon addition of several weight percent of alkaline metal nitrate or ammonium nitrate.¹⁵⁵ In addition to the acceleration of the reaction, a structure-directing effect was observed which is probably due to the salt inclusion within the MOF structure. Thus, the pillared–layered MOF based on a square grid was preferentially obtained using KNO_3 , NH_4NO_3 , Na_2SO_4 , $(\text{NH}_4)_2\text{SO}_4$, or K_2SO_4 , giving quantitatively a pillared–layered MOF based on a hexagonal (Kagome) grid.

4.4. Sonochemical Synthesis

Sonochemistry deals with the chemistry that takes place upon application of high-energy ultrasound to a reaction mixture. Fundamental principles of sonochemistry and its use for the synthesis of nanomaterials can be found, for example, in refs 156 and 157, but a basic summary is presented in the following paragraphs.

Ultrasound is cyclic mechanical vibration with a frequency between 20 kHz, the upper limit of human hearing, and 10 MHz. Since the wavelength is much larger than molecular dimensions, no direct interaction between ultrasound and molecules can be responsible for chemical reactions, but when high-energy ultrasound interacts with liquids, cyclic alternating areas of compression (high pressure) and rarefaction (low pressure) are formed. In the low-pressure region, the pressure drops below the vapor pressure of the solvent and/or the reactants and small bubbles, i.e. cavities, are formed. The bubbles grow (tens of micrometers) under the alternating pressure through the diffusion of solute vapor into the volume of the bubble. Thus, ultrasonic energy is accumulated. Once

Table 8. Summary of Studies Dealing with the Sonochemical Synthesis of Porous MOFs

MOF	comment	ref
Ditopic Linker		
MOF-5	variation of reaction time and temperature as well as power level	159
IRMOF-9 and -10	3^2 statistical design used for synthesis optimization; consecutive application of US and MW irradiation	113
Fe-MIL-53	control of catenation and its effect on CO ₂ adsorption; role of power level in US synthesis	160
Fe-MIL-88A	crystallization kinetics using CE, MW, and US methods; combination of MW and CE heating for nucleation/crystal growth; temperature control; variation of power level	79
	nanoparticles; flexible porous MOF; CE, MW, and US synthesis	105
Tritopic Linker		
[Zn ₃ (BTC) ₂]	synthesis of nanoparticles; selective sensing of organoamines	161
HKUST-1	time-dependent formation in DMF/ethanol/water mixture	162
	rapid room temperature synthesis; amount of DMF determines nature and morphology of reaction product	163
	competitive formation with [Cu ₂ (BTC)(OH)(H ₂ O)] using six synthesis methods	119
[Ln(BTC)(H ₂ O)] (Ln = Ce, Tb, Y)	short reaction time; particle size; luminescence	78
MOF-177	comparison among CE, MW, and US syntheses; short reaction time; high yield; small particles; improved sorption properties	117
PCN-6 and -6'	control of catenation and its effect on CO ₂ adsorption; role of power level in US synthesis	160

the bubbles reach their maximum size, they become unstable and collapse. This process of bubble formation, growth, and collapse is called cavitation and it leads to the rapid release of energy with heating and cooling rates of $>10^{10} \text{ K s}^{-1}$, temperatures of $\sim 5000 \text{ K}$, and pressures of $\sim 1000 \text{ bar}$. Thus, these "hot spots" present rather unusual conditions of short duration of extremely high temperature and pressures inside the collapsing bubble as well as in its vicinity (ring of $\sim 200 \text{ nm}$). At a little larger distance, intense shear forces are observed. There are a large number of parameters that govern the formation of cavities and the intensity of their collapse, and only a fraction of the input energy is transformed into cavitation. In addition to the acoustic frequency and intensity (based on the equipment used), parameters such as the choice of liquid (vapor pressure, viscosity, and chemical reactivity), the temperature, or the gas atmosphere play an important role. Volatile organic solvents are often not an effective medium for sonochemistry because the high vapor pressure reduces the intensity of cavitation collapse and hence the resulting temperatures and pressures.⁹¹

In the case of a solid surface in its vicinity, cavitation leads to the formation of microjets which clean, erode, or activate the surface. Agglomerations of smaller particles are dispersed. In a homogeneous liquid, chemical reactions can take place within the cavity (extreme conditions) at the interface (intermediate temperatures and pressures) or in the bulk media, where intense shear forces are present. The extreme conditions and intense shear forces (see mechanochemistry) can lead to the formation of molecules in an excited state, bond breakage, and the formation of radicals that will further react. At the same time, ultrasonication will improve dissolution of the starting materials. Sonochemistry has been extensively used in organic synthesis¹⁵⁸ and the synthesis of nanomaterials.¹⁵⁶ Starting in 2008, it was also applied to the investigation of MOFs but it is still largely unexplored. Table 8 summarizes the studies undertaken for the sonochemical synthesis of MOFs.

The primary goal of sonochemical synthesis in MOF science was to find a fast, energy-efficient, environmentally friendly, room-temperature method that can easily be carried out. This is of special interest for their future application, since fast reactions could allow the scaleup of MOFs. In addition, nanocrystalline particles, which

are often obtained by sonochemical syntheses, were also anticipated to be of advantage for their application. Systematic studies were carried out focusing on the role of reaction time and temperature, power level, and solvent. Short reaction times at ambient pressure were reported to lead to high yields of the desired product. Nevertheless, comparisons of the results must be regarded with caution due to the following reasons. The different studies were carried out using different equipment, i.e., ultrasonic cleaning baths that have normally lower power intensities or direct immersion of high power ultrasonic horns. In addition, reaction setups differ and sometimes they were not even reported. This is critical since the power introduced into the reaction system will strongly depend on the detailed setup. Some authors claim that room temperature syntheses were carried out. This may be true at the start of the reaction, but depending on the equipment used, a larger or smaller increase of temperature will occur in the reaction mixture. While in some cases the reaction temperature was monitored or even regulated by external cooling, in other cases the reaction temperature was not measured at all. The comparison of results obtained by sonochemistry or by other synthetic methods was also frequently reported. In some studies, the comparison is not valid, since optimized sonochemically synthesized products were compared to nonoptimized conventionally synthesized products. In addition, the formation of nanoparticles is claimed in some of the papers, but the results were only supported by a few TEM micrographs. To prove the formation of nanoparticles, additional characterization methods such as light-scattering techniques must be employed, as nicely shown in the study of MIL-88A.¹⁰⁵

Only a few studies are exclusively concerned with the sonochemical synthesis of MOFs, but the results are mostly compared with others obtained by MW-assisted, electrochemical, mechanochemical, or conventional synthesis. It is striking that up to now only known MOF structures have been sonochemically synthesized and that these compounds (e.g., MOF-5,³⁸ MOF-177,³⁸ HKUST-1¹¹⁹) can also be obtained under mild conditions or even at room temperature.

The first sonochemical investigations dealt with the synthesis of Zn carboxylates.¹⁶¹ [Zn₃(BTC)₂] was obtained from an aqueous solution of zinc acetate and H₃BTC in a mixture of

ethanol and water at room temperature in an ultrasonic bath. The only variable investigated was the reaction time. Compared to the solvothermal synthesis, which was carried out at 140 °C for 24 h, milder reaction conditions and faster reactions were reported. However, optimization of the solvothermal synthesis to shorten reaction time or reduce reaction temperature was not tested. The size and morphology of the reaction product varied with reaction time. Short reactions led to spherical particles in the 100–200 nm range, while reactions for 30 and 90 min resulted in long needles with a diameter of up to 900 nm.

High-quality MOF-5 crystals in the 5–25 μm range were obtained within 30 min in a horn-type reactor using NMP as the solvent.¹⁵⁹ Starting from a clear solution, the reaction time and power level were varied. After 8–30 min, the product formed and the temperature was measured to be between 129 and 164 °C, depending on the power applied. At low power levels, phase-impure samples were observed. Reaction times above 10 min and working at higher power levels led to the deterioration of the previously formed samples. Detailed characterization and comparison with a conventionally synthesized sample showed almost identical physical properties. In a more recent report on MOF-5, a very similar study was undertaken in DMF as the solvent, starting again from clear solutions.¹¹³ A temperature-regulated ultrasonic bath and microwave-assisted heating were consecutively used in a two-step process. Reactions were carried out at different temperatures for varying reaction times. Products with a narrow size distribution containing small particles (5 μm) could be obtained. However, the best samples were inferior to the ones obtained by using NMP as the solvent and ultrasonication exclusively.

Three studies were reported on the synthesis of HKUST-1.^{119,162,163} The first report investigated the influence of reaction time starting from copper acetate and H₃BTC in a mixed-solution of DMF/EtOH/H₂O.¹⁶² Using an ultrasonic bath and varying the reaction time, the desired product was obtained already after 5 min as a nanocrystalline (10–40 nm) powder. Increasing the reaction time led to larger crystals (50–200 nm) and higher yields, but long reaction times resulted in their partial decomposition. Only blurred TEM micrographs give a hint about the sizes and size distribution of the particles, which seem not to contain well-shaped crystals. Another study confirms these findings.¹⁶³ Using the same starting materials and the three solvents, the amount of DMF was increased stepwise and the reaction time was varied. In contrast to conventional and MW-assisted heating, DMF was necessary for the formation of HKUST-1. This was explained by a possible deprotonation of H₃BTC by DMF. After 1 min, a phase-pure and highly crystalline product was obtained. Short reaction times led to smaller and more homogeneous products (200–400 nm) compared to long reaction times, when agglomeration was observed. The concentration of DMF was found to have a strong influence on the physical properties of the product. In contrast to these studies, the third report concerns the successful synthesis of HKUST in a mixture of EtOH and H₂O, while a product of poor quality is formed in pure DMF.¹¹⁹ The physical measurements of all the optimized materials show that the specific surfaces (S_{BET}) are smaller (1100,¹⁶² 1156,¹⁶³ and 1253¹¹⁹ m^2g^{-1}) compared to the best materials. In the another study using the BTC³⁻ as the linker, the isostructural compounds [Ln(BTC)(H₂O)] (Ln = Ce, Tb, Y) were synthesized.⁷⁸ The Tb compound was previously obtained by conventional heating, but the reaction time and temperature could be significantly reduced to 20 min between 25

and 40 °C to yield well-crystalline particles in the 2–3 μm range. On the basis of N₂ sorption experiments, these compounds also showed improved physical properties. Interestingly, the synthesis rates for the three isostructural compounds differ substantially. The crystallization kinetics was established, and the nucleation and crystal growth rate were shown to correlate with the lability of the metal ions.

The use of the tritopic extended linker H₃BTB in sonochemical synthesis was described in the synthesis of the well-known Zn-based compound MOF-177.¹¹⁷ Using NMP as the solvent, a high yield (95.6%) of 5–50 μm -sized crystals was obtained within 40 min. Sonication time and power level were shown to have a strong influence on the product properties, and optimization of these parameters led to high-quality crystals matching the highest reported S_{BET} values for MOF-177.

In a comprehensive kinetic study on the synthesis of Fe–MIL-53, sonochemical reactions were carried out at various temperatures using an ultrasonic horn. The temperature was kept constant and the reaction time was varied to investigate the crystallization process. High crystallization rates were observed. Unexpectedly, the crystal size was found to be almost independent of reaction time or temperature, but dependent on the synthesis method (CE, US, MW). Thus, small, well-shaped crystals with homogeneous morphologies were observed for the sonochemically synthesized compound.

Several synthetic routes were investigated for the synthesis of Fe–MIL-88A with the goal to obtain monodisperse nanoparticles in a high yield. The study uses a number of characterization methods to determine the particle size and polydispersity, such as TEM, SEM, and dynamic light scattering. Different parameters, such as temperature (0, 20, and 50 °C), time (0.5, 1, 1.5, and 2 h), concentration, and pH (addition of acetic acid or NaOH), were evaluated, and an ultrasonic bath was used. Unfortunately, no information about the power input was given. The systematic study shows that the particle size increases as a function of concentration, reaction time, and temperature and that the crystallization rate increases with pH. Thus, by working at 0 °C, adding acetic acid, and using dilute conditions, monodisperse small particles (<200 nm) were obtained. Unfortunately, the yield was lower than 5%.

The most recent article demonstrates the unexpected influence of the ultrasonic power level on the product formation.¹⁶⁰ Two examples of interpenetrated and noninterpenetrated structures, i.e., PCN-6/PCN-6' and IRMOF-9/IRMOF-10, are presented. While at lower power levels the noninterpenetrated structure is obtained, intermediate power levels led to mixtures and higher power levels to phase-pure interpenetrated structure of the corresponding MOF. For all four compounds, small, well-shaped particles were obtained (1.5–2 μm for PCN-6', 4.5–6 μm for PCN-6, and ~5–20 μm for IRMOF-9 and -10).

5. VARIOUS ASPECTS OF MOF SYNTHESIS

As mentioned in the Introduction, concepts from zeolite chemistry were also used in MOF synthesis. Whereas structure-directing agents and mineralizers play an important role in zeolite science, they have been less frequently used in the synthesis of MOFs. On the other hand, approaches that are based on coordination chemistry have been proven suitable for the formation of MOFs. This includes the precursor route as well as the in situ linker synthesis. A phenomenon that is often observed with MOF structures is catenation. On the basis of the

reaction procedures, catenated and noncatenated MOFs can be sometimes selectively obtained. In the following sections, the use of solvents and structure-directing agents (section 5.1), mineralizers (section 5.2), precursors (section 5.3), as well as the in situ linker synthesis (section 5.4) and the selective synthesis of catenation polymorphs (section 5.5) will be covered.

5.1. Solvents and Structure-Directing Agents

The solvent is one of the most important parameters in the synthesis of MOFs, which has been investigated to a lesser extent in zeolite synthesis.⁶³ Although most often no direct interaction with the framework is observed, solvents are almost always incorporated in the as-synthesized MOF structures and thus act as space-filling molecules. Structure-directing agents (SDAs) have been mostly used in the field of zeolite synthesis,¹⁶⁴ where they act as counterions for charge balance, as space-filling molecules, or as “true” templates, in the case of well-defined host–guest interactions. SDAs have also been employed for the preparation of porous MOFs, but it is often hard to identify the role of the solvent as pore-filling molecule (SDA) or as pure reaction medium.

One challenge in the use of organic structure-directing agents, such as amines and ammonium ions, is their removal/exchange after the synthesis. This is due to strong host–guest interactions that lead to structural collapse upon removal of the guest molecules. Numerous examples of amine-templated compounds have been described, but most often the removal of the guest molecules was not reported.^{165–168}

5.1.1. Solvents. The influence of solvents on the product formation has been addressed in few systematic studies. As presented in section 3.1, high-throughput methods have been used to study the systems $\text{Fe}^{3+}/\text{H}_2\text{BDC}-\text{NH}_2/\text{solvent}$ and $\text{Al}^{3+}/\text{H}_2\text{BDC}-\text{NH}_2/\text{solvent}$.^{33,63} In both systems, the reaction medium has a profound impact on the product formation. This was shown to be due to the polarity of the solvent and the solubility of the organic linker and its protolysis properties. Thus, in acetonitrile as well as in methanol, at low temperatures, only $\text{Fe}-\text{MIL}-88\text{B}-\text{NH}_2$ was observed. With DMF only structures based on the trimeric inorganic brick $[\text{Fe}_3(\mu_3\text{-O})(\text{O}_2\text{C}-\text{R})_6]^+$, i.e., $\text{Fe}-\text{MIL}-88\text{B}-\text{NH}_2$ and $\text{Fe}-\text{MIL}-101-\text{NH}_2$, were isolated, while the reaction in water led to $\text{Fe}-\text{MIL}-53-\text{NH}_2$ in most of the cases. The systematic investigation on the influence of different solvents on the analogous Al^{3+} system was carried out with aluminum nitrate and chloride.³³ Aluminum nitrate led in all cases to the formation of $\text{Al}-\text{MIL}-53-\text{NH}_2$ using DMF, methanol, and water as the solvent. The use of aluminum chloride in DMF resulted in the formation of both $\text{Al}-\text{MIL}-53-\text{NH}_2$ and $\text{Al}-\text{MIL}-101-\text{NH}_2$. The reactions performed in methanol yielded a completely new MOF denoted as CAU-1, $[\text{Al}_4(\text{OH})_2(\text{OCH}_3)_4(\text{BDC}-\text{NH}_2)_3] \cdot x\text{H}_2\text{O}$, in which the solvent acted also as a reactant. In a similar study, the effect of solvent on the $\text{Cr}^{3+}/\text{H}_3\text{BTC}/\text{solvent}$ system was demonstrated.¹⁶⁹ $\text{Cr}-\text{MIL}-100$ was obtained as a pure phase using water as a solvent. The addition of small amounts of methanol to the aqueous synthesis mixture led to the coexistence of $\text{Cr}-\text{MIL}-100$ and $\text{Cr}-\text{MIL}-96$. Use of more methanol resulted in the formation of phase-pure $\text{Cr}-\text{MIL}-96$. However, if water was omitted, $\text{Cr}-\text{MIL}-96$ with poor crystallinity was obtained. The influence of the solvent was also observed for isoreticular compound based on the MIL-53 topology, $[\text{Al}(\text{OH})(\text{NDC})]$, denoted as $\text{Al}-\text{MIL}-69$ or DUT-4.¹⁷⁰ While MIL-53 exhibits a highly flexible structure, $[\text{Al}(\text{OH})(\text{NDC})]$ is rigid. Thus, the

synthesis in water led to a nonporous closed structure that could not be opened, while the synthesis in DMF as a solvent resulted in the open-pore modification called DUT-4 that also showed no flexibility.¹⁷¹

Solvents can also act as ligands during the synthesis. In a study on Zn benzobistriazolates, the variation of amide solvents (DMF vs DMA) led to two structurally different MOFs.¹³¹ While the product synthesized in DMF could be activated to yield a porous structure, the synthesis in DMA yielded a product with DMA coordinated to the metal ion. Removal of DMA led to the decomposition of the structure. Similarly, the variation of amide solvents in the amide/water solvent mixtures resulted in two similar yttrium–organic frameworks with different spatial arrangement of the BTC linkers around the Y^{3+} centers and 1D channels (along the *a*-axis), which are occupied by coordinated or occluded solvent molecules.¹⁷²

Hydrolysis of the solvent has been observed especially in the case of organic amides under solvothermal conditions.^{173,174} In a study on the synthesis of MOF-5 and in another study, concerning the use of ZnO in the synthesis of Zn terephthalates under acidic conditions, hydrolysis of DEF led to the formation of diethylammonium ions, which were, together with the solvent, incorporated in the final structure $(\text{H}_2\text{NEt}_2)_2[\text{Zn}_3(\text{BDC})_4] \cdot 3\text{DEF}$. Thus, this compound exhibits an anionic framework structure.

The use of room temperature ionic liquids (ILs) or deep eutectic solvents (DESs), which can act both as a solvent and a SDA, is called ionothermal synthesis.^{175,176} ILs are well-suitable for the dissolution of the inorganic components required for the synthesis. The lack of a detectable vapor pressure of ILs is also an advantage. A DES is a mixture of two or more compounds that has a melting point lower than that of either of its constituents. DESs exhibit also unusual solvent properties that are very similar to those exhibited by the ionic liquids. A number of coordination polymers have been obtained using ILs and DESs.^{175,176} Recently, the group of Morris and Bu demonstrated that chirality can be induced in the framework that is built up of nonchiral building blocks. Chiral ILs were used, but these were not observed in the final structure.^{177–179} The removal of the ionic component was not reported, but the authors expected the collapse of the frameworks upon removal of the guest molecules. In relatively rare cases, the framework contains the neutral component of the DES, the removal of which imparts porosity to the material. Thus, though an increasing number of MOFs (all of them are not cited here) has been synthesized so far under ionothermal conditions, the permanent porosity of only one compound, a samarium terephthalate,¹⁸⁰ was proven by sorption analysis.

5.1.2. Structure-Directing Agents. Space filling by unreacted linker molecules in addition to the solvent is quite often observed in as-synthesized MOF products. Depending on the flexibility of the framework, the guest molecules can have a strong influence on the pore dimension. Thus, $\text{M}-\text{MIL}-53$ ($\text{M} = \text{Fe}, \text{Al}, \text{Cr}$) can switch reversibly from a narrow pore (NP) into a large pore (LP) form with up to 60% variation of their unit cell volume without altering the framework topology.^{21,181,182} The Cr- and Al-based compounds show similar thermal and host–guest behavior. The as-synthesized (AS) materials contain guest terephthalic acid molecules and adopt the LP form. Removal of the guest molecules by thermal activation leads to the high-temperature form, which is identical to the LP form. Upon cooling down to room temperature, the compounds adsorb water from air and transform into the NP form. In case of the $\text{M}-\text{MIL}-88$ and -89

series ($M = \text{Fe}, \text{Cr}$), the ratio between the volumes of NP and LP forms can reach even more than 300%.¹⁸³

Benzene was observed to act as a SDA in the synthesis of pillared-layered MOFs. Depending on the presence or absence of hydrophobic benzene molecules in the hydrothermal reaction among Co^{2+} ion, H_2NDC , and BPE, two different MOFs were obtained,¹⁸⁴ in which the benzene-templated structure had larger pores and more favorable host-guest interactions than the nontemplated one.

Organic amines as SDAs were introduced in the synthesis of In-based MOFs.¹⁸⁵ Thus, the different SDAs HHPP, HIm, and H_2DACH were reacted with In^{3+} ions and 4,5-imidazolecarboxylic acid to form the zeolitic MOFs rho-ZMOF, sod-ZMOF, and usf-ZMOF, respectively. In the resulting anionic frameworks, protonated HHPP, HIm, and H_2DACH species acted as charge-balancing templates. The organic counterions in rho-ZMOF could be ion exchanged by Na^+ ions and subsequent thermal activation was accomplished. In another report, two zeolitic Cd-based MOFs incorporating the four-connected organic linker *cis*, *cis*-1,3,5-cyclohexanetricarboxylate were synthesized using piperazine and isopropanolamine as templates. In this case, the organic counterions were exchanged by K^+ ions prior to thermal activation.¹⁸⁶ Piperazine was also employed in order to prepare a zeolite-like MOF $[\text{Co}_5(\text{Im})_{10}]$. Though not observed in the crystalline structure, the piperazine apparently served as SDA, since parallel reactions with different SDAs resulted in different networks.¹⁸⁷ Furthermore, a precipitate isolated after 12 h at room temperature prior to solvothermal reaction exhibited an IR spectrum with a distinctive signature for an $-\text{NH}$ stretch. Tetramethylammonium (TMA) ions as SDA were used in the synthesis of lanthanide tris(2-carboxyethyl)isocyanurates.^{188,189} In the formation of isostructural 2D network structures using different lanthanides, TMA acted as a so-called “structure-blocking agent” that stops the formation of the 3D structure. Thus, in absence of the TMA ions, isostructural 3D frameworks were produced.

Inorganic templates such as alkaline metal ions or Keggin POM anions have also been investigated in the synthesis of MOFs. The role of the alkaline metal ion was studied in the system $\text{La}^{3+}/[(\text{H}_2\text{O}_3\text{P})_2\text{CH}-\text{C}_6\text{H}_4-\text{CH}(\text{PO}_3\text{H}_2)_2]/\text{NaOH}/\text{H}_2\text{O}$, and Na^+ was identified to be the best structure-directing agent for the anionic flexible open-framework metal phosphonate $[\text{NaLa}((\text{PO}_3\text{H})_2\text{CH}-\text{C}_6\text{H}_4-\text{CH}(\text{PO}_3\text{H})_2)]$.⁶⁹ Keggin ions were employed in the synthesis of HKUST-1^{190–192} and Al-MIL-101-NH₂.⁸⁴ In the room-temperature synthesis of HKUST-1 in water, no MOF product formed in absence of the POM $\text{H}_3\text{PW}_{12}\text{O}_{40}$.¹⁹⁰ The synthesis also failed if H_3BTC was added prior to POM. On the basis of the importance of the preparation sequence, it was presumed that Cu^{2+} ions arrange around the POM before coordinating with BTC. In the final framework structure, the POM ions reside in the smaller cages, since their geometry matches with the cage dimensions. Experimental evidence was provided in favor of the molecular mechanism for the spatial arrangement of Cu^{2+} ions surrounding the template. In another study,¹⁹¹ evidence was presented that the formation of HKUST-1 is significantly accelerated by adding Keggin POM ions to the synthesis solution. The use of EPR, XANES, and pH measurements presented evidence of changes in the Cu^{2+} speciation upon addition of $\text{H}_3\text{PW}_{12}\text{O}_{40}$. This enables paddle wheel formation and crystallization of HKUST-1 at room temperature. The POM-encapsulated HKUST-1 was shown to exhibit improved thermal stability. Steaming at up to 483 K did

not lead to a total decomposition of the crystal structure.¹⁹² The use of $\text{H}_3\text{PW}_{12}\text{O}_{40}$ as a template was also studied in the synthesis of Al-MIL-101-NH₂.⁸⁴ In-situ SAXS/WAXS measurements demonstrated that the POM ions act as nucleation sites. They also stabilize the precursor phase Al-MOF-235-NH₂, but this has almost no effect on the kinetics of the crystallization of Al-MIL-101-NH₂.

Surfactants and swelling agents have been used as SDAs, in analogy to mesostructured zeolite synthesis, to get hierarchically micro- and mesoporous MOFs. Triblock copolymers P123 and F127 in ethanol were used to synthesize hierarchically micro- and mesoporous Al-MIL-53 with two types of mesopore diameters.¹⁹³ The formation of the larger (5.4–7.6 nm) and the smaller (4.0 nm) pore diameters was attributed to block copolymers and solvent. It was presumed that ethanol reacts with 1,4-benzenedicarboxylic acid under the synthesis conditions and that the resulting organic product acts as a different surfactant creating smaller mesopores. In another study, the surfactant CTAB and the swelling agent TMB were employed to create mesoporous HKUST-1.¹⁹⁴ An increase in CTAB/ Cu^{2+} molar ratio enhanced the mesopore diameter from 3.8 to 5.6 nm. A further increase in the mesopore diameter up to 31 nm was achieved by carefully optimizing the TMB/CTAB molar ratio.

5.2. Mineralizers

In addition to helping solubilize the starting materials under the reaction conditions, mineralizers, such as fluorides, added to the reaction mixtures in the correct quantities favor the formation of well-crystalline phases of desired zeolites. Similarly, in the synthesis of carboxylate-based MOFs with trivalent metal ions, for example, Cr-MIL-53,²¹ Fe-MIL-53-X [$X = \text{CH}_3, \text{NH}_2, (\text{OH})_2, (\text{COOH})_2$],¹⁹⁵ MIL-71,¹⁹⁶ M-MIL-96 ($M = \text{Al},^{197} \text{Cr}^{169}$), M-MIL-100 ($M = \text{Cr},^{30} \text{Fe}^{198}$), and Cr-MIL-101,³¹ fluoride was used as a mineralizing agent to increase the crystallinity and to promote the crystal growth of the final product. In M-MIL-100 ($M = \text{Cr}, \text{Fe}$) and Cr-MIL-101, the fluoride ions are incorporated as terminal ligands at the trimeric metal clusters. Fluoride coordinates with the V^{3+} ions, forming corner-sharing $[\text{VO}_2(\text{OH})_2\text{F}_2]$ octahedra in MIL-71.¹⁹⁶ The complete replacement of the OH^- ions of Al-MIL-53, $[\text{Al}(\text{OH})(\text{BDC})]$, by F^- ions yielded the analogous compound $[\text{Al}(\text{F})(\text{BDC})]$.¹⁹⁹ Noteworthy, a significant drop in the BET surface area of the as-synthesized Cr-MIL-101 material was observed with an increase in fluoride concentration in the reaction solution.²⁰⁰ It has been proposed that fluoride ions strongly interact with Cr-trimers, thus inducing nucleation of Cr-MIL-101 during the hydrothermal reaction. Other studies were also conducted to increase crystallinity. Thus, TEOS and H_2O_2 have been used in order to synthesize Al-MIL-96¹⁹⁷ and MOF-5,^{37,201} respectively. The role of these additives was not explained.

5.3. Precursor Approach

MOF structures are obtained by a self-assembling process starting usually from isolated metal ions that assemble together with the linker molecules forming the inorganic brick. An alternative route is the use of molecular inorganic precursors, the so-called “precursor approach”. This involves the use of prebuilt polynuclear coordination complexes comprising structures and functions similar to or identical with the inorganic bricks constituting the MOF. The polynuclear “precursors” must maintain their structural integrity in the reaction media.

The exchange of the monotopic linkers of the precursors with polytopic linkers having similar functionalities can generate 3D

frameworks. The replacement of the acetate ligand of a trinuclear oxo-bridged basic iron(III) acetate by ditopic fumarate, NDC, and *trans,trans*-muconate enabled the syntheses of MIL-88A, MIL-88C, and MIL-89, respectively.^{202,203} However, no synthetic details were provided for MIL-88C. Notably, the EXAFS spectra recorded from crystallization solutions, amorphous intermediates, and crystalline products collected at different reaction times were very similar, demonstrating that the iron(III) acetate building units remained intact during crystallization of MIL-89.⁷⁵ The same group also substituted the monocarboxylate ligand of the zirconium methacrylate oxocluster $[\text{Zr}_6\text{O}_4(\text{OH})_4(\text{OMc})_{12}]$ with dicarboxylates (*trans,trans*-muconate and BDC), leading to Zr dicarboxylates exhibiting the UiO-66 architecture (Figure 5).²⁰⁴ The UiO-66 analogous structure with *trans,trans*-muconate was obtained using the Zr methacrylate oxocluster precursor as well as ZrCl_4 . In a similar study, tetranuclear oxo-centered basic zinc and beryllium acetates, $[(\text{M}_4(\mu_4\text{-O})(\text{OAc})_6)]$, were used as precursors to produce Zn–MOF-5 and Be–MOF-5, respectively.²⁰⁵ Since the analogous Co compound is not available, cobalt oxopivalate, which contains polynuclear complex ions composed of two $[\text{Co}_4\text{O}]^{6+}$ building units, was employed to prepare the isomorphous Co–MOF-5. The cobalt as well as the beryllium compound has not been obtained by another synthesis route up to now.

Exchange of a terminal ligand by a bridging ligand of different functionality can also lead to the formation of MOFs. The replacement of the labile axial solvent molecules of the molecular complex $[\text{Cu}_2(\text{CDC})_2(\text{DMA})(\text{EtOH})_6]$ with the ditopic linker BPY yielded a polyhedron-based MOF.²⁰⁶ The polyhedron-based MOF disassembled back into the molecular complexes in the presence of monotopic pyridine ligands, confirming the transformation as reversible. The chelating nitrate ligands of the tetrahedral symmetrical precursors $[\text{M}_5(\text{BTA})_6(\text{NO}_3)_4(\text{H}_2\text{O})_x]$ ($\text{M}^{2+} = \text{Zn}, \text{Co}, \text{Ni}; x = 1, 4$) were exchanged by either dicarboxylates (BDC, BDC–NH₂, and BPDC) or TCNQ radical anion, respectively, resulting in 3D MOF structures.^{207,208}

The precursor approach presents many advantages compared to the conventional synthesis, such as the control of the nature and topology of the final product and the possibility to use milder synthetic conditions (for example, lower temperature).²⁰⁴ The proof of the precursor concept is experimentally very demanding, but due to the large number of known metal carboxylate precursors, it might offer a versatile route to many new MOFs.²⁰⁹ Care must be taken due to the insolubility²⁰⁶ or hydrolytic instability of the precursor compounds.

5.4. In Situ Linker Synthesis

Traditionally, MOFs are prepared by reactions of presynthesized or commercially available linkers with metal ions. An alternative approach termed as “in situ linker synthesis”, in which the specified organic linkers are generated in the reaction media in situ from the starting materials, is attracting increasing interest in recent years. For the preparation of coordination compounds and coordination polymers, a wide variety of in situ organic transformation reactions were applied, which include oxidation, decarboxylation, hydrolysis, hydroxylation, cycloaddition, substitution, alkylation, acylation, amination, formation, or cleavage of C–C, S–S, and C–S bonds, and so on.²¹⁰ Only a few reaction types have been employed for the synthesis of porous MOFs, i.e., the hydrolysis, [2 + 3]-cycloaddition, decarboxylation, oxidation, and dimerization of the starting materials.

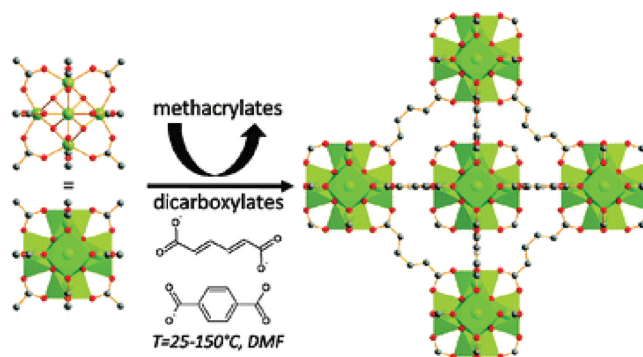


Figure 5. Zirconium–dicarboxylates (right) synthesized from $[\text{Zr}_6]$ methacrylate oxocluster (left) by applying the precursor approach. Color codes: Zr, green polyhedra; C, gray; O, red. Reproduced with permission from ref 204. Copyright 2010 Royal Society of Chemistry.

Hydrolysis of esters and nitriles to the corresponding carboxylates was employed to synthesize several MOFs. The ester trimethyl 1,3,5-benzenetricarboxylate was hydrolyzed in situ and the BTC^{3-} ions were incorporated into M–MIL-96 (M = Al,¹⁹⁷ Ga,²¹¹ In²¹²) and Al–MIL-100.²¹³ The in situ hydrolysis of the same ester led to the formation of two MOFs constructed from Y^{3+} ions and BTC^{3-} linkers.¹⁷² The rho-type zeolitic MOF $[\text{Cd}(\text{PYMC})]$ was obtained by in situ hydrolysis of the nitrile 2-pyrimidinonitrile.²¹⁴ Using the imidazole 4-amide-5-imidate linker, generated in situ by partial hydrolysis of 4,5-dicyano-2-methylimidazole, a Zn–imidazole MOF was synthesized.²¹⁵ A careful adjustment of the acidity of the reaction mixture was required to achieve the selective hydrolysis.

[2 + 3]-Cycloaddition reaction of an azide with nitriles in presence of a Lewis acid generates tetrazolates. The in situ formed tetrazolates were employed as linkers for the construction of a large variety of nonporous tetrazolate-based frameworks.²¹⁶ However, by using the 5-methyl-1H-tetrazole (MT) linker, formed in situ via cycloaddition of acetonitrile with Na azide in the presence of Cd^{2+} ions, the porous Cd-based MOF $[\text{Cd}(\text{Cl})(\text{MT})]$ was prepared.²¹⁷

Decarboxylation of esters and carboxylate ions was applied to prepare Cu- and Cd-based MOFs. The in situ formation of unfunctionalized tetrazolate (TZ) by decarboxylation of ethyl tetrazolate-5-carboxylate was used to synthesize MOFs of composition $[\text{M}_5(\text{TZ})_9][\text{NO}_3]$ ($\text{M}^{2+} = \text{Cu},^{218} \text{Cd}^{219}$). The linker 1,2,3-benzenetricarboxylic acid underwent decarboxylation followed by hydroxylation to produce 2-hydroxyisophthalic acid (HIP), which enabled the synthesis of the mixed-linker MOF $[\text{Cu}_3(\text{HIP})_2(\text{PYZ})_2]$.²²⁰

Oxidation reactions of three types were used to synthesize porous MOFs. The mixed-linker MOF $[\text{Eu}_2(\mu_2\text{-PZDC})(\mu_4\text{-PZDC})(\text{OX})(\text{H}_2\text{O})_4]$ was synthesized via in situ oxidation of 5-methylpyrazine-2-carboxylic acid using HNO_3 as an oxidant.²²¹ The in situ oxidation of dimethyl sulfoxide in the presence of nitrate ions led to sulfate ions, which were incorporated in the structure of PCN-17, $[\text{Yb}_4(\mu_4\text{-H}_2\text{O})(\text{TATB})_{8/3}(\text{SO}_4)_2]$.²²² In order to prepare PCN-46, the same group has employed 5,5'-(buta-1,3-diene-1,4-diyl)diisophthalic acid (H_4BDI), formed in situ through the oxidative coupling of 5-ethynylisophthalic acid (H_2EI) (Figure 6).²²³ It has been postulated that the combination of H_2EI bearing terminal acetylene groups with a slight excess of Cu^{2+} salt, which is readily reduced to Cu^+ ion under solvothermal conditions, generates the homocoupled diisophthalic acid H_4BDI . However, the exact chronological

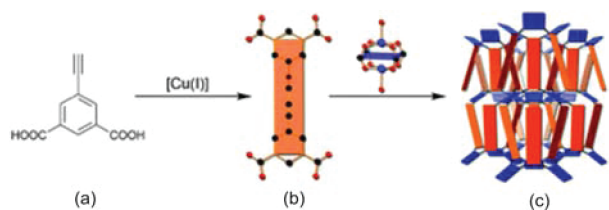


Figure 6. The linker 5,5'-(buta-1,3-diyne-1,4-diyl)diisophthalic acid (b), which is formed in situ under solvothermal conditions from 5-ethynylisophthalic acid (a), is incorporated in the PCN-46 framework (c). Reproduced with permission from ref 223. Copyright 2010 Royal Society of Chemistry.

sequence of events, such as the coupling of the precursors, the deprotonation of the diisophthalic acid, and the formation of the MOF, has not been deciphered.

Dimerization of *L*-aspartic acid resulted in *meso*-iminodisuccinate (IDS), which was used to synthesize the mixed-linker MOF [Zn₂(IDS)(BPY)].²²⁴

In situ linker synthesis has many advantages over conventional synthetic routes. This “one-pot” approach precludes the necessity of synthesizing the linkers, thus simplifying tedious synthesis and purification steps. The slow release of the in situ generated linkers in presence of metal ions can lead to the growth of better crystalline products or even larger single crystals. Moreover, the approach provides alternative pathways to MOFs with in situ synthesized linkers, which are inaccessible or not easily obtained by conventional synthetic methods. It should be mentioned that the discovery of some of the in situ synthesized linkers is serendipitous.²¹⁶

5.5. Control of Catenation

The self-assembly of multiple separate frameworks within each other, which is known as framework catenation, is a well-documented phenomena in MOF chemistry. Catenation is divided into two types: interpenetration and interweaving.²²⁵ In interpenetrated MOF structures, frameworks are maximally displaced from each other; in interwoven MOF structures, the distance between both frameworks is minimized. Catenation enhances the rigidity of the material at the expense of its porosity. However, there exists no established synthetic route to control catenation. For a given combination of inorganic building units and organic linkers, catenation has sometimes been regulated by changing the conventional solvothermal reaction conditions in a trial-and-error fashion.

Dilution of the synthesis mixtures or lowering the reaction temperature can be employed as a route to avoid catenation. The noncatenated (IRMOF-10, -12, -14, -16) and the catenated (IRMOF-9, -11, -13, -15) forms of the IRMOF-*n* series of compounds were synthesized in dilute and concentrated reaction solutions, respectively.²²⁶ In another report, a systematic variation of concentration as well as temperature affording control over the synthesis of a noncatenated form of [Cd(BPY)(BDC)]·3DMF·3H₂O and its catenated form [Cd(BPY)(BDC)] was carried out.²²⁷ Similar to the previous report, the noncatenated form of the framework was obtained from dilute reaction solution, whereas concentrated reaction solution resulted in its catenated form. Moreover, the noncatenated and the catenated forms of the frameworks were prepared in low and high temperatures, respectively. The authors explained the influences of concentration and temperature based on the following hypotheses. The dilution of a reaction solution reduces

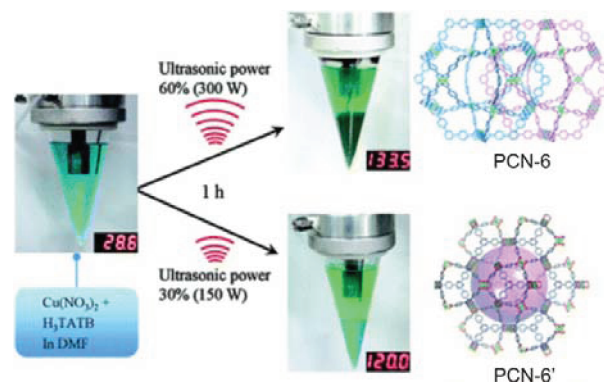


Figure 7. Phase-pure synthesis of the catenation isomers PCN-6 and -6' upon adjusting the ultrasonic power level. One benzoate moiety of each TATB linker in the PCN-6 structure has been omitted for simplicity. Reproduced with permission from ref 160. Copyright 2011 Royal Society of Chemistry.

the possibility of forming a sublattice in the voids of noncatenated structures as they are being formed. On the other hand, higher temperatures afford more thermodynamically stable and denser catenated structures.

MOF-5 is also known in an interpenetrated as well as a noncatenated form. In a study on the catenated form of MOF-5, the synthesis parameters were optimized by systematically varying the amount of water, temperature, time, and molar ratio of the reactants.²²⁸ In this case dilution of the reaction mixture did not lead to the noncatenated form of MOF-5. The solvent or template effect was suggested as the controlling factor for the catenation behavior of MOF-5. Recently, the pH of the reaction solution was found to be a key factor for the phase-pure synthesis of the catenated form of MOF-5.²²⁹

Ultrasonic power level was adjusted in order to develop a rapid, phase-pure synthesis route for PCN-6 and PCN-6' (Figure 7).¹⁶⁰ Employing this strategy, the control of catenation in the US synthesis of IRMOF-9 (catenated) and IRMOF-10 (noncatenated) pair was demonstrated. In both the cases, noncatenated and catenated isomers were synthesized at lower and higher sonication power levels, respectively. Unfortunately, the mechanistic implications of such power levels on the catenation are not understood.

Additives were used to control the catenation of MOFs containing paddle wheel units. Employing oxalic acid as an additive to the reactants, the noncatenated forms of PCN-6' and MOF-HTB' were obtained instead of the catenated forms PCN-6 and MOF-HTB.²³⁰ However, the role of the additive was not explained.

A layer-by-layer (LBL) approach, completely different from the above-mentioned strategies involving bulk synthesis, was applied to synthesize thin films of noncatenated form of MOF-508a, [Zn(BDC)(BPY)_{0.5}], at room temperature.²³¹ In the LBL method, a pyridyl-terminated Au surface was alternatively immersed in two different solutions: one containing metal salt and the other containing a mixture of the organic linkers. The substrate was rinsed in between the immersion steps to remove unreacted or physisorbed reactants. The pyridyl-terminated Au surface, which acts as a nucleation site and mimics the BPY linkers, probably lifts the equivalence of the two catenation isomers. However, the factors controlling the preferential formation of the particular isomer remain unclear.

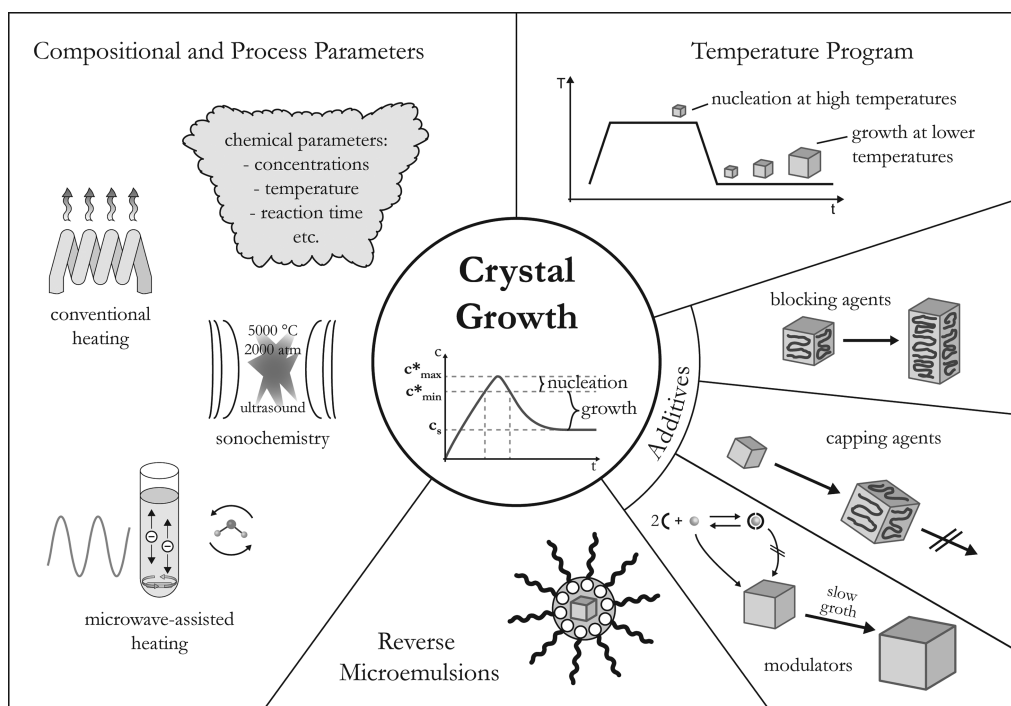


Figure 8. Summary of strategies for manipulating the crystal growth, i.e., size and morphology of MOF crystals.

6. MOF CRYSTALS, FILMS/MEMBRANES, AND COMPOSITES

Manipulation of the size and shape of the crystals is an emerging area in MOF research, since such manipulation is a means of optimizing the physical properties of the solids for specific applications.²³² For example, nanosized MOF crystals have been studied to investigate the influence of the particle size on the diffusion, i.e., the rate of adsorption. In addition, nanosized MOF crystals can be used for the fabrication of thin films or membranes.^{233–236} Notably, MOF thin films or membranes with well-defined porosity and chemical tunability are promising candidates for smart membranes, catalytic coatings, and chemical sensors.²³³ Nanoscale MOF particles have also been employed in magnetic resonance imaging²³⁷ and drug delivery.²³⁸ Beside thin films and membranes, MOF composites of different shapes have been prepared to easily handle and integrate them in gas storage/separation, catalytic, and biomedical systems. In the following paragraphs, the adjustment of crystal size and morphology (section 6.1) as well as the synthesis of films/membranes (section 6.2) and composites (section 6.3) will be discussed.

In addition to the results in the following sections, few other studies were reported that do not fit into the above categories. Therefore, these results are summarized in this paragraph. For the synthesis of an amorphous Fe–MIL-100 aerogel with dual micro- and mesoporosity, the MOF gel was synthesized by vigorous stirring of the reactants in ethanol at room temperature.²³⁹ However, no detailed synthesis procedure was reported. An excess amount of starting materials was removed by Soxhlet extraction, and the adsorbed ethanol was exchanged with supercritical CO₂ to yield the final aerogel. The densities of the aerogels increased with increasing concentration of the starting solution. Drying the gels slowly at low temperatures for several days yielded the corresponding xerogels. Aging of the gels prior to Soxhlet extraction led to xerogels with increased surface areas. Coating of MOF nanoparticles in order to

improve biocompatibility has also been described. Thus, nanoparticles of [Gd₂(BDC)₃(H₂O)₄] were coated with the copolymer poly(*N*-isopropylacrylamide)-*co*-poly(*N*-acryloxysuccinimide)-*co*-poly-(fluorescein *O*-methacrylate).²⁴⁰ Silica-coating of Fe–MIL-101–NH₂ was accomplished with a solution of Na–silicate under solvothermal conditions.¹⁰⁴ Nanorods of [Ln₂(BDC)₃(H₂O)₄] (Ln = Eu, Gd, Tb), which were obtained from a synthesis in a reverse microemulsion, were directly coated by treatment with TEOS at room temperature.²⁴¹ The thickness of the silica shells increased upon prolongation of reaction time.

6.1. Crystal Size and Morphology

Different strategies have been adopted to manipulate the size and morphology of MOF crystals in the micro/nano regimes (Figure 8). They involve variations that are related to any of the following issues: (1) compositional and process parameters, (2) temperature program, (3) additives, and (4) reverse microemulsions.

Compositional parameters that can be adjusted to manipulate the size and shape of MOF crystals include solvent, pH, metal source, reactant concentration, or molar ratio of the reactants. Process parameters, such as time, temperature, pressure, and heating source, can also have a strong influence on the crystal size and shape. In general, both US and MW synthesis produce relatively small and homogeneous crystals as compared to CE synthesis. Except this, no other general trends can be deduced about the control of crystal size by variation of compositional and process parameters, which have to be fine-tuned for each system in a trial-and-error approach. Temperature programs, which have an influence on the relative nucleation and crystal growth rates, have been also employed to synthesize nanoscale MOFs starting from supersaturated crystallization solutions. Various additives have been tested: thus, polymers can adsorb at certain crystal faces and slow down nucleation rates. Molecular blocking agents have been shown to slow down the crystal growth by adsorption

on certain crystal faces. Capping agents can be used to stop crystal growth, while modulators have been used to control the size and morphology of MOF crystals. The use of modulators relies on the addition of monodentate ligands (modulators), having the same chemical functionality as the multidentate linkers, to the reaction mixture. The modulators compete with the organic linkers in order to coordinate with the metal ions during nucleation and crystal growth. Thus, the size and morphology of the resulting crystals are greatly influenced. Microemulsions are thermodynamically stable mixtures of a hydrophobic liquid, water, and a surfactant, often in the presence of a cosurfactant, often short chain alcohols. They form spontaneously upon mixing of the starting materials. In case the dispersed phase is water and the continuous phase is the organic phase, these mixtures are called reverse microemulsions. The starting materials are usually dissolved in the aqueous phase and the collision between droplets or the application of an external stimulus (temperature, MW or US radiation) induces crystallization. Thus, the nanodroplets act as “nanocontainers”. The size and number of nanodroplets within the microemulsion can be tuned by varying the molar ratio (W) of continuous phase to surfactant. By changing the value of W , the size and morphology of the crystals can be adjusted.

6.1.1. Compositional and Process Parameters. Micro- and nanoscale MOF-5 were prepared in several reports at room temperature or by using CE heating, MW and US irradiation. In the room temperature synthesis, nanoscale (70–90 nm in diameter) MOF-5 and a new phase (100–150 nm in diameter) were produced when triethylamine (TEA) was directly added into a DMF solution containing the reactants.³⁷ Spherical (30–45 nm in diameter) and wire-shaped (~100 nm in diameter) nanocrystals with reduced sizes were synthesized when the direct-mixing approach occurred within a liquid crystalline phase (nonionic surfactant, polyoxyethylene(4) lauryl ether or Brij30) or in the ordered cylindrical channels (diameter 100 nm) of an anodic alumina membrane, respectively. In the CE synthesis of microscale MOF-5, the profound effect of the Zn salt on the morphology of the microcrystals was demonstrated.⁴² Employment of zinc nitrate and zinc oxide led to strongly intergrown big cubic crystals (>100 μm), whereas in the case of zinc acetate, smaller well-defined cubic crystals were formed (<10 μm). This was assigned to the higher nucleation rate when starting with zinc acetate, resulting in higher basicity compared with zinc nitrate, and better solubility of the Zn source compared with zinc oxide. In the MW synthesis of microscale MOF-5 ($4 \pm 1 \mu\text{m}$), both size and regularity of the cubic shaped crystals decreased down to 1 μm by reducing the concentration of H_2BDC in the starting solution.¹¹⁰ By varying the reaction time from 25 s to 1 min, the size of the microcrystals did not change remarkably. The reduction in size has been attributed to the quick depletion of the available reactants during the crystal growth. In another study concerning the MW synthesis of microscale MOF-5 (20–25 μm), the increase in irradiation time, power level, and concentration of the substrates beyond an optimal condition led to a reduction in synthesis time at the expense of crystal quality.¹¹¹ It has been speculated that the excess Zn clusters, formed at increased MW heating time, competes with the BDC linkers in the preformed crystals. Thus, the BDC linkers dissolve back in solution, causing defects in the crystal faces. In the US synthesis of microscale MOF-5 (5–25 μm), the formation of platelike crystals as an impurity was suppressed by increasing the power level.¹⁵⁹ Similar to the MW synthesis of MOF-5,¹¹¹ an increase in

US irradiation time and concentration of the reactants deteriorated the crystal quality. The decrease in crystal quality was attributed to high temperatures generated by the prolonged irradiation time. However, the replacement of the commonly used solvent DEF by low-cost NMP increased the crystal quality. This was ascribed to the higher vapor pressure produced by the more volatile DEF compared to NMP, reducing the intensity of cavitation collapse and hence the resulting temperatures and pressures. In another work, microscale MOF-5 crystals (5–15 μm) were synthesized by using US and MW-assisted heating consecutively, and the results were compared to reaction products obtained by CE heating.¹¹³ In this study, CE heating led to less regularly shaped crystals. The crystal size decreased with increasing ultrasonic bath temperature and sonication time. This was attributed to the combined effects of US and MW irradiation, which promoted uniform and fast nucleation.

Microscale MOF-177 was obtained in a variety of shapes (filaments, rods, needles, cuboids, cubes) using CE heating.²⁴² A low temperature (90 °C) and a short reaction time (24 h) favored the growth of well-dispersed cubic crystals (10–25 μm). A slow cooling rate (0.1 °C min^{-1}) enabled the formation of rod-shaped crystals (length ~ 60 μm , diameter ~ 10 μm) that were less aggregated than those obtained without applying any cooling program. However, a detailed investigation demonstrating the precise control of the morphology was not performed. In another work on MOF-177, the US synthesis yielded microsized crystals (5–20 μm), which were smaller in size compared to those prepared by using CE heating (0.5–1.5 mm) or MW irradiation (5–50 μm).¹¹⁷ The size of the sonochemically synthesized crystals remained invariant to the reaction time. It has been reasoned that the significantly accelerated nucleation in US synthesis quickly depletes the reagent concentration below the critical nucleation concentration.

The influence of the reaction parameters on the crystal size of HKUST-1 was systematically investigated in two reports.^{42,118} The choice of the metal salt has a strong influence on the crystal size. Thus, the use of acetate as the counterion led to smaller crystals, which was related to the change in nucleation rate. Increasing the reaction temperature leads to the formation of Cu_2O as a side product. Only low reaction temperatures (348 K) resulted in octahedrally shaped crystals (~15 μm) while higher temperatures led to crystals with less-defined faces and edges. The overall concentration of the reaction mixtures was also investigated. At low concentrations, intergrowth of truncated octahedral crystals was observed. Intermediate concentrations led to well-defined octahedra and high concentrations to less defined irregular products. In another report, the results of MW and CE syntheses were compared.¹¹⁸ While the crystal size increased at prolonged reaction time in the MW synthesis, the reverse was observed in the CE synthesis. The crystal size also increased in both cases when higher concentrated solutions were used. MW-assisted heating was found to be the method of choice to rapidly synthesize HKUST-1 crystals in the range of 10–20 μm in high yields (~90%) within 60 min.

Nanoscale ZIF-8 (~50 nm) was synthesized in methanol at room temperature, using an excess of HMIIm relative to the Zn source.³⁹ The product contained agglomerated, nonuniform, rhombic dodecahedrally shaped crystals. It was assumed that the excess linker molecules in the protonated form acted as a stabilizing agent for the colloidal particles. Focusing and defocusing of the particle size distribution was observed at earlier and later stages of growth, respectively.⁸⁷ In another

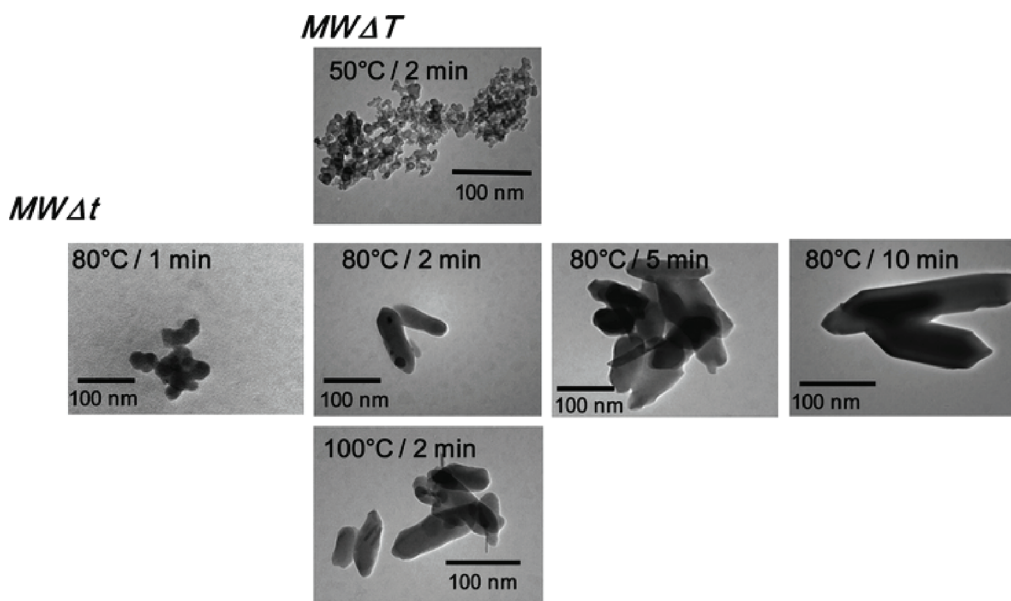


Figure 9. TEM images of Fe–MIL-88A crystals synthesized by MW-assisted heating at various reaction temperatures and reaction times. Reproduced with permission from ref 105. Copyright 2011, Royal Society of Chemistry.

report, nanoscale ZIF-8 (~ 85 nm) was prepared by using a molar ratio HMiM: $\text{Zn}(\text{NO}_3)_2 \cdot 6\text{H}_2\text{O}$ of 70 and replacing methanol by water.²⁴³ Variation of the molar ratio was shown to reduce the crystal size, but it had little effect on the morphology of the crystals. Thus, the size of the crystals decreased from ~ 85 nm to ~ 50 nm when the molar ratio was increased from 70 to 100.

Fe–MIL-53 crystal size varied with the synthesis method applied.⁷⁹ Starting from identical reaction mixtures, CE heating as well as US and microwave irradiation were employed. While CE heating led to large, irregular-shaped crystals of varying size, MW-assisted heating and US radiation resulted in well-shaped crystals with crystal sizes around 1 and $0.5 \mu\text{m}$, respectively.

Nanoscale MIL-88A was synthesized by using various synthesis methods, i.e., static hydro/solvothermal synthesis, dynamic ambient pressure synthesis, sonochemical as well as microwave-assisted hydrothermal conditions.¹⁰⁵ Reaction parameters such as solvent, pH, reaction time, and temperature as well as overall concentration were studied. Optimized reaction conditions yielded relative large crystals for common hydrothermal synthesis (250 nm). Sonochemistry resulted in particles of around 100 nm but only in small yields. The best results were obtained by MW-assisted heating. Particles smaller than 100 nm were obtained in high yield that also showed a narrow particle size distribution (Figure 9).

Nanoscale Cr–MIL-101 was prepared in water using HF and MW-assisted heating.¹⁰² The dimensions of the particles increased (from 40–80 to 70–90 nm) and became more homogeneous in size with increasing reaction time. Later, the researchers avoided the use of HF, and nanocrystals of Cr–MIL-101 with sizes of around 50 nm were obtained by lowering the reactant concentration or increasing the pH of the reaction mixture.¹⁰³ However, the particle size was not affected by the reaction time. The decrease in particle size with lowering of the reactant concentration is not easy to understand, but the authors attributed it to a faster rate of nucleation compared with that of crystal growth. It was also argued that high pH promoted

dissolution and deprotonation of H_2BDC and thus formation of Cr trimers, leading to an increase in nucleation rate and as a consequence to a decrease in particle size.

Microscale PCN-6 and -6' ($1.5\text{--}2 \mu\text{m}$ for PCN-6', $4.5\text{--}6 \mu\text{m}$ for PCN-6), which are formed in the $\text{Cu}^{2+}/\text{TATB}^{3-}/\text{DMF}$ system, increased in size with an increase in sonication power level.¹⁶⁰ A mixture of crystals of two different sizes was obtained at an intermediate power level. It has been proposed that the smaller, larger, and mixed crystal sizes belong to PCN-6' (noncatenated), PCN-6 (catenated), and their mixtures, respectively. A similar effect of the sonication power level was found on the crystal sizes of IRMOF-9 and -10 ($\sim 5\text{--}20 \mu\text{m}$ for both), suggesting that catenation seemingly produced bigger crystals.

6.1.2. Temperature Program. Three studies have dealt with the synthesis of the nanocrystals of IRMOF-1, IRMOF-3, and HKUST-1 by using temperature programs and additives. The nanocrystals of IRMOF-1⁸⁶ and HKUST-1⁸⁵ were synthesized in three steps: (a) incubation of the reaction solution, (b) initiation of nucleation by heating at a high temperature, and (c) initiation of growth by cooling down to low temperature. The combination of faster nucleation (b) and comparatively slow crystal growth (c) for MOF-5 led to homogeneous nanocrystals. However, for HKUST-1, the nucleation continued also at lower temperatures and thus overlapped with the crystal growth. Thus, crystal growth up to 200 nm in particle size within 10 min was observed, but continuous new nucleation was proven by SLS measurements and SEM images.

The influence of the presence of a surfactant (CTAB) to regulate the nucleation was also investigated.²⁴⁴ The steps for the preparation of the monodisperse nanocrystals of IRMOF-1 and -3 with regular shape and uniform size of 200–300 nm included (a) incubation of the reaction solution at a lower temperature, (b) addition of the CTAB to decrease the rate of nucleation, (c) initiation of growth at a higher temperature, and (d) increment of growth rate by adding TEA.²⁴⁴ Step a led to the formation of inorganic building units. Its exclusion led to crystals with poor monodispersity and crystallinity. Nucleation (b) and crystal

growth (c) were influenced by the addition of CTAB as the surfactant, and upon addition of the amine (d), rapid growth was accomplished. Surprisingly, replacing TEA with other amines in step d resulted in products with various crystal shapes. Thus, addition of decylamine or piperidine led to relatively large crystals with rodlike or octahedral shapes, respectively. Lowering the reactant concentration resulted in spherical and flower-shaped crystals.

6.1.3. Additives. The polymer PVSA was added as an additive in different concentrations in the crystallization of $[\text{Cu}_2(\text{PZDC})_2(\text{PYZ})]$ at room temperature to tune the size (mean sizes in the range 1–100 μm) and shape of the resulting crystals (Figure 10).²⁴⁵ Larger crystals have been obtained with an increase in PVSA/ Cu^{2+} molar ratio, which is opposite to the conventional route for size tuning of crystals using additives. The addition of PVSA to the reaction mixture led to a slow rate of nucleation and consequently provided larger crystals. The direction of crystal growth upon addition was also influenced and larger amounts of PVSA resulted in crystal growth parallel to the *ac*-plane and thus to the formation of platelets. The micropore volumes of the products were independent of crystal size. However, the elongation of the 1D channels, which are parallel to the *a*-axis in the larger crystals, decreased the rate of adsorption.

A blocking agent like pyridine was added in the solvothermal synthesis of In–MIL-53 to manipulate the morphology of the micro-sized crystals. The employment of 0, 1, 2, and 25 equiv of pyridine resulted in long rod, short rod, lump, and disk-shaped crystals, respectively.²⁴⁶ It has been argued that control of the crystal shape is achieved through a crystal growth blocking event involving the interaction of blocking agents with particular facets of MOFs and the simultaneous crystal growth interruption in a specific direction. Thus, the crystal growth rate in a certain direction was manipulated by using a variable amount of the blocking agent.

Modulators have been employed to adjust the size and shape of MOF crystals in seven reports.^{86,87,105,247–250} Mostly monocarboxylic acids and their salts were used for the synthesis of metal carboxylates, but N-heterocycles and alkylamines were also employed for the synthesis of ZIFs.

Acetic acid was added as a modulator in the CE synthesis under reflux conditions of nanosized, pillared–layered $[\text{Cu}_2(\text{NDC})_2(\text{DABCO})]$ to control the morphology of the crystals.²⁴⁷ Lower concentration of acetic acid induced rapid crystallization, producing intergrown nanocrystals with low crystallinity. A higher concentration of acetic acid decelerated the rate of crystallization and facilitated the formation of well-dispersed nanorods with high crystallinity. Notably, Cu–NDC and Cu–DABCO interactions predominate in the [100] and [001] directions, respectively, in the tetragonal framework. Acetate ions compete with NDC ions, disturbing Cu–NDC interaction and thus inhibiting crystal growth in the [100] direction. However, Cu–DABCO interaction, which remains unaffected in presence of acetic acid, favors crystal growth in the [001] direction. Therefore, the aspect ratios of the nanorods increased at higher concentration of acetic acid. The formation of the nanorods was shown to be even more complicated, since nanoparticles with a size of around 5 nm, nanocubes with an average size of around 80 nm, and nanorods with different length but diameters of approximately 80 nm were observed (Figure 11). Thus, an oriented attachment mechanism was proposed, in which the initially produced nanoparticles assemble to nanocubes, which subsequently assemble to nanorods at later stages of the reaction. At an optimal concentration of acetic acid, prolongation of reaction

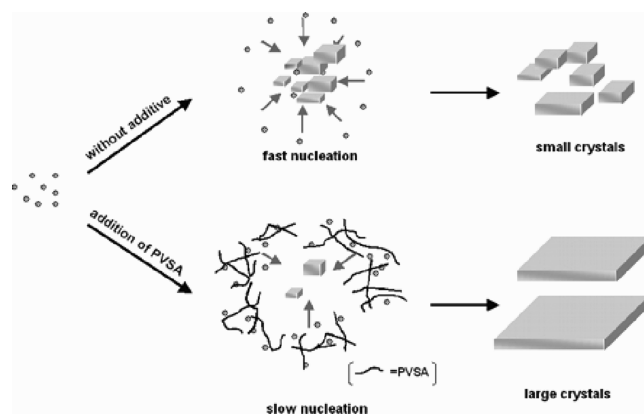


Figure 10. Control of crystal size for the preparation of $[\text{Cu}_2(\text{PZDC})_2(\text{PYZ})]$. Reproduced with permission from ref 245. Copyright 2006 American Chemical Society.

time increased the number of nanocubes and the aspect ratio of the nanorods, demonstrating oriented attachment growth mechanism. This mechanism was also supported by the fact that the aspect ratio of the nanorods increased at higher concentrations of all the reactants.

In the CE synthesis of nanoscale MIL-88A the addition of acetic acid had the reverse effect. The increasing of the concentration resulted in a decrease of particle size.¹⁰⁵

Acetic acid or benzoic acid as a modulator was added to regulate the size and morphology of isoreticular Zr-based MOFs with UiO-66, -67, and -68 structures.²⁴⁸ Without modulation, the MOFs were obtained as micro-sized aggregates of nanocrystals. By adding increasing amounts of the modulator, Zr–BDC samples evolved from aggregated small crystals to separated octahedrally shaped nanocrystals of increasing size. For Zr–BPDC, increasing the amount of the modulator resulted in the formation of individual octahedral microcrystals. Upon addition of suitable amounts of benzoic acid, single crystals of Zr–TPDC– NH_2 were obtained. An increase in the amount of modulator presumably decreased the rate of nucleation, resulting in fewer nuclei and hence larger crystals.

Lauric acid (LA, $\text{C}_{11}\text{H}_{23}\text{COOH}$) was used as a modulator in the MW synthesis of HKUST-1 to tune the size of the crystals in the nano- to microscale range.²⁴⁹ Nanocrystalline powder with less defined morphology was obtained in the absence of the modulator. Lower as well as higher concentrations of LA in butanol (BuOH) led to globular and cubic nanocrystals, respectively. The replacement of LA by acetic acid (AcOH) generated less-defined crystals of different sizes. The change of solvent to ethanol led to highly intergrown nanoparticles, regardless of the modulator (LA or AcOH). Thus, the combination LA/BuOH was selected for further studies. For a given LA/BuOH ratio, lowering of the reactant concentration decreased the sizes of the cubic nanocrystals. At a fixed reactant concentration, increasing the LA content promoted the growth of larger crystals. Small fused nanoparticles, cubic nanocrystals, and cubic microcrystals were received at lower, intermediate, and higher concentrations of LA, respectively. Whereas the higher concentration of LA decelerated the rate of nucleation, leading to larger crystals with greater polydispersity, the reverse was true at lower concentration. This tendency has also been observed using a polymer additive (compare Figure 10).²⁴⁵ The sorption capacity of the small fused nanoparticles or cubic microcrystals was significantly

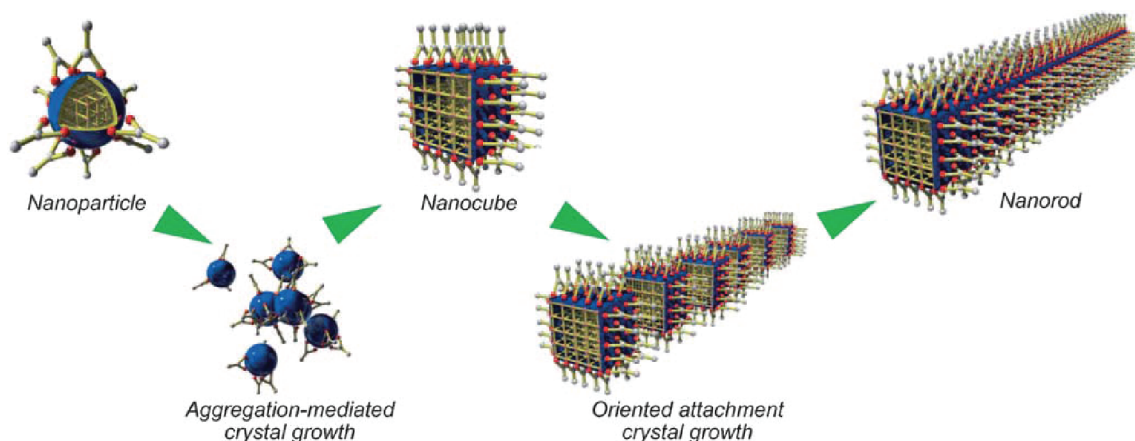


Figure 11. Proposed growth mechanism for $[\text{Cu}_2(\text{NDC})_2(\text{DABCO})]$ nanorods. The growth process of nanocubes is a consequence of nanoparticle aggregation-mediated crystal growth. The selective coordination modulation on the (100) surfaces of the nanocubes induces the oriented attachment leading to the growth of nanorods in the [001] direction. Reproduced with permission from ref 247. Copyright 2009 Wiley-VCH Verlag GmbH & Co. KGaA.

higher than the ill-defined nanocrystalline powder and was comparable to the microcrystals produced by static CE heating. The sudden increase in adsorption at high relative pressure, observed for nanoparticles but absent for microcrystals, was attributed to the condensation of the adsorptive in the space between the nanoparticles (textural porosity).

Sodium carboxylates were used as modulators in the CE synthesis of nanoscale $[\text{Ln}(\text{BTC})(\text{H}_2\text{O})]$ ($\text{Ln} = \text{Dy}, \text{Eu}, \text{Tb}$).²⁵⁰ The crystallinity of the compounds increased in presence of the modulators. Rod-shaped microcrystals were obtained in the absence of the modulators, while the addition of sodium formate resulted in uniform, bean-shaped nanocrystals. Smaller nanocrystals were obtained when sodium acetate was used. However, sodium oxalate led to needle-shaped microcrystals. The influence of the additive on the crystal morphology was not explained.

Ligands with different functionalities (carboxylate, N-heterocycle, and alkylamine) were employed as modulators to tune the size and shape of ZIF-8 crystals. A rapid room-temperature synthesis was developed that allowed the synthesis of nanocrystals (10–65 nm) and microcrystals ($\sim 1 \mu\text{m}$).⁸⁷ The addition of *n*-butylamine to a reaction solution containing excess of the bidentate ligand HMiM resulted in spherical nanocrystals, whereas rhombic dodecahedrally shaped microcrystals were obtained by adding 1-methylimidazole or sodium formate to the same solution. It was surmised that the modulators acted as competitive ligands in the coordination equilibria and that the bases influence the deprotonation equilibria during crystallization. The growth of microcrystals was proposed to be dominated by a particle-monomer attachment mechanism, although coalescence of nanocrystals during early stages of growth is also indicated by the results of the SLS measurements. ZIF-8 nanocrystals exhibited a type-H2 hysteresis loop in the adsorption–desorption isotherm at high relative pressure, originating from interparticle mesopores (textural porosity).

While modulators, which are usually added to the reaction solution from the beginning, influence the crystal growth, other additives, termed as capping agents, prevent the crystal growth.^{105,247,249} Thus, the size of the growing nanocrystals of MOF-5 was adjusted by adding *p*-perfluoromethylbenzoic acid in a supersaturated mother solution at room temperature.⁸⁶

6.1.4. Reverse Microemulsions. CTAB/isooctane/1-hexanol/water microemulsions were used to prepare uniform nanorods of $[\text{Ln}_2(\text{BDC})_3(\text{H}_2\text{O})_4]$ ($\text{Ln} = \text{Eu}, \text{Gd}, \text{Tb}$) at room temperature in 84% yield.²⁵¹ Higher water/CTAB molar ratios led to particles with higher aspect ratios, resulting from a decrease of nucleation sites within the microemulsion droplets. The particle size also decreased with lowering of reactant concentration. Luminescent nanorods were synthesized by using Eu^{3+} and Tb^{3+} ions as dopants in the Gd-based compound. Although a high yield was observed, the method required high volumes of solvents. Moreover, the removal of the surfactants from the nanoparticle surface required harsh conditions or multiple washing steps.

The nonaqueous AOT/*n*-heptane/DMF microemulsion system was employed to synthesize nanorods of $[\text{Zn}(\text{IP})(\text{BPY})]$ at room temperature.²⁵² The compound exhibits a flexible interdigitated layered structure. US irradiation was mandatory to induce fast nucleation in the microemulsion and thus to control the crystal growth. Absence of US irradiation resulted in a gel-like amorphous material. At a molar ratio of DMF to AOT (*W*) of 1, nanocrystals having dimensions of $\sim 300 \text{ nm} \times 50 \text{ nm} \times 15 \text{ nm}$ were observed, which were larger than the microemulsion droplets. The nanoparticle growth was therefore explained by aggregation of the growing nanocrystals followed by the coordination of AOT on the crystal surface, thus changing the crystal growth behavior. The morphology of the particles was unaffected upon variation of reaction time. Increasing *W* led to larger nanorods, but at $W > 3$, nonuniform particles resulted due to instability of the microemulsion. The adsorption properties of the resulting MOFs depend strongly on the synthesis procedure. While the overall adsorption capacity was identical for nanocrystals and bulk microcrystals synthesized using CE heating, the shape of the sorption isotherms varied considerably. This is probably due to the adsorption of surfactant on the crystal surface. At the same time, nanocrystals were shown to exhibit faster adsorption due to shorter diffusion lengths compared to the bulk material.

6.2. Thin Films and Membranes

Various functionalized and nonfunctionalized substrates such as silica, alumina, titania, graphite, or nylon have been used to deposit thin films and membranes. Especially continuous,

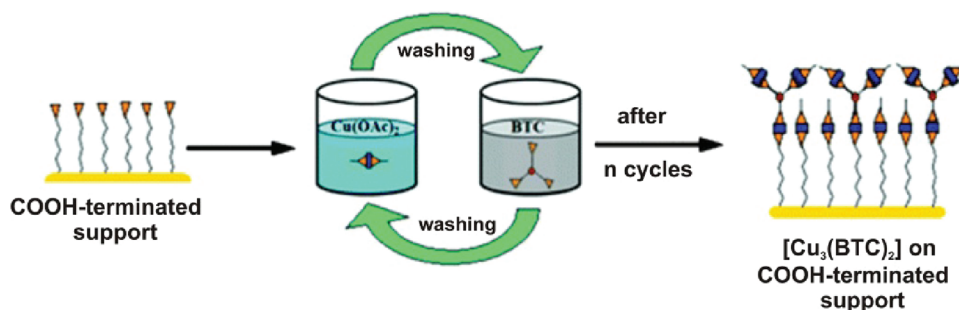


Figure 12. Layer-by-layer growth of HKUST-1 thin films on COOH-terminated support. The substrate is repeatedly immersed in solutions of $\text{Cu}(\text{OAc})_2$ and H_3BTC , with an intermediate washing between successive steps. Reproduced with permission from ref 275. Copyright 2008 Royal Society of Chemistry.

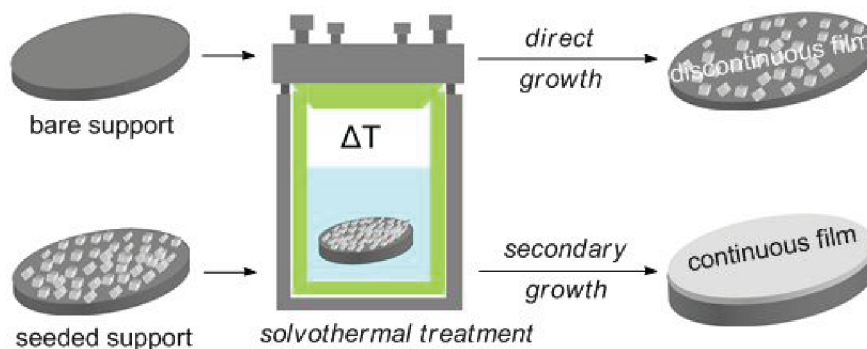


Figure 13. Comparison between direct and secondary growth methods for the preparation of MOF thin films under solvothermal conditions. Immersion of the bare or seeded supports in the reaction solution and subsequent solvothermal treatment lead to discontinuous or continuous films, respectively.

well-intergrown, and oriented films are of interest, which could be useful for efficient gas/liquid separation applications. For the use in sensors, the preparation of patterned films is also of interest.^{136,137,253} Different strategies have been described in the literature to fabricate thin films or membranes of MOFs. These can be categorized as follows: (1) direct growth, (2) layer-by-layer growth, (3) secondary growth, and (4) chemical solution deposition.

Direct growth techniques rely on the immersion of the supports in the reaction solutions containing the metal salts and linkers. Application of CE or MW-assisted heating generates nucleation sites on the supports, thus enabling the growth of crystals on the substrate. These crystals can intergrow to form films having a thickness of several micrometers. Alternatively, supports can be immersed in preheated reaction mixture in which nucleation has occurred and crystallization is about to begin. For both methods, it has been observed that the preparation of continuous thin films on bare substrates is difficult due to poor heterogeneous nucleation. Therefore, chemical modifications of the supports turn out to be indispensable for high quality films.

The layer-by-layer (LBL) approach (Figure 12) for the growth of MOF thin films at room temperature involves repeated cycles of immersion of a substrate in solutions of the metal salt and solutions of organic linker. Between successive deposition steps, the substrate is rinsed with an appropriate solvent to remove unreacted or physisorbed reaction components. Compared to direct growth, the LBL method leads to homogeneous, nanoscale films with precise control of orientation and thickness for each single step. However, the LBL route includes the prefunctionalization of substrates with SAMs,

which is a nontrivial task. Moreover, the repetitive process of immersion/washing cycles is time-consuming. The full description of the method is summarized in several review articles.^{233–235,254}

Secondary or seeded growth offers a better control over thickness and orientation of the film or membrane, compared to direct growth (Figure 13). Prior to secondary growth, the substrate is coated with a seed layer, and the most versatile seeding method is spin- or dip-coating. The seeded supports are then immersed in a reaction solution of the particular MOF, and thin films or membranes on the seeded surface are produced in a procedure similar to direct growth. Due to the pre-existence of nuclei on the support surface, the influence of the surface chemistry is eliminated. More often, secondary growth is used to prepare membranes, since direct growth does not lead to good coverage of crystallites on bare substrates.

The chemical solution deposition route for the preparation of thin films employs stable dispersions of nanocrystals that are spin- or dip-coated on the substrates. Films with increasing thickness can be prepared by multiple depositions. This method is simple, rapid, and cheap. Because of its low-cost and the possibility of large-area processing, this technique is also used in industry.

6.2.1. Direct Growth. Direct growth of MOF thin films was demonstrated on flat substrates, as well as on beads. The substrate-free direct growth at liquid–liquid interface of two immiscible solvents was also shown that resulted in free-standing films and capsules.

Unfunctionalized substrates were used for the direct growth of thin films of only a few MOFs.^{128,255–257} Alumina or graphite was

used as a substrate to grow thin films of $[\text{Mn}(\text{HCO}_2)_2]$.²⁵⁵ Since only poor coverage was observed, Al_2O_3 was treated under basic conditions (NaOH) and graphite was partially oxidized in air. The pretreatment led to even lower crystal densities, but changing the reaction conditions, i.e., replacing formic acid with sodium formate, resulted in an improved coverage due to more favorable electrostatic attraction between oxidized graphite and the $[\text{Mn}(\text{HCO}_2)_2]$ nuclei. SEM images demonstrated the intergrowth of the MOF crystals into the porous graphite. Dense, crack-free films of M-CPO-27 with $\text{M} = \text{Co}^{2+}$, Ni^{2+} , and Mg^{2+} were synthesized by applying the direct growth method on bare alumina.²⁵⁶ When the metal source was changed to Zn^{2+} or Mn^{2+} salts, only large individual crystals were deposited on the surface in a discontinuous fashion. This suggested a strong effect of the nature of the cation on the growth mechanism and binding to the substrate. The influence of the surface chemistry on the crystal growth of the three MOFs $[\text{Zn}_2(\text{BDC})_2(\text{DABCO})]$, MOF-5, and HKUST-1 was also investigated.^{265,266} MOF-5 and HKUST-1 did not grow on unfunctionalized silica but did on nonfunctionalized *c*-sapphire (*c*- Al_2O_3). Compared to silica, *c*-sapphire is more basic and therefore could promote the growth of MOF crystals due to better deprotonation of the carboxylic acids. Changing to ALD-alumina, which is amorphous and more basic compared to silica, increased surface coverage of all the three MOFs. Only $[\text{Zn}_2(\text{BDC})_2(\text{DABCO})]$ could also be grown on silica, probably due to the basic DABCO linkers, which favored H-bonding interactions. The crystals of HKUST-1 showed an oriented growth mode on both *c*-sapphire and COOH-terminated silica. In a report on ZIF-8, a dense, crack-free membrane was deposited on bare titania using the direct growth method and MW irradiation.¹²⁸ The so-called contra-diffusion method was employed in order to fabricate a continuous and compact film of ZIF-8 on an organic polymer as the support. Individual solutions of the metal salt and the linker are separated by a porous nylon membrane, and crystallization occurs on membrane surfaces via diffusion of both starting materials.²⁵⁷ The reactant concentration was systematically varied and the growth was repeated to improve the quality of the film, but only on the zinc nitrate side was a continuous film accomplished.

Modified substrates were more often used for the direct growth of thin films of MOFs.^{114,258–263} MOF-5 films were deposited on porous alumina, which was coated with a thin conductive layer of graphite, under MW irradiation.¹¹⁴ The authors argued that the strong interaction between graphite layer and MW radiation resulted in a rapid temperature increase in alumina, which enhanced direct growth of MOF-5 on alumina. However, oriented but poorly intergrown crystals were produced. In another report on MOF-5, a continuous, well-intergrown MOF-5 membrane was grown on porous α -alumina disk that was treated with a H_2BDC solution prior to solvothermal reaction.²⁵⁸ The use of almost dehydrated zinc nitrate improved the quality of the film, and the crystal size was found to decrease with lowering of the reactant concentration. In a recent study on the direct growth of thin films of MOF-5, the surface of alumina was modified by depositing a drop of a suspension containing α -hopeite $[\text{Zn}_3(\text{PO}_4)_2 \cdot 4(\text{H}_2\text{O})]$ microparticles, which acted as nucleation sites.²⁵⁹ For the direct growth of continuous films of HKUST-1, an oxidized Cu net was used, which provided homogeneous nucleation sites as well as Cu^{2+} ions.²⁶⁰ The syntheses of thin films of ZIFs have been described in four reports. In order to prepare continuous, well-intergrown films of ZIF-7 and -8, sodium formate was added to the reaction mixture to enable the complete deprotonation of the linker molecules.

The α -alumina substrate was pretreated with a solution of the imidazole linker at 200 °C, which resulted in strong covalent bonds between the linker and the substrate.²⁶¹ For the preparation of continuous membranes of ZIF-7, -8, -22, and -90, the titania and α -alumina supports were functionalized with APTES, which created fixed nucleation sites on the supports, acting as covalent linker molecules between the ZIFs and the supports.^{262,263} For ZIF-90, it was hypothesized that the ethoxy groups of APTES reacted first with the hydroxyl groups of alumina, which was followed by the condensation of the amine groups of APTES with the aldehyde groups of imidazole-2-carboxaldehyde.

Surface modification employing SAMs has been extensively used for the direct growth of MOF thin films.^{264–271} Depending on the functional groups of the SAM, oriented growth was observed in most cases. The orientation depends on the crystal structure of the MOFs and specific interactions of the surface with the inorganic bricks or the growing nuclei. However, mostly discontinuous films were obtained. To accomplish direct growth, the SAM-modified substrates were either directly immersed in the reaction mixture or in a filtered preheated solution of the starting materials, which supposedly contained nuclei of the desired MOF phase. In addition, diffusion of the starting materials through a polymer gel was reported.

In the preparation of thin films of MOF-5 on a bifunctional CF_3 -/COOH-terminated Au surface, the crystals grew only on COOH-terminated parts.²⁶⁴ Comparative studies on unfunctionalized, CF_3 - and COOH-terminated Au surfaces revealed that well-adherent films were formed only in the later case. The same group also reported a similar selective growth of films of MOF-5, HKUST-1, and $[\text{Zn}_2(\text{BDC})_2(\text{DABCO})]$ on CF_3 - and COOH-terminated *c*-sapphire and silica.^{265,266} The difference between CF_3 - and COOH-terminated surfaces was attributed to the ability of the latter to mimic the carboxylate-based organic linker. Highly oriented thin films of HKUST-1 were obtained after 8 days at room temperature on a COOH- and OH-terminated Au surface,^{267,268} while the CH_3 -terminated Au substrate yielded nonoriented crystals due to the absence of specific interactions. The same researchers also synthesized highly ordered thin films of MIL-88B on a COOH-terminated Au surface.²⁶⁹ The selective formation of Fe-MIL-88B over Fe-MIL-53 was ascribed to the possible symmetry transfer between hexagonally ordered SAMs and the hexagonal structure of MIL-88B. The growth of CAU-1 on OH-, COOH-functionalized gold surface at room temperature starting from pretreated crystallization solutions was also investigated.²⁷⁰ While oriented growth is independent of the reaction conditions for the COOH-terminated surface, crystal orientation at the OH-terminated SAM can be tuned by changing the synthesis procedure. In a recent report on the synthesis of oriented nanoscale films of HKUST-1 and MIL-88B at room temperature, the same group used the gel-layer approach, in which the gel layer containing the COOH-functionalized Au substrate and the metal salt was covered with the solution containing the linker molecules.²⁷¹ Slow diffusion of the reactants through the gel layer produced thin films on the modified Au surface. The film thickness was adjusted by lowering the reactant concentration.

Patterned films of HKUST-1 have been described in three reports. By modifying the bulk electrochemical synthesis of HKUST-1,⁵² densely packed films of this MOF were grown on a Cu anode, a patterned Cu, or a Cu-coated Au electrode.¹³⁶ The crystal size decreased upon increasing of voltage or lowering of

water content in the synthesis mixture. For the synthesis of a patterned film of HKUST-1 on a nonconducting substrate, the same group has used the galvanic displacement method, which precludes the need of voltage supply and interconnectivity among the metallic patterns as opposed to anodic oxidation.¹³⁷ The spin-coating of a solution containing AgNO₃ and H₃BTC on a Cu surface, patterned on glass, ensured the release of Cu²⁺ ions upon reduction of Ag⁺ ions. Subsequently, the reaction of Cu²⁺ ions with H₃BTC molecules during evaporation of the solvent yielded patterned films. In another study, patterned polydimethylsiloxane stamps were used to generate patterned films of oriented crystals of HKUST-1 by evaporation of the solvent from the reaction mixture confined under the protrusions of the stamp.²⁵³

Beads were also used as substrates. Thin films of SIM-1 and ZIF-7 were grown on α - or γ -alumina beads using the direct growth method.²⁷² SIM-1 is isostructural to ZIF-8 but contains 4-methyl-5-imidazolecarboxaldehyde instead of 2-methylimidazole. Since ZIF-8 crystals did not grow on γ -alumina under similar conditions, it was postulated that the linker in SIM-1 is attached to the alumina surface, probably through bond formation to the C(2)-atom of the linker molecule.

Direct growth at a liquid–liquid interface, termed as interfacial or biphasic synthesis, has led to the formation of thin films and/or hollow capsules of HKUST-1 and ZIF-8.²⁷³ The method takes advantage of the preferential solubility of the metal salts and linkers in water and organic solvents, respectively. Free-standing thin films of HKUST-1 and ZIF-8 were obtained at the interface between two immiscible liquids by layering an organic solution (typically 1-octanol) of the linker on top of the aqueous solution of the metal salt at room temperature. Nucleation occurred at the liquid–liquid interface. For the synthesis of hollow capsules of HKUST-1, aqueous droplets containing the metal salt were added to a coflowing stream of the organic solution of linker flowing through hydrophobic tubing. In this case, nucleation took place inside the droplets. Concentrated solutions of the reactants were used to avoid a reduction in crystallization rate due to reactant depletion near the interface. The selection of copper acetate decreased the preparation time when compared to copper nitrate. The addition of an organic amine base accelerated the MOF formation by deprotonation of the linker. A small amount of the water-soluble emulsifier polyvinyl alcohol, which was added to the interior phase, avoided coalescence of the droplets and was also incorporated in the capsule wall, enhancing mechanical stability of the capsules. Exchanging 1-octanol with cyclohexanol had a negligible influence. However, the addition of ethanol to the aqueous droplets increased the thickness of capsule walls, possibly due to the formation of less well-defined interface as the ethanol diffused out.

6.2.2. Layer-By-Layer Growth. The LBL preparation was developed and demonstrated for thin films of HKUST-1^{88,274–276} and the mixed-ligand, pillared–layered MOFs [M(L₁)(L₂)_{0.5}] (M = Zn, Cu; L₁ = BDC, BDC-F₄, NDC; L₂ = DABCO, BPY).^{231,233} The stepwise formation of HKUST-1 was investigated on differently functionalized SAMs on a Au surface employing SPR spectroscopy. Highly oriented growth was observed for substrates with different functionalization, such as COOH or OH. The growth rate depends on the surface termination as well as the metal source. Copper acetate was observed to be the Cu source of choice, which was explained by the presence of paddle wheel units in the starting solution.⁸⁸ Film growth was also selectively observed on COOH-functionalized

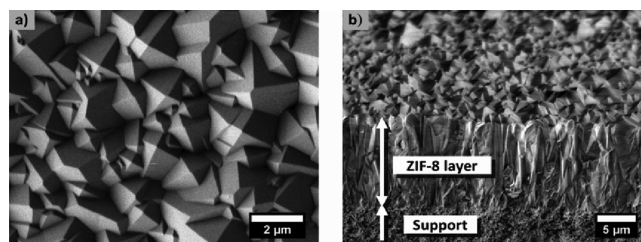


Figure 14. (a) Top- and (b) cross-sectional view the ZIF-8 membrane synthesized by secondary growth technique. Reproduced with permission from ref 278. Copyright 2011 American Chemical Society.

areas of a bifunctional CH₃-/COOH-terminated Au surface.²⁷⁵ Applying the same method, thin films of HKUST-1 were prepared on flexible polyester fabrics.²⁷⁶

Employing the LBL technique, the same group was able to deposit thin films of the highly oriented noncatenated form of [Zn(BDC)(DABCO)_{0.5}], on a pyridyl-terminated Au surface (see section 4.5).²³¹ The isorecticular Zn- and Cu-based compounds with various dicarboxylate ions and dinitrogen pillar ligand molecules were obtained. Surprisingly, the orientation of the film was observed to depend on the sequence of addition of the reactants. In the case of a two-step process, i.e., addition of an equimolar mixture of both ligands, growth along the [001] direction was observed while the three-step process with consecutive addition of all three components resulted in the deposition along the [100] direction on COOH-terminated SAMs.²⁷⁷

6.2.3. Secondary Growth. Several preparative strategies have been developed to deposit a seed layer on the substrate prior to secondary growth. Those are (1) spin- or dip-coating, (2) direct growth, (3) rubbing, and (4) LBL growth.

Spin- or dip-coating of a dispersion of as-synthesized or presynthesized crystals on the substrates can be used to produce a seed layer. For the preparation of seed layers of ZIF-7 and -8, α -alumina was dip-coated with dispersions containing presynthesized nanocrystals and PEI (Figure 14).^{129,278,279} Later, the same group added PEI in the reaction solution during the room temperature synthesis of ZIF-7 to obtain a stable colloidal dispersion, which was dip-coated on alumina.²⁸⁰ PEI supposedly enhanced the attachment between the seeds and the support via H-bonding. In all cases, continuous and oriented membranes were produced. In a study on HKUST-1, dip-coating of an α -alumina substrate in a dispersion of preformed seeds led to poor crystal densities in the resulting membrane.²⁸¹ Spin-coating of the support with a dispersion of a 1D Cu(II)-BTC coordination polymer or an amorphous MOF material, followed by secondary growth, resulted in the formation of HKUST-1 films. These exhibited improved crystal coverage; however, membrane-quality coatings of HKUST-1 were not obtained.

Direct growth, which often leads to poor crystal densities on substrates, can be used to create a seed layer for secondary growth. Thus, repeated direct growth was employed at room temperature for the fabrication of continuous and ordered thin films of [Cu₂(PZDC)₂(PYZ)]²⁸² and ZIF-8.²⁸³ In a similar way, continuous films of MOF-5¹¹⁵ and ZIF-8²⁶¹ were prepared. During secondary growth, the bases EDIPA and sodium formate were added to the starting mixtures of MOF-5 and ZIF-8, respectively. EDIPA led to the deprotonation of H₂BDC and thus prevented dissolution of the MOF-5 seeds. Analogously, sodium formate ensured the complete deprotonation of HMiM in the synthesis of ZIF-8. The same group also prepared hybrid

IRMOF-3/IRMOF-1 films using IRMOF-1 crystals as seeds and adding EDIPA in the reaction solution of IRMOF-3 during secondary growth.²⁸⁴ In another work concerning the preparation of continuous membranes of Al–MIL-53, a uniform seed layer was synthesized on α -alumina, which acted as the inorganic source in the reaction with the organic linker. Secondary growth under hydrothermal reaction conditions led to the formation of homogeneous, crack-free membranes.²⁸⁵

Rubbing the substrate surface with grounded presynthesized crystals can also generate a seed layer. Using this route, discontinuous films of $[\text{Mn}(\text{HCO}_2)_2]^{255}$ and continuous films of ZIF-8²⁸⁶ were obtained after secondary growth. In a study regarding $[\text{Cu}(\text{HFIPBB})(\text{H}_2\text{HFIPBB})_{0.5}]$, the α -alumina surface was modified with PEI before rubbing the seeds on the surface.²⁸⁷ Secondary growth led to well-intergrown and ordered films.

LBL growth can also be applied to prepare a seed layer. Applying this approach, continuous and ordered thin films of $[\text{Cu}(\text{NDC})(\text{DABCO})_{0.5}]$ were formed on bare SiO_2 , Al_2O_3 , Ta_2O_5 , and Si_3N_4 .²⁸⁸ These films were used as a seed layer for the secondary growth of thicker films.

6.2.4. Chemical Solution Deposition. Spin-coating a suspension of presynthesized nanocrystals on ITO glass enabled the preparation of thin films of $[\text{Ln}_{1-x}\text{Tb}_x(\text{BTC})]$.²⁵⁰ The resulting films showed strong luminescence properties. Dip-coating was also used in order to synthesize high-quality optical thin films of Fe–MIL-89,²⁸⁹ Cr–MIL-101,²⁹⁰ and ZIF-8.²⁹¹ In these cases, silicon wafers were dip-coated with colloidal dispersions of as-synthesized or presynthesized nanocrystals. The thickness and density of the ZIF-8 films were tuned by varying the withdrawal speed and the concentration of nanoparticles. For MIL-89, only the use of the trimeric precursor $[\text{Fe}_3\text{O}(\text{OAc})_6(\text{H}_2\text{O})_3]$ in combination with *trans,trans*-muconic acid resulted in stable colloidal dispersions, which was deposited on the surface. The thin films of Cr–MIL-101 or ZIF-8 displayed a dual hierarchical porous structure due to the textural porosity.

Instead of using flat substrates, the inner surface of a silica capillary column was coated with thin films of Cr–MIL-101,²⁹² ZIF-*n* (*n* = 7, 8),²⁹³ and IRMOF-*n* (*n* = 1, 3).²⁹⁴ Suspensions of presynthesized nanocrystals of Cr–MIL-101, the ZIFs, or IRMOFs were first filled into the column under gas pressure and then pushed through the column at a steady speed to leave a wet coating layer on the inner wall. To avoid acceleration of the suspension near the exit of the column, a buffer tube was attached to the column end as a restrictor. Before the GC separation experiments, the columns were treated using different temperature programs.

6.3. Composites

Composites are multicomponent materials comprising multiple different (nongaseous) phase domains in which at least one type of phase domain is a continuous phase.²⁹⁵ They are often used in industrial processes, since the composites combine the properties of the phases and tuning of the properties is possible. Thus, they have been studied, for example, to improve gas sorption properties or in gas separation. In addition, handling of the composites is often easier compared to the crystalline MOFs. Especially in catalysis, composites are of interest since the catalytic activity of the dispersed phase is combined with superior stability of the continuous phase, which also allows the easy recovery of the catalyst.

In the following section composites will be described containing the MOF as the dispersed phase. The sections are organized

according to composites containing an organic (section 6.3.1) and inorganic matrix (section 6.3.2). Monoliths, membranes, fibers, or beads were used as the continuous phase. The section does not cover MOF-based composites where the MOF is the continuous phase. Numerous examples for these kinds of composites have been reported, which include also metals,²⁹⁶ magnetic particles,²⁹⁷ CNTs,²⁹⁸ or polymers²⁹⁹ as the dispersed phase.

6.3.1. MOF–Organic Matrix Composites. Natural and synthetic polymers were used for the formation of composites composed of an organic matrix and MOF crystals.

One study on the use of a monolithic material has been reported. HKUST-1 crystals were deposited within the interconnected voids of a monolithic macroporous hydrophilic poly-HIPE, which was obtained by polymerization of 4-vinylbenzyl chloride and divinylbenzene. Hydrophilization was mandatory to obtain homogenous distribution of the crystals throughout the monolith, which was easily detected by the light blue color of the composite material. The formation of the composite was accomplished by treatment of the activated monolith with the reaction mixture followed by the solvothermal reaction.³⁰⁰ A HKUST-1 monolithic structure (Figure 15a) was also manufactured in a two-step process. Presynthesized crystals were first mixed with a liquid binding agent and a plasticizer in a lab-scale kneader until the molding batch appeared as homogeneous. In a second step, the molding batch was extruded to a monolithic structure.³⁰¹

Synthetic polymer–MOF composite membranes have been investigated using a polyimide (Matrimid) and a polysulfone polymer as the matrix. Composite membranes of MOF-5 and ZIF-8 with Matrimid were prepared by the solution blending approach.^{302–304} A dispersion of preformed MOF-5 or ZIF-8 was added to a solution of Matrimid in CHCl_3 . Dispersion of the MOF crystals was accomplished by sonication. The composite membrane was formed by evaporation of the solvent. Plastic deformation of the composite membrane indicated strong interaction between the polymer matrix and the MOF-5 nanocrystals. Applying the same approach, composite membranes of HKUST-1, MIL-47, MIL-53, and ZIF-8 with Matrimid or polysulfone were also produced.^{305,306} Better quality composite membranes were formed by pretreatment of the MOF crystals with the silylating agent *N*-methyl-*N*-(trimethylsilyl)trifluoroacetamide. In a similar study, ZIF-8–polysulfone membranes were also obtained by the solution blending approach.³⁰⁷ The CO_2 diffusion properties of the composite membranes were studied, and the ZIF-8 crystals were shown to improve the transport of the gas through the membrane.

Synthetic polymer fibers were also employed as the substrate, and the composites were obtained by electrospinning. In the first report, ZIF-8/polyvinylpyrrolidone (PVP) composite nanofibers were synthesized starting from a PVP solution with well-dispersed ZIF-8 nanocrystals (Figure 15b).³⁰⁸ The diameter of the nanofibers in the fiber mat was adjusted by varying the polymer concentration. Using other polymers like polystyrene and polyethylene oxide allowed increasing the fibers' stability. Higher ZIF-8 loadings were achieved by tuning the synthesis parameters and functionalizing the surface of the ZIF-8 nanocrystals with less polar molecules. The second report describes the preparation of MOF/polymer (MOF: HKUST-1, MIL-100; polymer: PS, PVP, polyacrylonitrile, polypropylene) composite fibers with different mechanical stabilities.³⁰⁹ A small difference between particle size and fiber diameter led to a pearl necklace-like morphology with lower MOF loadings. Fortunately, particles in combination with

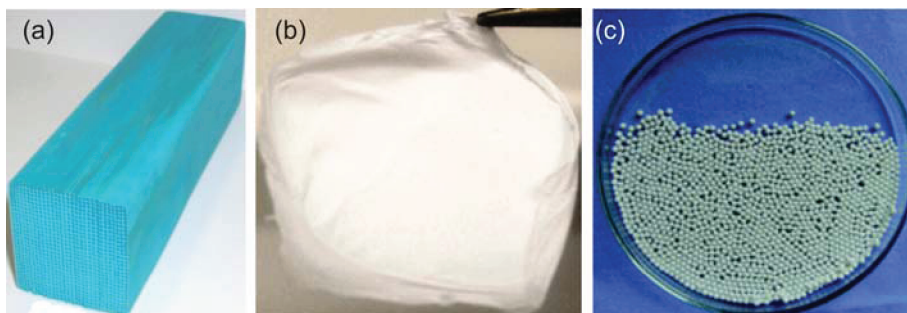


Figure 15. Digital images of (a) HKUST-1 monolith, (b) ZIF-8/PVP fiber mat, and (c) HKUST-1/PAM beads. Reproduced with permissions from ref 301, 308, and 311, respectively. Copyright 2010 American Ceramic Society, 2011 Royal Society of Chemistry, and 2010 Royal Society of Chemistry, respectively.

significantly smaller fibers resulted in a spiderlike morphology at higher MOF loadings.

Natural polymer fibers were also used to form composites. Differently treated pulps were employed. Addition of the crystalline powder of HKUST-1 to the pulp slurry was found to yield an inhomogeneous distribution of the powder.³¹⁰ Pulp fibers with crystals homogeneously distributed over the surface area were obtained by the direct growth method. In these experiments, the degree of coverage increased with increasing lignin contents in the fibers. This was explained by the presence of carboxyl groups in lignin.

PAM beads were used as a matrix, due to their hydrophilicity, in combination with HKUST-1 and Co-CPO-27³¹¹ with the goal to enhance mechanical stability and facilitate handling compared to bulk HKUST-1. Two methods were employed: formation under solvothermal conditions and immersion of the beads into preheated crystallization solutions. Using copper nitrate, HKUST-1/PAM composites (Figure 15c) were synthesized under solvothermal conditions, and the presence of HKUST-1 crystals within the beads was confirmed by SEM images. Preswelling of the beads in an ethanol/water (1:1) mixture prior to solvothermal treatment led to growth of the crystals only on the external surface, indicating a large barrier to diffusion compared to the rate of nucleation and crystal growth. The ratio of MOF:polymer could be adjusted by changing the concentration of the HKUST-1 reaction mixture. The immersion procedure of untreated beads did not lead to the formation of HKUST-1 crystals. Therefore, pretreatment, i.e., preswelling of the PAM beads in a solution of copper acetate, was carried out and led to the formation of HKUST-1/PMA composites. Independent of the pretreatment, solvothermally prepared Co-CPO-27/PAM beads exclusively exhibited crystals on the external surface. In addition to pure organic beads, composite SiO₂/PAM beads were also tested. Applying the immersion method, HKUST-1 crystals were grown on SiO₂/PAM beads.

6.3.2. MOF-Inorganic Matrix Composites. Four different types of inorganic matrices—graphite oxide (GO), silica, alumina, and cordierite or combinations thereof—were employed for the formation of composites.

Two studies were reported on the coating of a cordierite monolith.^{301,312} Uniform coatings of Cr-MIL-101 nanocrystals inside the macropores of a cylindrical cordierite monolith were accomplished by employing the secondary growth technique.³¹² Two methods were employed: (a) a suspension of α -alumina was dip-coated on the substrate prior to seeding with preformed Cr-MIL-101 nanocrystals and (b) the suspension of α -alumina

together with preformed Cr-MIL-101 nanocrystals was dip-coated on the substrate. Dense, uniform coating was observed for optimized reaction conditions, i.e., rotating of the autoclave during the secondary growth step as well as the right choice of the size of seeds and the seeding procedure. The composite was tested in liquid-phase oxidation reactions and showed good stability. In the second study, a cordierite monolith was also used as the substrate.³⁰¹ Solvothermal synthesis of HKUST-1 resulted in low crystal coverage on the cutting edges of the honeycomb structure.

In order to enhance gas adsorption capacities of graphite oxide (GO), composites of MOF-5³¹³ and HKUST-1³¹⁴ were synthesized by dispersing GO in the synthesis mixtures prior to the solvothermal reactions. GO/MOF-5 composites with various ratios of the components were obtained. With increased GO content, a decrease in microporosity was observed. The composites likely adopted lamellar structures constructed from alternating layers of GO and MOF, which was explained by possible interactions between the epoxy groups on graphene and the oxide clusters in MOF-5. GO/HKUST-1 composites were also reported, and the porosity of the composite was claimed to exceed that of the parent materials. Unfortunately, a specific surface of 900 m²/g of HKUST-1 for their material was reported by the authors, which is far below the state of the art values known for HKUST-1. Recently also the formation GO/Fe-MIL-100 composites was also investigated. In these studies increasing amounts of an amorphous phase were observed with higher GO contents.³¹⁵

Using a nonionic surfactant, the formation of hierarchical micro- and mesoporous HKUST-1/alumina and HKUST-1/silica composites was investigated. These were prepared by applying MW irradiation to a dispersion containing starting materials of HKUST-1 and the alumina (boehmite) or silica (TEOS) source together with the triblock copolymer Pluronic P123.³¹⁶ Microporosity as well as mesoporosity could be demonstrated for the composites by sorption experiments, and the presence of HKUST-1 was confirmed by XRPD measurements.

Silica as well as alumina beads were also employed as substrates for the synthesis of HKUST-1 composites. Monodisperse mesoporous silica beads (Nucleosil 100-3) were impregnated with the starting mixture, and the solvent was evaporated.³¹⁷ The monodisperse MOF-silica composites were tested as the HPLC stationary phase and showed good separation properties. In another report,³¹¹ silica and SiO₂/Al₂O₃ composite beads were used. Two methods were employed: formation under solvothermal conditions and immersion of the beads into preheated crystallization solutions. No HKUST-1 growth was detected on silica beads, but growth was observed using mixed SiO₂/Al₂O₃

beads. This was attributed to the more basic properties of the alumina. No information regarding bead surface growth or growth within the macropores of the beads was reported.

7. CONCLUSIONS AND FUTURE PROSPECTS

Although MOF synthesis was originally set out for making new compounds and structures with interesting properties, the field has matured and is broadening its scope. This holds for the synthesis methods applied as well as the areas of application. While conventional syntheses methods have been widely used, the fields of mechano-, sono-, and electrochemical synthesis as well as microwave-assisted syntheses are just emerging. They have demonstrated to be applicable for some compounds, often under milder reaction conditions, yielding materials with different particle sizes and properties. This could be of interest for up-scaling of syntheses and the application of MOFs. However, mainly well-known compounds have been reproduced by these alternative routes, and the reproducibility of the synthesis procedures needs to be established. Great care must be exerted upon the actual input of energy by the different synthetic procedures. Therefore, systematic studies under well-defined conditions need to be performed. High-throughput methods are the ideal tools to accomplish this task, but unfortunately, they are still not well-established in the MOF community. Their extension to the study of other reaction parameters or other synthesis methods would definitely be beneficial. Thus, the reaction temperature can be systematically varied using a gradient oven. This setup could be extended to higher reactions temperatures. While the HT methodology was recently extended to microwave-assisted heating, setups can be envisioned, with different degrees of miniaturization and parallelization, that would even allow the HT investigation using sonochemical or mechanochemical syntheses. A method that has been much neglected, probably due to the complexity of the equipment and the chemistry involved, is the electrochemical synthesis of MOFs. Especially when working at elevated reaction temperatures, this method could lead to new MOFs structures with unusual metals in uncommon oxidation states.

As shown, concepts from other research areas, and especially from zeolite chemistry, have found their way in MOF synthesis, but they need to be extended and pursued in more detail. MOFs offer an even larger playground compared to zeolites. For example, due to the variety of possible organic linkers, some positively as well as negatively charged framework compounds have been obtained. Thus, MOFs can be imagined that contain zwitterionic linker molecules. In addition, the use of charged linkers in combination with structure-directing agents could allow discovery of new compounds. Alternative synthesis methods applied in zeolite synthesis, such as dry-gel or steam-assisted conversion, could be an easy candidate to obtain some of the compounds as recently described for the first time.³¹⁸ While expanding the variety of MOFs, there is also a need to learn more about the formation of these compounds. Systematic studies can help to identify specific parameters, but in situ and ex situ methods comprising various analytical tools in combination with theoretical methods are necessary to study the different stages of crystallization. These studies could not only help to explain the crystallization, but they could even help in the synthesis of metastable polymorphs and/or MOFs with new or improved properties.³¹⁹

A large variety of distinct preparative approaches, such as the use of structure-directing agents, ionic liquids, biphasic solvent mixtures, molecular precursors, or in situ linker synthesis, have been undertaken in the last 2 decades. The modulator approach or reverse microemulsion systems in combination with different energy sources have shown to be useful to tune size and morphology of MOF crystals. Most of these studies have dealt with a few prototypical MOFs. Considering that a wide variety of compounds are available, future investigations must be extended to these and also to the shaping of MOFs with potential applications. In addition to the most-studied thin films and membranes, other shaped composite materials could be envisaged for desired industrial applications.

Finally, we want to raise concern about the comparison of results reported on the synthesis and characterization, especially sorption properties, of MOFs. Great care must be exerted not only to the synthesis but also to the activation and characterization in order to allow for reliable comparisons. Verification of results by different groups such as established in the zeolite synthesis community in the book on “*Verified Synthesis of Zeolites*” would benefit the synthesis community and the groups working on the application of MOFs.³²⁰

AUTHOR INFORMATION

Corresponding Author

*E-mail: stock@ac.uni-kiel.de.

Notes

[†]Dedicated to Prof. Férey on the occasion of his 70th birthday in July 2011.

BIOGRAPHIES



Norbert Stock has received his Ph.D. degree in chemistry with Prof. Schnick in 1998 at the University of Bayreuth and has spent the next 15 months as a postdoc in the groups of Prof. Férey, Prof. Cheetham, and Prof. Stucky at the University of Versailles and University of California at Santa Barbara. In 2000, he joined the group of Prof. Bein at the Ludwig-Maximilians University of Munich, where he finished his habilitation in 2004. In the same year, he became Professor at the Institute of Inorganic Chemistry at the Christian-Albrechts-University in Kiel. His research interests are within the field of inorganic–organic hybrid compounds. He has been involved in the development and application of high-throughput methods for reactions under solvothermal conditions. Thus, he is interested in the discovery of new hybrid

compounds, in understanding their formation, as well as in setting up synthesis–structure relationships.



Shyam Biswas received his M.Sc. in chemistry from Indian Institute Technology Kanpur in 2006. He completed his Ph.D. in 2010 from University of Ulm under the supervision of Prof. Dirk Volkmer in the area of coordination compounds and coordination polymers based on 1,2,3-triazolate ligands. He is currently a postdoc with Prof. Norbert Stock. His research interests include functional coordination compounds, catalytic and gas storage properties of metal–organic frameworks.

ACKNOWLEDGMENT

Deutsche Forschungsgemeinschaft (DFG, SPP 1362 “Porous Metal–Organic Frameworks”, grant agreement no. STO 643/5-2) and European Union (Seventh Framework Programme FP7/2007-2013, grant agreement no. 228862) are gratefully acknowledged for their financial support. The authors thank Tim Ahnfeldt (University of Kiel) and Prof. Paul Wright (University of St. Andrews) for helpful discussions, and Lars-Hendrik Schilling (University of Kiel) for drawing Figures 1 and 8. N.S. thanks Prof. Karl-Petter Lillerud and the research team at the Norwegian National Centre of Research inGAP (University of Oslo) for their hospitality and support during his sabbatical.

LIST OF ACRONYMS AND ABBREVIATIONS

2D	two-dimensional
3D	three-dimensional
AFM	atomic force microscopy
ALD	atomic layer deposition
AOT	dioctyl sulfosuccinate, sodium salt
APTES	3-aminopropyltriethoxysilane
AS	as-synthesized
BBTA	1 <i>H</i> ,5 <i>H</i> -benzo[1,2- <i>d</i> :4,5- <i>d'</i>]bistriazole
BDC	1,4-benzenedicarboxylic acid
BDC-(OH) ₂	2,5-dihydroxybenzenedicarboxylate
BDC-NH ₂	2-aminoterephthalate
BDI	5,5'-(buta-1,3-diyne-1,4-diyl)diisophthalate
BDPB	1,4-bis[(3,5-dimethyl)pyrazol-4-yl]benzene
BET	Brunauer–Emmett–Teller
BIm	benzimidazole
BPDC	4,4'-bipyridinedicarboxylate
BPE	<i>trans</i> -1,2-bis(4-pyridyl)ethylene

BPY	4,4'-bipyridine
BTA	1,2,3-benzotriazole
BTB	benzene-1,3,5-tribenzoate
BTC	1,3,5-benzenetricarboxylate
BTDD	bis(1 <i>H</i> -1,2,3-triazolo[4,5- <i>b</i>],[4',5'- <i>i</i>])dibenzo[1,4]dioxin
BTEC	1,2,4,5-benzenetetracarboxylate
BTT	1,3,5-benzenetristetrazolate
cam	D-camphorate
CAU	Christian-Albrechts University
CDC	9 <i>H</i> -carbazole-3,6-dicarboxylate
CE	conventional electric
CNT	carbon nano tube
CPO	coordination polymer of Oslo
CTAB	cetyltrimethylammonium bromide
DABCO	1,4-diazabicyclo[2.2.2]octane
DACH	1,2-diaminocyclohexane
DEF	<i>N,N'</i> -diethylformamide
DES	deep eutectic solvent
DMA	<i>N,N'</i> -dimethylacetamide
DMF	<i>N,N'</i> -dimethylformamide
DMSO	dimethyl sulfoxide
DPNI	<i>N,N'</i> -di-(4-pyridyl)-1,4,5,8-naphthalene tetracarboxy-diimide
DUT	Dresden University of Technology
EC	electrochemistry
EDIPA	<i>N</i> -ethyl-diisopropylamine
EDXRD	energy-dispersive X-ray diffraction
EI	5-ethynylisophthalate
EIm	2-ethylimidazole
EPR	electron paramagnetic resonance
ESI-MS	electron spray ionization–mass spectrometry
EXAFS	extended X-ray absorption fine structure
FMA	fumarate
GLU	glutarate
GO	graphite oxide
H ₂ HFIPBB	4,4'-(hexafluoroisopropylidene)bis(benzoic acid)
HIP	2-hydroxyisophthalate
HIPE	high internal phase emulsion
HKUST	Hong Kong University of Science and Technology
HPP	1,3,4,6,7,8-hexahydro-2 <i>H</i> -pyrimido[1,2- <i>a</i>]pyrimidine
HT	high-throughput
HTB	<i>s</i> -heptazine tribenzoate
IDS	<i>meso</i> -iminodisuccinate
IL	ionic liquid
ILAG	ion- and liquid-assisted grinding
Im	imidazole
INA	isonicotinate
IP	isophthalate
IRMOF	isoreticular metal–organic framework
L	[(HO ₃ P) ₂ CH–C ₆ H ₄ –CH(PO ₃ H) ₂]
L'	1,3,5-trimethylimidazole-2,4,6-triethylbenzene
LA	lauric acid
LAG	liquid-assisted grinding
LBL	layer-by-layer
LP	large pore
MC	mechanochemistry
MIL	Material of Institute Lavoisier
MIm	2-methylimidazole
MOF	metal–organic framework
MT	5-methyl-1 <i>H</i> -tetrazole

MW	microwave
NDC	2,6-naphthalenedicarboxylate
NMP	N-methyl-2-pyrrolidone
NP	narrow pore
OAc	acetate
OBA	4,4'-oxidibenzoate
OMc	methacrylate
OX	oxalate
PAM	polyacrylamide
PCN	porous coordination network
PEI	polyethyleneimine
POM	polyoxometalate
PS	polystyrene
PVP	polyvinylpyrrolidone
PYDC	2,5-pyridinedicarboxylate
PYMC	2-pyrimidinedicarboxylate
PYZ	pyrazine
PZDC	2,5-pyrazinedicarboxylate
QCMB	quartz crystal microbalance
SAM	self-assembled monolayer
SAXS	small-angle X-ray scattering
SBA	structure-blocking agent
SDA	structure-directing agent
SEM	scanning electron microscopy
SIM	substituted imidazolate-based metal–organic framework
SLS	static light scattering
SPR	surface plasmon resonance
STY	space–time yield
TATB	4,4',4''-s-triazine-2,4,6-triyltribenzoate
TCNQ	7,7,8,8-tetracyano- <i>p</i> -quinodimethane
TEA	triethylamine
TEM	transmission electron microscopy
TEOS	tetraethyl orthosilicate
TG	thermogravimetric
TG–MS	thermogravimetric–mass spectroscopy
TMA	trimethylammonium
TMB	1,3,5-trimethylbenzene
TZ	tetrazolate
UiO	University of Oslo
US	ultrasonic or ultrasound
WAXS	wide-angle X-ray scattering
XANES	X-ray absorption near edge structure
XRPD	X-ray powder diffraction
ZIF	zeolitic imidazolate framework
ZMOF	zeolitic metal–organic framework

REFERENCES

- (1) Kitagawa, S.; Kitaura, R.; Noro, S.-I. *Angew. Chem., Int. Ed.* **2004**, *43*, 2334.
- (2) Rowsell, J. L. C.; Yaghi, O. M. *Microporous Mesoporous Mater.* **2004**, *73*, 3.
- (3) Férey, G. *Chem. Soc. Rev.* **2008**, *37*, 191.
- (4) Janiak, C.; Vieth, J. K. *New J. Chem.* **2010**, *34*, 2366.
- (5) O'Keeffe, M. *Chem. Soc. Rev.* **2009**, *38*, 1215.
- (6) <http://www.merriam-webster.com>.
- (7) Hoskins, B. F.; Robson, R. *J. Am. Chem. Soc.* **1990**, *112*, 1546.
- (8) Cheetham, A. K.; Férey, G.; Loiseau, T. *Angew. Chem. Int. Ed.* **1999**, *38*, 3268.
- (9) Cundy, C. S.; Cox, P. A. *Chem. Rev.* **2003**, *13*, 663.
- (10) Tanabe, K. K.; Cohen, S. M. *Chem. Soc. Rev.* **2011**, *40*, 498.
- (11) Biradha, K.; Ramanan, A.; Vittal, J. J. *Cryst. Growth Des.* **2009**, *9*, 2969.
- (12) Bailar, J. C., Jr. *Prep. Inorg. React.* **1964**, *1*, 1.
- (13) Hoskins, B. F.; Robson, R. *J. Am. Chem. Soc.* **1989**, *111*, 5962.
- (14) Robson, R. *Dalton Trans.* **2008**, 5113.
- (15) Yaghi, O. M.; Li, G.; Li, H. *Nature* **1995**, *378*, 703.
- (16) Yaghi, O. M.; Li, H. *J. Am. Chem. Soc.* **1995**, *117*, 10401.
- (17) Kondo, M.; Yoshitomi, T.; Seki, K.; Matsuzaka, H.; Kitagawa, S. *Angew. Chem., Int. Ed. Engl.* **1997**, *36*, 1725.
- (18) Li, H.; Eddaoudi, M.; O'Keeffe, M.; Yaghi, O. M. *Nature* **1999**, *402*, 276.
- (19) Chui, S. S.-Y.; Lo, S. M.-F.; Charmant, J. P. H.; Orpen, A. G.; Williams, I. D. *Science* **1999**, *283*, 1148.
- (20) Barthelet, K.; Marrot, J.; Riou, D.; Férey, G. *Angew. Chem., Int. Ed.* **2002**, *41*, 281.
- (21) Serre, C.; Millange, F.; Thouvenot, C.; Noguès, M.; Marsolier, G.; Louër, D.; Férey, G. *J. Am. Chem. Soc.* **2002**, *124*, 13519.
- (22) Serre, C.; Mellot-Draznieks, C.; Surblé, S.; Audebrand, N.; Filinchuk, Y.; Férey, G. *Science* **2007**, *315*, 1828.
- (23) Eddaoudi, M.; Kim, J.; Rosi, N.; Vodak, D.; Wachter, J.; O'Keeffe, M.; Yaghi, O. M. *Science* **2002**, *295*, 469.
- (24) Dybtsev, D. N.; Chun, H.; Kim, K. *Angew. Chem., Int. Ed.* **2004**, *43*, 5033.
- (25) Seki, K.; Mori, W. *J. Phys. Chem. B* **2002**, *106*, 1380.
- (26) Tian, Y.-Q.; Cai, C.-X.; Ji, Y.; You, X.-Z.; Peng, S.-M.; Lee, G.-H. *Angew. Chem., Int. Ed.* **2002**, *41*, 1384.
- (27) Park, K. S.; Ni, Z.; Côté, A. P.; Choi, J. Y.; Huang, R.; Uribe-Romo, F. J.; Chae, H. K.; O'Keeffe, M.; Yaghi, O. M. *P. Natl. Acad. Sci. U.S.A.* **2006**, *103*, 10186.
- (28) Dietzel, P. D. C.; Panella, B.; Hirscher, M.; Blom, R.; Fjellvag, H. *Chem. Commun.* **2006**, 959.
- (29) Cavka, J. H.; Jakobsen, S.; Olsbye, U.; Guillou, N.; Lamberti, C.; Bordiga, S.; Lillerud, K. P. *J. Am. Chem. Soc.* **2008**, *130*, 13850.
- (30) Férey, G.; Serre, C.; Mellot-Draznieks, C.; Millange, F.; Surblé, Dutour, S. J.; Margiolaki, I. *Angew. Chem., Int. Ed.* **2004**, *43*, 6296.
- (31) Férey, G.; Mellot-Draznieks, C.; Serre, C.; Millange, F.; Dutour, J.; Surblé, S.; Margiolaki, I. *Science* **2005**, *309*, 2040.
- (32) Dan-Hardi, M.; Serre, C.; Frot, T.; Rozes, L.; Maurin, G.; Sanchez, C.; Férey, G. *J. Am. Chem. Soc.* **2009**, *131*, 10857.
- (33) Ahnfeldt, T.; Guillou, N.; Gunzermann, D.; Margiolaki, I.; Loiseau, T.; Férey, G.; Senker, J.; Stock, N. *Angew. Chem., Int. Ed.* **2009**, *48*, 5163.
- (34) Banerjee, R.; Phan, A.; Wang, B.; Knobler, C.; Furukawa, H.; O'Keeffe, M.; Yaghi, O. M. *Science* **2008**, *319*, 939.
- (35) Byrappa, K.; Yoshimura, M. In *Handbook of Hydrothermal Technology (Materials and Processing Technology)*; Noyes Publications: New York, 2002; Chapter 1.2.
- (36) Rabenau, A. *Angew. Chem., Int. Ed. Engl.* **1985**, *24*, 1026.
- (37) Huang, L.; Wang, H.; Chen, J.; Wang, Z.; Sun, J.; Zhao, D.; Yan, Y. *Microporous Mesoporous Mater.* **2003**, *58*, 105.
- (38) Tranchemontagne, D.; Hunt, J.; Yaghi, O. M. *Tetrahedron* **2008**, *64*, 8553.
- (39) Cravillon, J.; Münzer, S.; Lohmeier, S. J.; Feldhoff, A.; Huber, K.; Wiebcke, M. *Chem. Mater.* **2009**, *21*, 1410.
- (40) Forster, P. M.; Stock, N.; Cheetham, A. K. *Angew. Chem., Int. Ed.* **2005**, *44*, 7608.
- (41) Bauer, S.; Stock, N. *Angew. Chem. Int. Ed.* **2007**, *46*, 6857.
- (42) Biemmi, E.; Christian, S.; Stock, N.; Bein, T. *Microporous Mesoporous Mater.* **2009**, *117*, 111.
- (43) Millange, F.; Osta, R. E.; Medina, M. E.; Walton, R. I. *Cryst. Eng. Commun.* **2011**, *13*, 103.
- (44) Schubert, M.; Müller, U.; Tonigold, M.; Ruetz, R. Patent WO2007/023134 A1.
- (45) Schubert, M.; Müller, U.; Mattenheimer, H.; Tonigold, M. Patent WO2007/023119.
- (46) Jhung, S. H.; Chang, J.-S. Patents KR 0627634; JP 4610531.
- (47) Chang, J.-S.; Hwang, Y. K.; Jhung, S. H.; Hwang, J.-S.; Seo, Y.-K. Patent KR 0803945.

- (48) Chang, J.-S.; Hwang, Y. K.; Jhung, S. H. Patent WO2008/066293 A1.
- (49) Czaja, A. U.; Trukhan, N.; Müller, U. *Chem. Soc. Rev.* **2009**, *38*, 1284.
- (50) Seo, Y.-K.; Yoon, J. W.; Lee, J. S.; Lee, U.-H.; Hwang, Y. K.; Jun, C.-H.; Chang, J.-S.; Serre, C. *Microporous Mesoporous Mater.* **2011** manuscript submitted.
- (51) Wang, Q. M.; Shen, D.; Bülow, M.; Lau, M. L.; Deng, S.; Fitch, F. R.; Lemcoff, N. O.; Semanscin, J. *Microporous Mesoporous Mater.* **2002**, *55*, 217.
- (52) Müller, U.; Schubert, M.; Teich, F.; Pütter, Schierle-Arndt, H. K.; Pastre, J. *J. Mater. Chem.* **2006**, *16*, 626.
- (53) BASF SE, Press release P-10-428; October 5, 2010.
- (54) Gritzner, G.; Kreysa, G. *Pure Appl. Chem.* **1993**, *65*, 1009.
- (55) Available through Sigma-Aldrich, catalogue search, June 12, 2011.
- (56) Mueller, U.; Puetter, H.; Hesse, M.; Wessel, H. WO 2005/049892.
- (57) Chang, J.-S. Korea Research Institute of Chemical Technology, private communication.
- (58) Stock, N. *Microporous Mesoporous Mater.* **2010**, *129*, 287.
- (59) Moliner, M.; Serra, J. M.; Corma, A.; Argente, E.; Valero, S.; Botti, V. *Microporous Mesoporous Mater.* **2005**, *78*, 73.
- (60) Stock, N.; Bein, T. *Angew. Chem., Int. Ed.* **2004**, *43*, 749.
- (61) Sumida, K.; Horike, S.; Kaye, S. S.; Herm, Z. R.; Queen, W. L.; Brown, C. M.; Grandjean, F.; Long, G. J.; Dailly, A.; Long, J. R. *Chem. Sci.* **2010**, *1*, 184.
- (62) Akporiaye, D. E.; Dahl, I. M.; Karlsson, A.; Wendelbo, R. *Angew. Chem., Int. Ed.* **1998**, *37*, 3369.
- (63) Bauer, S.; Serre, C.; Devic, T.; Horcajada, P.; Marrot, J.; Férey, G.; Stock, N. *Inorg. Chem.* **2008**, *47*, 7568.
- (64) Ahnfeldt, T.; Gunzelmann, D.; Loiseau, T.; Hirsemann, D.; Senker, J.; Férey, G.; Stock, N. *Inorg. Chem.* **2009**, *48*, 3057.
- (65) Volkringer, C.; Loiseau, T.; Guillou, N.; Férey, G.; Haouas, M.; Taulelle, F.; Elkaim, E.; Stock, N. *Inorg. Chem.* **2010**, *49*, 9852.
- (66) Reinsch, H.; Krüger, M.; Wack, J.; Senker, J.; Salles, F.; Maurin, G.; Stock, N. *Microporous Mesoporous Mater.* **2011**, DOI: 10.1016/j.micromeso.2011.05.029.
- (67) Sonnauer, A.; Hoffmann, F.; Fröba, M.; Kienle, L.; Duppl, V.; Thommes, M.; Serre, C.; Férey, G.; Stock, N. *Angew. Chem., Int. Ed.* **2009**, *48*, 3791.
- (68) Maniam, P.; Stock, N. *Inorg. Chem.* **2011**, *50*, S085.
- (69) Plabst, M.; Köhn, R.; Bein, T. *CrystEngComm* **2010**, *12*, 1920.
- (70) Chen, B.; Eddaoudi, M.; Hyde, S. T.; O'Keeffe, M.; Yaghi, O. M. *Science* **2001**, *291*, 1021.
- (71) Ma, S.; Sun, D.; Ambrogio, M.; Fillinger, J. A.; Parkin, S.; Zhou, H.-C. *J. Am. Chem. Soc.* **2007**, *129*, 1858.
- (72) Seki, K.; Takamizawa, S.; Mori, W. *Chem. Lett.* **2001**, *30*, 332.
- (73) Chun, H.; Dymbtsev, D. N.; Kim, H.; Kim, K. *Chem.—Eur. J.* **2005**, *11*, 3521.
- (74) Shimizu, G. K. H.; Vaidhyanathan, R.; Taylor, J. M. *Chem. Soc. Rev.* **2009**, *38*, 1430.
- (75) Surblé, S.; Millange, F.; Serre, C.; Férey, G.; Walton, R. I. *Chem. Commun.* **2006**, 1518.
- (76) Rood, J. A.; Boggess, W. C.; Noll, B. C.; Henderson, K. W. *J. Am. Chem. Soc.* **2007**, *129*, 13675.
- (77) Haque, E.; Jeong, J. H.; Jhung, S. H. *CrystEngComm* **2010**, *12*, 2749.
- (78) Khan, N. A.; Haque, Md. M.; Jhung, S. H. *Eur. J. Inorg. Chem.* **2010**, 4975.
- (79) Haque, E.; Khan, N. A.; Park, J. H.; Jhung, S. H. *Chem.—Eur. J.* **2010**, *16*, 1046.
- (80) Venna, S. R.; Jasinski, J. B.; Carreon, M. A. *J. Am. Chem. Soc.* **2010**, *51*, 18033.
- (81) Ahnfeldt, T.; Moellmer, J.; Guillerm, V.; Staudt, R.; Serre, C.; Stock, N. *Chem.—Eur. J.* **2011**, *23*, 6462.
- (82) Millange, F.; Medina, I. M.; Guillou, N.; Férey, G.; Golden, K. M.; Walton, R. I. *Angew. Chem. Int. Ed.* **2010**, *49*, 763.
- (83) Juan-Alcañiz, J.; Goesten, M.; Martinez-Joaristi, A.; Stavitski, E.; Petukhov, A. V.; Gascon, J.; Kapteijn, F. *Chem. Commun.* **2011**, *47*, 8578.
- (84) Stavitski, E.; Goesten, M.; Juan-Alcañiz, J.; Martinez-Joaristi, A.; Serra-Crespo, P.; Petukhov, A. V.; Gascon, J.; Kapteijn, F. *Angew. Chem., Int. Ed.* **2011**, *50*, 9624.
- (85) Zacher, D.; Liu, J. N.; Huber, K.; Fischer, R. A. *Chem. Commun.* **2009**, 1031.
- (86) Hermes, S.; Witte, T.; Hikov, T.; Zacher, D.; Bahnmüller, S.; Langstein, G.; Huber, K.; Fischer, R. A. *J. Am. Chem. Soc.* **2007**, *129*, 5324.
- (87) Cravillon, J.; Nayuk, R.; Springer, S.; Feldhoff, A.; Huber, K.; Wiebcke, M. *Chem. Mater.* **2011**, *23*, 2130.
- (88) Shekhah, O.; Wang, H.; Zacher, D.; Fischer, R. A.; Wöll, C. *Angew. Chem., Int. Ed.* **2009**, *48*, 5038.
- (89) Shoaee, M.; Anderson, M. W.; Attfield, M. P. *Angew. Chem., Int. Ed.* **2008**, *47*, 8525.
- (90) John, N. S.; Scherb, C.; Shoaee, M.; Anderson, M. W.; Attfield, M. P.; Bein, T. *Chem. Commun.* **2009**, 6294.
- (91) Shono, T.; Mingos, D. M. P.; Baghurst, D. R.; Lickiss, P. D. Novel Energy Sources for Reactions. In *The New Chemistry*; Hall, N., Ed.; The Press Syndicate of the University of Cambridge: Cambridge, 2000, Chapter 4.
- (92) Bang, J. H.; Suslick, K. S. *Adv. Mater.* **2010**, *22*, 1039.
- (93) Keskin, S.; Kizilel, S. *Ind. Eng. Chem. Res.* **2011**, *50*, 1799.
- (94) Hafizovic, J.; Bjørgen, M.; Olsbye, U.; Dietzel, P. D. C.; Bordiga, S.; Prestipino, C.; Lamberti, C.; Lillerud, K. P. *J. Am. Chem. Soc.* **2007**, *129*, 3612.
- (95) Kaye, S. S.; Dailly, A.; Yaghi, O. M.; Long, J. R. *J. Am. Chem. Soc.* **2007**, *129*, 14176.
- (96) Mingos, D. M. P.; Baghurst, D. R. *Chem. Soc. Rev.* **1991**, *20*, 1.
- (97) Kappe, C. O.; Dallinger, D.; Murphree, S. In *Practical Microwave Synthesis for Organic Chemists: Strategies, Instruments, and Protocols*; Wiley VCH: Weinheim, 2008.
- (98) Kappe, C. O. *Chem. Soc. Rev.* **2008**, *37*, 1127.
- (99) Klinowski, J.; Paz, F. A. A.; Rocha, J. *Dalton Trans.* **2011**, 40, 321.
- (100) Jhung, S. H.; Lee, J.-H.; Chang, J.-S. *Bull. Korean Chem. Soc.* **2005**, *26*, 880.
- (101) Horcajada, P.; Chalati, T.; Serre, C.; Gillet, B.; Sebrie, C.; Baati, T.; Eubank, J. F.; Heurtaux, D.; Clayette, P.; Kreuz, C.; Chang, J. S.; Hwang, Y. K.; Marsaud, V.; Bories, P. N.; Cynober, L.; Gil, S.; Férey, G.; Couvreur, P.; Gref, R. *Nat. Mater.* **2010**, *9*, 172.
- (102) Jhung, S. H.; Lee, J.-H.; Yoon, J. W.; Serre, C.; Férey, G.; Chang, J.-S. *Adv. Mater.* **2007**, *19*, 121.
- (103) Khan, N. A.; Kang, I. J.; Seok, H. Y.; Jhung, S. H. *Chem. Eng. J.* **2011**, *166*, 1152.
- (104) Taylor-Pashow, K. M. L.; Rocca, J. D.; Xie, Z.; Tran, S.; Lin, W. *J. Am. Chem. Soc.* **2009**, *131*, 14261.
- (105) Chalati, T.; Horcajada, P.; Gref, R.; Couvreur, P.; Serre, C. *J. Mater. Chem.* **2011**, *21*, 2220.
- (106) Centrone, A.; Harada, T.; Speakman, S.; Hatton, T. A. *Small* **2010**, *6*, 1598.
- (107) Centrone, A.; Yang, Y.; Speakman, S.; Bromberg, L.; Rutledge, G. C.; Hatton, T. A. *J. Am. Chem. Soc.* **2010**, *132*, 15687.
- (108) Silva, P.; Valente, A. A.; Rocha, J.; Paz, F. A. A. *Cryst. Growth Des.* **2010**, *10*, 2025.
- (109) Choi, J. Y.; Kim, J.; Jhung, S. H.; Kim, H.-K.; Chang, J.-S.; Chae, H. K. *Bull. Korean Chem. Soc.* **2006**, *27*, 1523.
- (110) Ni, Z.; Masel, R. *J. Am. Chem. Soc.* **2006**, *128*, 12394.
- (111) Choi, J. S.; Son, W. J.; Kim, J.; Ahn, W. S. *Microporous Mesoporous Mater.* **2008**, *116*, 727.
- (112) Lu, C.-M.; Liu, J.; Xiao, K.; Harris, A. T. *Chem. Eng. J.* **2010**, *156*, 465.
- (113) Sabouni, R.; Kazemian, H.; Rohani, S. *Chem. Eng. J.* **2010**, *165*, 966.
- (114) Yoo, Y.; Jeong, H.-K. *Chem. Commun.* **2008**, 2441.
- (115) Yoo, Y.; Lai, Z. P.; Jeong, H.-K. *Microporous Mesoporous Mater.* **2009**, *123*, 100.

- (116) Kim, D. O.; Park, J.; Ahn, G. R.; Jeon, H. J.; Kim, J. S.; Kim, D. W.; Jung, M. S.; Lee, S. W.; Shin, S. H. *Inorg. Chim. Acta* **2011**, *370*, 76.
- (117) Jung, D. W.; Yang, D. A.; Kim, J.; Kim, J.; Ahn, W. S. *Dalton Trans.* **2010**, *39*, 2883.
- (118) Seo, Y.-K.; Hundal, G.; Jang, I. T.; Hwang, Y. K.; Jun, C.-H.; Chang, J.-S. *Microporous Mesoporous Mater.* **2009**, *119*, 331.
- (119) Schlesinger, M.; Schulze, S.; Hietschold, M.; Mehring, M. *Microporous Mesoporous Mater.* **2010**, *132*, 121.
- (120) Khan, N. A.; Haque, E.; Jhung, S. H. *Phys. Chem. Chem. Phys.* **2010**, *12*, 2625.
- (121) Xiang, Z. H.; Cao, D. P.; Shao, X. H.; Wang, W. C.; Zhang, J. W.; Wu, W. Z. *Chem. Eng. Sci.* **2010**, *65*, 3140.
- (122) Jhung, S. H.; Lee, J. H.; Forster, P. M.; Férey, G.; Cheetham, A. K.; Chang, J. S. *Chem.—Eur. J.* **2006**, *12*, 7899.
- (123) Lee, J. S.; Halligudi, S. B.; Jang, N. H.; Hwang, D. W.; Chang, J.-S.; Hwang, Y. K. *Bull. Korean Chem. Soc.* **2010**, *31*, 1489.
- (124) Liu, B.; Zou, R.-Q.; Zhong, R.-Q.; Han, S.; Shioyama, H.; Yamada, T.; Maruta, G.; Takeda, V.; Xu, Q. *Microporous Mesoporous Mater.* **2008**, *111*, 470.
- (125) Liu, H.-K.; Tsao, T.-H.; Zhang, Y.-T.; Lin, C.-H. *CrystEngComm* **2009**, *11*, 1462.
- (126) Wang, X.-F.; Zhang, Y.-B.; Huang, H.; Zhang, J.-P.; Chen, X.-M. *Cryst. Growth Des.* **2008**, *8*, 4559.
- (127) Park, J. H.; Park, S. H.; Jhung, S. H. *J. Korean Chem. Soc.* **2009**, *53*, 553.
- (128) Bux, H.; Liang, F.; Li, Y.; Cravillon, J.; Wiebcke, M.; Caro, J. *J. Am. Chem. Soc.* **2009**, *131*, 16000.
- (129) Li, Y.-S.; Liang, F.-Y.; Bux, H.; Feldhoff, A.; Yang, W.-S.; Caro, J. *Angew. Chem., Int. Ed.* **2010**, *49*, 548.
- (130) Tonigold, M.; Lu, Y.; Bredenkötter, B.; Rieger, B.; Bahn Müller, S.; Hitzbleck, J.; Langstein, G.; Volkmer, D. *Angew. Chem., Int. Ed.* **2009**, *48*, 7546.
- (131) Biswas, S.; Grzywa, M.; Nayek, H. P.; Dehnen, S.; Senkovska, S.; Kaskel, S.; Volkmer, D. *Dalton Trans.* **2009**, 6487.
- (132) Denysenko, D.; Grzywa, M.; Tonigold, M.; Streppel, B.; Krljusz, I.; Hirscher, M.; Mugnaioli, E.; Kolb, U.; Hanss, J.; Volkmer, D. *Chem.—Eur. J.* **2011**, *17*, 1837.
- (133) Bae, Y.-S.; Mulfort, K. L.; Frost, H.; Ryan, P.; Punathanam, S.; Broadbelt, L. J.; Hupp, J. T.; Snurr, R. Q. *Langmuir* **2008**, *24*, 8592.
- (134) Richter, I.; Schubert, M.; Müller, U. Patent WO 2007/131955.
- (135) Hartmann, M.; Kunz, S.; Himsl, D.; Tangermann, O.; Ernst, S.; Wagener, A. *Langmuir* **2008**, *24*, 8634.
- (136) Ameloot, R.; Stappers, L.; Franssaer, J.; Alaerts, L.; Sels, B. F.; De Vos, D. E. *Chem. Mater.* **2009**, *21*, 2580.
- (137) Ameloot, R.; Pandey, L.; Van der Auweraer, M.; Alaerts, L.; Sels, B. F.; De Vos, D. E. *Chem. Commun.* **2010**, *46*, 3735.
- (138) Fernández-Bertran, J. F. *Pure Appl. Chem.* **1999**, *71*, 581.
- (139) Boldyrev, V. V.; Tkacova, K. *J. Mater. Synth. Proc.* **2000**, *8*, 121.
- (140) Kaupp, G. *CrystEngComm* **2009**, *11*, 388.
- (141) Lazuen-Garay, A.; Pichon, A.; James, S. L. *Chem. Soc. Rev.* **2007**, *36*, 846.
- (142) Beyer, M. K.; Clausen-Schaumann, H. *Chem. Rev.* **2005**, *105*, 2921.
- (143) Friščić, T. *J. Mater. Chem.* **2010**, *20*, 7599.
- (144) Pichon, A.; Lazuen-Garay, A.; James, S. L. *CrystEngComm* **2006**, *8*, 211.
- (145) Pichon, A.; James, S. L. *CrystEngComm* **2008**, *10*, 1839.
- (146) Yuan, W.; Lazuen-Garay, A.; Pichon, A.; Clowes, R.; Wood, C. D.; Cooper, A. I.; James, S. L. *CrystEngComm* **2010**, *12*, 4063.
- (147) Klimakow, M.; Klobes, P.; Thünnemann, A. F.; Rademann, K.; Emmerling, F. *Chem. Mater.* **2010**, *22*, 5216.
- (148) Yang, H.; Orefuwa, S.; Goudy, A. *Microporous Mesoporous Mater.* **2011**, *143*, 37.
- (149) Yuan, W.; O'Connor, J.; James, S. L. *CrystEngComm* **2010**, *12*, 3515.
- (150) Beldon, P. J.; Fábíán, L.; Stein, R. S.; Thirumurugan, A.; Cheetham, A. K.; Friščić, T. *Angew. Chem. Int. Ed.* **2010**, *49*, 9640.
- (151) Willans, C. E.; French, S.; Anderson, K. M.; Barbour, L. J.; Gertenbach, J.-A.; Lloyd, G. O.; Dyer, R. J.; Junk, P. C.; Steed, J. W. *Dalton Trans.* **2011**, *40*, 573.
- (152) Friščić, T.; Fábíán, L. *CrystEngComm* **2009**, *11*, 743.
- (153) Fujii, K.; Lazuen-Garay, A.; Hill, J.; Sbircea, E.; Pan, Z.; Xu, M.; Apperley, D. C.; James, S. L.; Harris, K. D. M. *Chem. Commun.* **2010**, *46*, 7572.
- (154) Yuan, W.; Friščić, T.; Apperley, D.; James, S. L. *Angew. Chem., Int. Ed.* **2010**, *49*, 3916.
- (155) Friscic, T.; Reid, D. G.; Halasz, I.; Stein, R. S.; Dinnebier, R. E.; Duer, M. J. *Angew. Chem., Int. Ed.* **2010**, *49*, 712.
- (156) Bang, J. H.; Suslick, K. S. *Adv. Mater.* **2010**, *22*, 1039.
- (157) Mason, T. J.; Peters, D. In *Practical Sonochemistry: Power Ultrasound Uses and Applications*; Horwood Publishing: Chichester, 2003.
- (158) Fillion, H.; Luche, J.-L. In *Synthetic Organic Sonochemistry*; Luche, J.-L., Ed.; Plenum Press: New York, 1998.
- (159) Son, W.-J.; Kim, J.; Kim, J.; Ahn, W.-S. *Chem. Commun.* **2008**, 6336.
- (160) Kim, J.; Yang, S.-T.; Choi, S. B.; Sim, J.; Kim, J.; Ahn, W.-S. *J. Mater. Chem.* **2011**, *21*, 3070.
- (161) Qiu, L.-G.; Li, Z.-Q.; Wu, Y.; Wang, W.; Xu, T.; Jiang, S. *Chem. Commun.* **2008**, 3642.
- (162) Li, Z.-Q.; Qiu, L.-G.; Su, T.; Wu, Y.; Wang, W.; Wu, Z.-Y.; Jiang, X. *Mater. Lett.* **2009**, *63*, 78.
- (163) Khan, N. A.; Jhung, S. H. *Bull. Korean Chem. Soc.* **2009**, *30*, 2921.
- (164) Cundy, C. Y.; Cox, P. A. *Microporous Mesoporous Mater.* **2005**, *82*, 1.
- (165) de Lill, D. T.; Cahill, C. L. *Cryst. Growth Des.* **2007**, *7*, 2390.
- (166) de Lill, D. T.; de Bettencourt-Dias, A.; Cahill, C. L. *Inorg. Chem.* **2007**, *46*, 3960.
- (167) Cahill, C. L.; de Lill, D. T.; Frisch, M. *CrystEngComm* **2007**, *9*, 15.
- (168) Sun, Z. G.; Ren, Y. P.; Long, L. S.; Huang, R. B.; Zheng, L. S. *Inorg. Chem. Commun.* **2002**, *5*, 629.
- (169) Long, P.; Wu, H.; Zhao, Q.; Yang, Y.; Dong, J.; Li, J. *Microporous Mesoporous Mater.* **2011**, *142*, 489.
- (170) Loiseau, T.; Mellot-Drazniéks, C.; Muguerra, H.; Férey, G.; Haouas, M.; Taulelle, F. C. R. *Chim.* **2005**, *8*, 765.
- (171) Senkovska, I.; Hoffmann, F.; Fröba, M.; Getzschmann, J.; Böhlmann, W.; Kaskel, S. *Microporous Mesoporous Mater.* **2009**, *122*, 93.
- (172) Dong, B.-X.; Gu, X.-J.; Xu, Q. *Dalton Trans.* **2010**, *39*, 5683.
- (173) Biemmi, E.; Bein, T.; Stock, N. *Solid State Sci.* **2006**, *8*, 363.
- (174) Burrows, A. D.; Cassar, K.; Friend, R. M. W.; Mahon, M. F.; Rigby, S. P.; Warren, J. E. *CrystEngComm* **2005**, *7*, 548.
- (175) Cooper, E. R.; Andrews, C. D.; Wheatley, P. S.; Webb, P. B.; Wormald, P.; Morris, R. E. *Nature* **2004**, *430*, 1012.
- (176) Parnham, E. R.; Morris, R. E. *Acc. Chem. Res.* **2007**, *40*, 1005.
- (177) Xu, L.; Choi, E. Y.; Kwon, Y. U. *Inorg. Chem.* **2007**, *46*, 10670.
- (178) Zhang, J.; Chen, S.; Bu, X. *Angew. Chem., Int. Ed.* **2008**, *47*, 5434.
- (179) Chen, S. M.; Zhang, J.; Bu, X. H. *Inorg. Chem.* **2008**, *47*, 5567.
- (180) Zhang, J.; Wu, T.; Chen, S.; Feng, P.; Bu, X. H. *Angew. Chem., Int. Ed.* **2009**, *121*, 3538.
- (181) Millange, F.; Serre, C.; Guillou, N.; Férey, G.; Walton, R. I. *Angew. Chem., Int. Ed.* **2008**, *47*, 4100.
- (182) Loiseau, T.; Serre, C.; Huguenard, C.; Fink, G.; Taulelle, F.; Henry, M.; Bataille, T.; Férey, G. *Chem.—Eur. J.* **2004**, *10*, 1373.
- (183) Serre, C.; Férey, G. *Chem. Soc. Rev.* **2009**, *38*, 1380.
- (184) Choi, E.-Y.; Park, K.; Yang, C.-M.; Kim, H.; Son, J.-H.; Lee, S. W.; Lee, Y. H.; Min, D.; Kwon, Y.-U. *Chem.—Eur. J.* **2004**, *10*, 5535.
- (185) Liu, Y. L.; Kravtsov, V.; Larsen, R.; Eddaoudi, M. *Chem. Commun.* **2006**, 1488.
- (186) Fang, Q.-R.; Zhu, G.-S.; Xue, M.; Sun, J.-Y.; Qiu, S.-L. *Dalton Trans.* **2006**, 2399.
- (187) Tian, Y.-Q.; Cai, C.-X.; Ji, J.; You, X.-Z.; Peng, S.-M.; Lee, G.-H. *Angew. Chem., Int. Ed.* **2002**, *41*, 1384.

- (188) Ghosh, S. K.; Zhang, J. -P.; Kitagawa, S. *Angew. Chem., Int. Ed.* **2007**, *46*, 7965.
- (189) Ghosh, S. K.; Bureekaew, S.; Kitagawa, S. *Angew. Chem., Int. Ed.* **2008**, *47*, 3403.
- (190) Bajpe, S. R.; Kirschhock, C. E. A.; Aerts, A.; Breynaert, E.; Absillis, G.; Parac-Vogt, T. N.; Giebel, L.; Martens, J. A. *Chem.—Eur. J.* **2010**, *16*, 3926.
- (191) Bajpe, S. R.; Breynaert, E.; Mustafa, D.; Jobbágy, M.; Maes, A.; Martens, J. A.; Kirschhock, C. E. A. *J. Mater. Chem.* **2011**, *21*, 9768.
- (192) Mustafa, D.; Breynaert, E.; Bajpe, S. R.; Martens, J. A.; Kirschhock, C. E. A. *Chem. Commun.* **2011**, *47*, 8037.
- (193) Xuan-Dong, D.; Vinh-Thang, H.; Kaliaguine, S. *Microporous Mesoporous Mater.* **2011**, *141*, 135.
- (194) Qiu, L.; Xu, T.; Li, Z.; Wu, Y.; Jiang, X.-Y.; Zhang, L.-D. *Angew. Chem.* **2008**, *47*, 9487.
- (195) Devic, T.; Horcajada, P.; Serre, C.; Salles, F.; Maurin, G.; Moulin, B.; Heurtaux, D.; Clet, G.; Vimont, A.; Grenèche, J.-M.; Le Ouay, B.; Moreau, Magnier, E.; Filinchuk, Y.; Marrot, J.; Lavalley, J.-C.; Daturi, M.; Férey, G. *J. Am. Chem. Soc.* **2010**, *132*, 1127.
- (196) Barthelet, K.; Adil, K.; Millange, F.; Serre, C.; Riou, D.; Férey, G. *J. Mater. Chem.* **2003**, *13*, 2208.
- (197) Loiseau, T.; Lecrog, L.; Volkringer, C.; Marrot, J.; Férey, G.; Haouas, M.; Taulelle, F.; Bourrelly, S.; Llewellyn, P. L.; Latroche, M. *J. Am. Chem. Soc.* **2006**, *128*, 10223.
- (198) Horcajada, P.; Surblé, S.; Serre, C.; Hong, D.; Seo, Y.; Chang, J.; Grenèche, J.; Margiolaki, I.; Férey, G. *Chem. Commun.* **2007**, 2820.
- (199) Liu, L.; Wang, X.; Jacobson, A. J. *Dalton Trans.* **2010**, *39*, 1722.
- (200) Hong, D.-Y.; Hwang, Y. K.; Serre, C.; Férey, G.; Chang, J.-S. *Adv. Funct. Mater.* **2009**, *19*, 1537.
- (201) Panella, B.; Hirscher, M. *Adv. Mater.* **2005**, *17*, 538.
- (202) Serre, C.; Millange, F.; Surblé, S.; Férey, G. *Angew. Chem., Int. Ed.* **2004**, *43*, 6285.
- (203) Surblé, S.; Serre, C.; Mellot-Draznieks, C.; Millange, F.; Férey, G. *Chem. Commun.* **2006**, 284.
- (204) Guillermin, V.; Gross, S.; Serre, C.; Devic, T.; Bauer, M.; Férey, G. *Chem. Commun.* **2010**, *46*, 767.
- (205) Hausdorf, S.; Baitalow, F.; Böhle, T.; Rafaja, D.; Mertens, F. O. R. L. *J. Am. Chem. Soc.* **2010**, *132*, 10978.
- (206) Li, J. R.; Timmons, D. J.; Zhou, H. C. *J. Am. Chem. Soc.* **2009**, *131*, 6368.
- (207) Wang, X. L.; Qin, C.; Wu, S. X.; Shao, K. Z.; Lan, Y. Q.; Wang, S.; Zhu, D. X.; Su, Z. M.; Wang, E. B. *Angew. Chem., Int. Ed.* **2009**, *48*, 5291.
- (208) Bai, Y.-L.; Tao, J.; Huang, R.-B.; Zheng, L.-S. *Angew. Chem., Int. Ed.* **2008**, *47*, 5344.
- (209) Tranchemontagne, D. J.; Mendoza-Cortés, J. L.; O’Keeffe, M.; Yaghi, O. M. *Chem. Soc. Rev.* **2009**, *38*, 1257.
- (210) Zhang, X.-M. *Coord. Chem. Rev.* **2005**, *249*, 1201.
- (211) Volkringer, C.; Loiseau, T.; Férey, G.; Morais, C. M.; Taulelle, F.; Montouillout, V.; Massiot, D. *Microporous Mesoporous Mater.* **2007**, *105*, 111.
- (212) Volkringer, C.; Loiseau, T. *Mater. Res. Bull.* **2006**, *41*, 948.
- (213) Volkringer, C.; Popov, D.; Loiseau, T.; Férey, G.; Burghammer, M.; Riekel, C.; Haouas, M.; Taulelle, F. *Chem. Mater.* **2009**, *21*, 5695.
- (214) Zhang, J.-Y.; Cheng, A.-L.; Yue, Q.; Sun, W.-W.; Gao, E.-Q. *Chem. Commun.* **2008**, 847.
- (215) Debatin, F.; Thomas, A.; Kelling, A.; Hedin, N.; Bacsik, Z.; Senkovska, I.; Kaskel, S.; Junginger, M.; Müller, H.; Schilde, U.; Jäger, C.; Friedrich, A.; Holdt, H.-J. *Angew. Chem., Int. Ed.* **2010**, *49*, 1258.
- (216) Zhao, H.; Qu, Z. R.; Ye, H. Y.; Xiong, R. G. *Chem. Soc. Rev.* **2008**, *37*, 84.
- (217) Qiu, Y. C.; Deng, H.; Mou, J. X.; Yang, S. H.; Zeller, M.; Batten, S. R.; Wu, H. H.; Li, J. *Chem. Commun.* **2009**, 5415.
- (218) Zhong, D.-C.; Lu, W.-G.; Jiang, L.; Feng, X.-L.; Lu, T.-B. *Cryst. Growth Des.* **2010**, *10*, 739.
- (219) Zhong, D. C.; Lin, J. B.; Lu, W. G.; Jiang, L.; Lu, T. B. *Inorg. Chem.* **2009**, *48*, 8656.
- (220) Nadeem, M. A.; Thornton, A. W.; Hill, M. R.; Stride, J. A. *Dalton Trans.* **2011**, *40*, 3398.
- (221) Ma, D.; Wang, W.; Li, Y.; Li, J.; Daiguebonne, C.; Calvez, G.; Guillou, O. *CrystEngComm* **2010**, *12*, 4372.
- (222) Ma, S.; Wang, X.-S.; Yuan, D.; Zhou, H.-C. *Angew. Chem., Int. Ed.* **2008**, *47*, 4130.
- (223) Zhao, D.; Yuan, D. Q.; Yakovenko, A.; Zhou, H.-C. *Chem. Commun.* **2010**, *46*, 4196.
- (224) Gould, J. A.; Bacsá, J.; Park, H.; Claridge, J. B.; Fogg, A. M.; Ramanathan, V.; Warren, J. E.; Rosseinsky, M. J. *Cryst. Growth Des.* **2010**, *10*, 2977.
- (225) Han, S. S.; Mendoza-Cortés, J. L.; Goddard, W. A., III. *Chem. Soc. Rev.* **2009**, *38*, 1460.
- (226) Eddaoudi, M.; Kim, J.; Rosi, N. L.; Vodak, D. T.; Wachter, J.; O’Keeffe, M.; Yaghi, O. M. *Science* **2002**, *295*, 469.
- (227) Zhang, J. J.; Wojtas, L.; Larsen, R. W.; Eddaoudi, M.; Zaworotko, M. J. *J. Am. Chem. Soc.* **2009**, *131*, 17040.
- (228) Chen, B.; Wang, X.; Zhang, Q.; Xi, X.; Cai, J. W.; Qi, H.; Shi, S. H.; Wang, J.; Yuan, D.; Fang, M. *J. Mater. Chem.* **2010**, *20*, 3758.
- (229) Kim, H.; Das, S.; Kim, M. G.; Dybtsev, D. N.; Kim, Y.; Kim, K. *Inorg. Chem.* **2011**, *50*, 3691.
- (230) Ma, S.; Sun, D.; Ambrogio, M.; Fillinger, J. A.; Parkin, S.; Zhou, H.-C. *J. Am. Chem. Soc.* **2007**, *129*, 1858.
- (231) Shekhah, O.; Wang, H.; Paradinas, M.; Ocal, C.; Schupbach, B.; Terfort, A.; Zacher, D.; Fischer, R. A.; Wöll, C. *Nat. Mater.* **2009**, *8*, 481.
- (232) Renzo, F. D. *Catal. Today* **1998**, *41*, 37.
- (233) Shekhah, O.; Liu, J.; Fischer, R. A.; Wöll, C. *Chem. Soc. Rev.* **2011**, *40*, 1081.
- (234) Zacher, D.; Shekhah, O.; Wöll, C.; Fischer, R. A. *Chem. Soc. Rev.* **2009**, *38*, 1418.
- (235) Zacher, D.; Schmid, R.; Wöll, C.; Fischer, R. A. *Angew. Chem., Int. Ed.* **2011**, *50*, 176.
- (236) Gascon, J.; Kapteijn, F. *Angew. Chem., Int. Ed.* **2010**, *49*, 1530.
- (237) Della Rocca, J.; Lin, W. *Eur. J. Inorg. Chem.* **2010**, 3725.
- (238) Taylor-Pashow, K. M. L.; Rocca, J. D.; Huxford, R. C.; Lin, W. *Chem. Commun.* **2010**, *46*, 5832.
- (239) Lohe, M.; Rose, M.; Kaskel, S. *Chem. Commun.* **2009**, 6056.
- (240) Rowe, M. D.; Thamm, D. H.; Kraft, S. L.; Boyes, S. G. *Biomacromolecules* **2009**, *10*, 983.
- (241) Rieter, W. J.; Taylor, K. M.; Lin, W. *J. Am. Chem. Soc.* **2007**, *129*, 9852.
- (242) Li, X.; Cheng, F.; Zhang, S.; Chen, J. *J. Power Sources* **2006**, *160*, 542.
- (243) Pan, Y.; Liu, Y.; Zeng, G.; Zhao, L.; Lai, Z. *Chem. Commun.* **2011**, *47*, 2071.
- (244) Ma, M.; Zacher, D.; Zhang, X.; Fischer, R. A.; Metzler-Nolte, N. *Cryst. Growth Des.* **2011**, *11*, 185.
- (245) Uemura, T.; Hoshino, Y.; Kitagawa, S. *Chem. Mater.* **2006**, *18*, 992.
- (246) Cho, W.; Lee, H.-J.; Oh, M. *J. Am. Chem. Soc.* **2008**, *130*, 16943.
- (247) Tsuruoka, T.; Furukawa, S.; Takashima, Y.; Yoshida, K.; Isoda, S.; Kitagawa, S. *Angew. Chem., Int. Ed.* **2009**, *48*, 4739.
- (248) Schaate, A.; Roy, P.; Godt, A.; Lippke, J.; Waltz, F.; Wiebecke, M.; Behrens, P. *Chem.—Eur. J.* **2011**, *17*, 6643.
- (249) Diring, S.; Furukawa, S.; Takashima, Y.; Tsuruoka, T.; Kitagawa, S. *Chem. Mater.* **2010**, *22*, 4531.
- (250) Guo, H. L.; Zhu, Y. Z.; Qiu, S. L.; Lercher, J. A.; Zhang, H. J. *Adv. Mater.* **2010**, *22*, 4190.
- (251) Rieter, W. J.; Taylor, K. M. L.; An, H.; Lin, W.; Lin, W. *J. Am. Chem. Soc.* **2006**, *128*, 9024.
- (252) Tanaka, D.; Henke, A.; Albrecht, K.; Moeller, M.; Nakagawa, K.; Kitagawa, S.; Groll, J. *Nat. Chem.* **2010**, *2*, 410.
- (253) Ameloot, R.; Gobechiya, E.; Uji-i, H.; Martens, J. A.; Hofkens, J.; Alaerts, L.; Sels, B. F.; De Vos, D. E. *Adv. Mater.* **2010**, *22*, 2685.
- (254) Shekhah, O. *Materials* **2010**, *3*, 1302.

- (255) Arnold, M.; Kortunov, P.; Jones, D. J.; Nedellec, Y.; Karger, J.; Caro, J. *Eur. J. Inorg. Chem.* **2007**, 60.
- (256) Bétard, A.; Zacher, D.; Fischer, R. A. *CrystEngComm* **2010**, *12*, 3678.
- (257) Yao, J.; Dong, D.; Li, D.; He, L.; Xu, G.; Wang, H. *Chem. Commun.* **2011**, 47, 2559.
- (258) Liu, Y.; Ng, Z.; Khan, E. A.; Jeong, H.-K.; Ching, C.-b.; Lai, Z. *Microporous Mesoporous Mater.* **2009**, *118*, 296.
- (259) Falcaro, P.; Hill, A. J.; Nairn, K. M.; Jasieniak, J.; Mardel, J. L.; Bastow, T. J.; Mayo, S. C.; Gimona, M.; Gomez, D.; Whitfield, H. J.; Riccò, R.; Patelli, A.; Marmiroli, B.; Amenitsch, H.; Colson, T.; Villanova, L.; Buso, D. *Nat. Commun.* **2011**, *2*, 1.
- (260) Guo, H. L.; Zhu, G. S.; Hewitt, I. J.; Qiu, S. L. *J. Am. Chem. Soc.* **2009**, *131*, 1646.
- (261) McCarthy, M. C.; Varela-Guerrero, V.; Barnett, G. V.; Jeong, H.-K. *Langmuir* **2010**, *26*, 14636.
- (262) Huang, A.; Bux, H.; Steinbach, F.; Caro, J. *Angew. Chem.* **2010**, *49*, 4958.
- (263) Huang, A.; Dou, W.; Caro, J. *J. Am. Chem. Soc.* **2010**, *132*, 15562.
- (264) Hermes, S.; Schröder, F.; Chelmoski, R.; Wöll, C.; Fischer, R. A. *J. Am. Chem. Soc.* **2005**, *127*, 13744.
- (265) Hermes, S.; Zacher, D.; Baunemann, A.; Wöll, C.; Fischer, R. A. *Chem. Mater.* **2007**, *19*, 2168.
- (266) Zacher, D.; Baunemann, A.; Hermes, S.; Fischer, R. A. *J. Mater. Chem.* **2007**, *17*, 2785.
- (267) Biemmi, E.; Scherb, C.; Bein, T. *J. Am. Chem. Soc.* **2007**, *129*, 8054.
- (268) Biemmi, E.; Darga, A.; Stock, N.; Bein, T. *Microporous Mesoporous Mater.* **2008**, *113*, 380.
- (269) Scherb, C.; Schödel, A.; Bein, T. *Angew. Chem., Int. Ed.* **2008**, *47*, 5777.
- (270) Hinterholzinger, F.; Scherb, C.; Ahnfeldt, T.; Stock, N.; Bein, T. *Phys. Chem. Chem. Phys.* **2010**, *12*, 4515.
- (271) Schödel, A.; Scherb, C.; Bein, T. *Angew. Chem., Int. Ed.* **2010**, *49*, 7225.
- (272) Aguado, S.; Canivet, J.; Farrusseng, D. *Chem. Commun.* **2010**, *46*, 7999.
- (273) Ameloot, R.; Vermoortele, F.; Vanhove, W.; Roefiaers, M. B. J.; Sels, B. F.; Vos, D. E.; De Nat. *Mater.* **2011**, *3*, 382.
- (274) Shekhah, O.; Wang, H.; Kowarik, S.; Schreiber, F.; Paulus, M.; Tolan, M.; Sternemann, C.; Evers, F.; Zacher, D.; Fischer, R. A.; Wöll, C. *J. Am. Chem. Soc.* **2007**, *129*, 15118.
- (275) Munuera, C.; Shekhah, O.; Wang, H.; Woll, C.; Ocal, C. *Phys. Chem. Chem. Phys.* **2008**, *10*, 7257.
- (276) Meilikhov, M.; Yusenko, K.; Schollmeyer, E.; Mayer, C.; Buschmann, H.-J.; Fischer, R. A. *Dalton Trans.* **2011**, 40, 4838.
- (277) Zacher, D.; Yusenko, K.; Bétard, A.; Henke, S.; Molon, M.; Ladnorg, T.; Shekhah, O.; Schüpbach, B.; de los Arcos, T.; Krasnopolski, M.; Meilikhov, M.; Winter, J.; Terfort, A.; Wöll, C.; Fischer, R. A. *Chem.—Eur. J.* **2011**, *17*, 1448.
- (278) Bux, H.; Feldhoff, A.; Cravillon, J.; Wiebcke, M.; Li, Y.-S.; Caro, J. *Chem. Mater.* **2011**, *23*, 2262.
- (279) Li, Y.; Liang, F.; Bux, H.; Yang, W.; Caro, J. *J. Membr. Sci.* **2010**, *354*, 48.
- (280) Li, Y. S.; Bux, H.; Feldhoff, A.; Li, G. L.; Yang, W. S.; Caro, J. *Adv. Mater.* **2010**, *22*, 3322.
- (281) Gascon, J.; Aguado, S.; Kapteijn, F. *Microporous Mesoporous Mater.* **2008**, *113*, 132.
- (282) Kubo, M.; Chaikittisilp, W.; Okubo, T. *Chem. Mater.* **2008**, *20*, 2887.
- (283) Lu, G.; Hupp, J. T. *J. Am. Chem. Soc.* **2010**, *132*, 7832.
- (284) Yoo, Y.; Jeong, H.-K. *Cryst. Growth Des.* **2010**, *10*, 1238.
- (285) Hu, Y.; Dong, X.; Nan, J.; Jin, W.; Ren, X.; Xua, N.; Lee, Y. M. *Chem. Commun.* **2011**, 47, 737.
- (286) Venna, S. R.; Carreon, M. A. *J. Am. Chem. Soc.* **2010**, *132*, 76.
- (287) Ranjan, R.; Tsapatsis, M. *Chem. Mater.* **2009**, *21*, 4920.
- (288) Yusenko, K.; Meilikhov, M.; Zacher, D.; Wieland, F.; Sternemann, C.; Stammer, X.; Ladnorg, T.; Wöll, C.; Fischer, R. A. *CrystEngComm* **2010**, *12*, 2086.
- (289) Horcajada, P.; Serre, C.; Grosso, D.; Boissière, C.; Perruchas, S.; Sanchez, C.; Férey, G. *Adv. Mater.* **2009**, *21*, 1931.
- (290) Demessence, A.; Horcajada, P.; Serre, C.; Boissière, C.; Grosso, D.; Sanchez, C.; Férey, G. *Chem. Commun.* **2009**, 7149.
- (291) Demessence, A.; Boissière, C.; Grosso, D.; Horcajada, P.; Serre, C.; Férey, G.; Soler-Illia, G. J. A. A.; Sanchez, C. *J. Mater. Chem.* **2010**, *20*, 7676.
- (292) Gu, Z.-Y.; Yan, X.-P. *Angew. Chem., Int. Ed.* **2010**, *49*, 1477.
- (293) Chang, N.; Gu, Z.-Y.; Yan, X.-P. *J. Am. Chem. Soc.* **2010**, *132*, 13645.
- (294) Gu, Z.-Y.; Jiang, J.-Q.; Yan, X.-P. *Anal. Chem.* **2011**, *83*, 5093.
- (295) Work, W. J.; Horie, K.; Hes, M.; Stepto, R. F. T. *Pure Appl. Chem.* **2004**, *76*, 1985.
- (296) Hermes, S.; Schröter, M.-K.; Schmid, R.; Khodeir, L.; Muhler, M.; Tissler, A.; Fischer, R. W.; Fisher, R. A. *Angew. Chem., Int. Ed.* **2005**, *44*, 6237.
- (297) Lohe, M. R.; Gedrich, K.; Freudenberg, T.; Kockrick, E.; Dellmann, T.; Kaskel, S. *Chem. Commun.* **2011**, 47, 3075.
- (298) Yang, S. J.; Choi, J. Y.; Chae, H. K.; Cho, J. H.; Nahm, K. S.; Park, C. R. *Chem. Mater.* **2009**, *21*, 1893.
- (299) Uemura, T.; Yanai, N.; Kitagawa, S. *Chem. Soc. Rev.* **2009**, *38*, 1228.
- (300) Schwab, M. G.; Senkovska, I.; Rose, M.; Koch, M.; Pahnke, J.; Jonschker, G.; Kaskel, S. *Adv. Eng. Mater.* **2008**, *10*, 1151.
- (301) Küsgens, P.; Zgaverdea, A.; Fritz, H.-G.; Siegle, S.; Kaskel, S. *J. Am. Ceram. Soc.* **2010**, *93*, 2476.
- (302) Perez, E. V.; Balkus, K. J., Jr.; Ferraris, J. P.; Musselman, I. H. *J. Membr. Sci.* **2009**, *328*, 165.
- (303) Ordoñez, M. J. C.; Balkus, K. J., Jr.; Ferraris, J. P.; Musselman, I. H. *J. Membr. Sci.* **2010**, *361*, 165.
- (304) Ordoñez, M. J. C.; Balkus, K. J., Jr.; Ferraris, J. P.; Musselman, I. H. *J. Membr. Sci.* **2010**, *361*, 165.
- (305) Basu, S.; Cano-Odena, A.; Vankelecom, I. F. J. *J. Membr. Sci.* **2010**, *362*, 478.
- (306) Basu, S.; Maes, M.; Cano-Odena, A.; Alaerts, L.; De Vos, D. E.; Vankelecom, I. F. J. *J. Membr. Sci.* **2009**, *344*, 190.
- (307) Díaz, G.; Garrido, L.; López-González, M.; Castillo, L. F.; del Riande, E. *Macromolecules* **2010**, *43*, 316.
- (308) Ostermann, R.; Cravillon, J.; Weidmann, C.; Wiebcke, M.; Smarsly, B. M. *Chem. Commun.* **2011**, 47, 442.
- (309) Rose, M.; Bohringer, B.; Jolly, M.; Fischer, R.; Kaskel, S. *Adv. Eng. Mater.* **2011**, *13*, 356.
- (310) Küsgens, P.; Siegle, S.; Kaskel, S. *Adv. Eng. Mater.* **2009**, *11*, 93.
- (311) O'Neill, L. D.; Zhang, H.; Bradshaw, D. *J. Mater. Chem.* **2010**, *20*, 5720.
- (312) Ramos-Fernandez, E. V.; Garcia-Domingos, M.; Juan-Alcañiz, J.; Gascon, J.; Kapteijn, F. *Appl. Catal., A* **2011**, *391*, 261.
- (313) Petit, C.; Bandosz, T. J. *Adv. Mater.* **2009**, *21*, 4753.
- (314) Petit, C.; Burrell, J.; Bandosz, T. J. *Carbon* **2011**, *49*, 563.
- (315) Petit, C.; Bandosz, T. J. *Adv. Funct. Mater.* **2011**, *21*, 2108.
- (316) Górka, J.; Fulvio, P. F.; Pikus, S.; Jaroniec, M. *Chem. Commun.* **2010**, 6798.
- (317) Ameloot, R.; Liekens, A.; Alaerts, L.; Maes, M.; Galarneau, A.; Coq, B.; Desmet, G.; Sels, B. F.; Denayer, J. F. M.; De Vos, D. E. *Eur. J. Inorg. Chem.* **2010**, 3735.
- (318) Shi, Q.; Chen, Z.; Song, Z.; Li, J.; Dong, J. *Angew. Chem., Int. Ed.* **2011**, *50*, 672.
- (319) Pienack, N.; Bensch, W. *Angew. Chem., Int. Ed.* **2011**, *50*, 2014.
- (320) Robson, H. In *Verified Synthesis of Zeolites*; Lillerud, K. P., Ed.; Elsevier: Amsterdam, 2001.